

AD-A009 432

**ILS GLIDE SLOPE PERFORMANCE PREDICTION.
VOLUME B**

S. Morin, et al

Transportation Systems Center

Prepared for:

Federal Aviation Administration

September 1974

DISTRIBUTED BY:

NTIS

**National Technical Information Service
U. S. DEPARTMENT OF COMMERCE**

**Best
Available
Copy**

Technical Report Documentation Page

| | | | |
|---|--|--|-------------------|
| 1. Report No. FAA-RD-74-157.B | 2. Government Accession No. | 3. Recipient's Catalog No. <i>RD-A009 432</i> | |
| 4. Title and Subtitle ILS GLIDE SLOPE PERFORMANCE PREDICTION VOLUME B | | 5. Report Date September 1974 | |
| | | 6. Performing Organization Code | |
| 7. Author(s) S. Morin, D. Newsom, D. Kahn, L. Jordan | | 8. Performing Organization Report No. DOT-TSC-FAA-74-14.B | |
| 9. Performing Organization Name and Address U.S. Department of Transportation Transportation Systems Center Kendall Square Cambridge MA 02142 | | 10. Work Unit No. (TRAIS) FA507/P5123 | |
| | | 11. Contract or Grant No. | |
| 12. Sponsoring Agency Name and Address U.S. Department of Transportation Federal Aviation Administration Systems Research and Development Service Washington DC 20591 | | 13. Type of Report and Period Covered Fiscal Year 1974 Final Report and Operational Handbook | |
| | | 14. Sponsoring Agency Code | |
| 15. Supplementary Notes This report consists of two volumes. Volume A includes figure foldouts. Volume B does not include figure foldouts. The text, appendixes, and all figures are identical in both volumes. | | | |
| 16. Abstract A mathematical model for predicting the performance of ILS glide slope arrays in the presence of certain types of terrain irregularities has been developed. The model is discussed in detail and then applied to a number of typical glide slope siting problems for purposes of illustration. A User's Manual for exercising the model forms Part 2 of this report. | | | |
| 17. Key Words ILS, Glide Slope, CDI | | 18. Distribution Statement DOCUMENT IS AVAILABLE TO THE PUBLIC THROUGH THE NATIONAL TECHNICAL INFORMATION SERVICE, SPRINGFIELD, VIRGINIA 22161 | |
| 19. Security Classif. (of this report) Unclassified | 20. Security Classif. (of this page) Unclassified | 21. No. of Pages 170 | 22. Price 6.25 |

Form DOT F 1700.7 (8-72)

Reproduced by
NATIONAL TECHNICAL
INFORMATION SERVICE
U.S. Department of Commerce
Springfield, VA, 22151

Prices Subject to Change

PREFACE

In order to quickly assess the effect of certain types of terrain irregularities on the performance of ILS Glide Slope antenna systems, a mathematical-electromagnetic scattering computer model has been developed.

This work was performed by members of the Modeling and Analysis Section of the Electromagnetic Technology Division, Transportation Systems Center for the Category 1 and 2 ILS Section of the Terminal Navigation Branch of the Systems Research and Development Service, Federal Aviation Administration (FAA).

CONTENTS

| <u>Section</u> | <u>PAGE</u> |
|--|-------------|
| PART I THEORY | |
| 1. INTRODUCTION..... | 1-1 |
| 2. THEORY..... | 2-1 |
| 3. NUMERICAL RESULTS..... | 3-1 |
| 3.1 Introduction..... | 3-1 |
| 3.2 Flat Terrain..... | 3-4 |
| 3.3 Terrain Discontinuity..... | 3-7 |
| 3.3.1 Adjusted Antenna Element Heights..... | 3-15 |
| 3.4 20-Foot Dropoff..... | 3-15 |
| 3.4.1 Adjusted Antenna Element Heights..... | 3-29 |
| 3.5 Dropoff and Upgrade..... | 3-30 |
| 3.5.1 Adjusted Antenna Element Heights..... | 3-44 |
| 3.6 Upgrade, Dropoff and Upgrade..... | 3-51 |
| 3.6.1 Adjusted Antenna Element Heights..... | 3-59 |
| 3.7 Hill Terrain..... | 3-67 |
| 3.7.1 Adjusted Antenna Element Heights..... | 3-75 |
| PART II USER'S MANUAL | |
| 1. INTRODUCTION; DEFINITION OF INSTRUMENT LANDING SYSTEM..... | 4-1 |
| 2. ANTENNA PATTERNS..... | 4-3 |
| 3. SIMULATION DESCRIPTION OF ILSGLD..... | 4-6 |
| 3.1 Method of Simulation..... | 4-7 |
| 3.2 Operation..... | 4-9 |
| 3.3 Conclusion..... | 4-9 |
| 4. FMAKE PROGRAM DESCRIPTION..... | 4-10 |
| 4.1 Switch: Y..... | 4-10 |
| 4.2 Switch: G..... | 4-10 |
| 4.3 Switch: P..... | 4-12 |
| 4.4 Switch: A..... | 4-13 |
| 5. GLDPLT PROGRAM DESCRIPTION..... | 4-16 |
| APPENDIX A - LISTING OF ILSGLD..... | A-1 |
| APPENDIX B - FMAKE LISTING..... | B-1 |
| APPENDIX C - GLDPLT LISTING..... | C-1 |
| APPENDIX D - EXAMPLE..... | D-1 |

LIST OF ILLUSTRATIONS

| <u>Figure</u> | <u>Page</u> |
|---|-------------|
| 1. Geometry of a Typical One-Dimensional Ground Reflection Problem..... | 2-4 |
| 2. Null Reference Array, Level Run Flight, Flat Terrain..... | 3-5 |
| 2A. Null Reference Array, Flyability Run, Flat Terrain..... | 3-6 |
| 3. Terrain Discontinuity..... | 3-8 |
| 3A. Null Reference Array, Level Run Flight, Terrain Discontinuity..... | 3-9 |
| 3B. Sideband Reference Array, Level Run Flight, Terrain Discontinuity..... | 3-10 |
| 3C. Capture Effect Array, Level Run Flight, Terrain Discontinuity..... | 3-11 |
| 3D. Null Reference Array, Flyability Run, Terrain Discontinuity..... | 3-12 |
| 3E. Sideband Reference Array, Flyability Run, Terrain Discontinuity..... | 3-13 |
| 3F. Capture Effect Array, Flyability Run, Terrain Discontinuity..... | 3-14 |
| 3G. Adjusted Null Reference Array, Level Run Flight, Terrain Discontinuity..... | 3-16 |
| 3H. Adjusted Sideband Reference Array, Level Run Flight, Terrain Discontinuity..... | 3-17 |
| 3I. Adjusted Capture Effect Array, Level Run Flight, Terrain Discontinuity..... | 3-18 |
| 3J. Adjusted Null Reference Array, Flyability Run, Terrain Discontinuity..... | 3-19 |
| 3K. Adjusted Sideband Reference Array, Flyability Run, Terrain Discontinuity..... | 3-20 |
| 3L. Adjusted Capture Effect Array, Flyability Run, Terrain Discontinuity..... | 3-21 |
| 4. 20-Foot Dropoff..... | 3-22 |

LIST OF ILLUSTRATIONS (CONTINUED)

| <u>Figure</u> | <u>Page</u> |
|---|-------------|
| 4A. Null Reference Array, Level Run Flight, 20-Foot Dropoff..... | 3-23 |
| 4B. Sideband Reference Array, Level Run Flight, 20-Foot Dropoff..... | 3-24 |
| 4C. Capture Effect Array, Level Run Flight, 20-Foot Dropoff..... | 3-25 |
| 4D. Null Reference Array, Flyability Run, 20-Foot Dropoff..... | 3-26 |
| 4E. Sideband Reference Array, Flyability Run, 20-Foot Dropoff..... | 3-27 |
| 4F. Capture Effect Array, Flyability Run, 20-Foot Dropoff..... | 3-28 |
| 4G. Adjusted Null Reference Array, Level Run Flight, 20-Foot Dropoff..... | 3-31 |
| 4H. Adjusted Sideband Reference Array, Level Run Flight, 20-Foot Dropoff..... | 3-32 |
| 4I. Adjusted Capture Effect Array, Level Run Flight, 20-Foot Dropoff..... | 3-33 |
| 4J. Adjusted Null Reference Array, Flyability Run, 20-Foot Dropoff..... | 3-34 |
| 4K. Adjusted Sideband Reference Array, Flyability Run, 20-Foot Dropoff..... | 3-35 |
| 4L. Adjusted Capture Effect Array, Flyability Run, 20-Foot Dropoff..... | 3-36 |
| 5. Dropoff and Upgrade..... | 3-37 |
| 5A. Null Reference Array, Level Run Flight, Dropoff and Upgrade..... | 3-38 |
| 5B. Sideband Reference Array, Level Run Flight, Dropoff and Upgrade..... | 3-39 |
| 5C. Capture Effect Array, Level Run Flight, Dropoff and Upgrade..... | 3-40 |
| 5D. Null Reference Array, Flyability Run, Dropoff and Upgrade..... | 3-41 |

LIST OF ILLUSTRATIONS (CONTINUED)

| <u>Figure</u> | <u>Page</u> |
|---|-------------|
| SE. Sideband Reference Array, Flyability Run, Dropoff and Upgrade..... | 3-42 |
| SF. Capture Effect Array, Flyability Run, Dropoff and Upgrade..... | 3-43 |
| SG. Adjusted Null Reference Array, Level Run Flight, Dropoff and Upgrade..... | 3-45 |
| SH. Adjusted Sideband Reference Array, Level Run Flight, Dropoff and Upgrade..... | 3-46 |
| SI. Adjusted Capture Effect Array, Level Run Flight, Dropoff and Upgrade..... | 3-47 |
| SJ. Adjusted Null Reference Array, Flyability Run, Dropoff and Upgrade..... | 3-48 |
| SK. Adjusted Sideband Reference Array, Flyability Run, Dropoff and Upgrade..... | 3-49 |
| SL. Adjusted Capture Effect Array, Flyability Run, Dropoff and Upgrade..... | 3-50 |
| 6. Upgrade, Dropoff and Upgrade..... | 3-52 |
| 6A. Null Reference Array, Level Run Flight, Upgrade, Dropoff and Upgrade..... | 3-53 |
| 6B. Sideband Reference Array, Level Run Flight, Upgrade, Dropoff and Upgrade..... | 3-54 |
| 6C. Capture Effect Array, Level Run Flight, Upgrade, Dropoff and Upgrade..... | 3-55 |
| 6D. Null Reference Array, Flyability Run, Upgrade, Dropoff and Upgrade..... | 3-56 |
| 6E. Sideband Reference Array, Flyability Run, Upgrade, Dropoff and Upgrade..... | 3-57 |
| 6F. Capture Effect Array, Flyability Run, Upgrade, Dropoff and Upgrade..... | 3-58 |
| 6G. Adjusted Null Reference Array, Level Run Flight, Upgrade, Dropoff and Upgrade..... | 3-60 |
| 6H. Adjusted Sideband Reference Array, Level Run Flight, Upgrade, Dropoff and Upgrade..... | 3-61 |

LIST OF ILLUSTRATIONS (CONTINUED)

| <u>Figure</u> | <u>Page</u> |
|---|-------------|
| 6I. Adjusted Capture Effect Array, Level Run Flight, Upgrade, Dropoff and Upgrade..... | 3-62 |
| 6J. Adjusted Null Reference Array, Flyability Run, Upgrade, Dropoff and Upgrade..... | 3-63 |
| 6K. Adjusted Sideband Reference Array, Flyability Run, Upgrade, Dropoff and Upgrade..... | 3-64 |
| 6L. Adjusted Capture Effect Array, Flyability Run, Upgrade, Dropoff and Upgrade..... | 3-65 |
| 7. Hill (5° Upgrade)..... | 3-68 |
| 7A. Null Reference Array, Level Run Flight, Hill..... | 3-69 |
| 7B. Sideband Reference Array, Level Run Flight, Hill..... | 3-70 |
| 7C. Capture Effect Array, Level Run Flight, Hill..... | 3-71 |
| 7D. Null Reference Array, Flyability Run, Hill..... | 3-72 |
| 7E. Sideband Reference Array, Flyability Run, Hill..... | 3-73 |
| 7F. Capture Effect Array, Flyability Run, Hill..... | 3-74 |
| 7G. Adjusted Null Reference Array, Level Run Flight, Hill..... | 3-76 |
| 7H. Adjusted Sideband Reference Array, Level Run Flight, Hill..... | 3-77 |
| 7I. Adjusted Capture Effect Array, Level Run Flight, Hill..... | 3-78 |
| 7J. Adjusted Null Reference Array, Flyability Run, Hill... | 3-79 |
| 7K. Adjusted Sideband Reference Array, Flyability Run, Hill..... | 3-80 |
| 7L. Adjusted Capture Effect Array, Flyability Run, Hill... | 3-81 |
| USER'S MANUAL | |
| 8. Antenna Patterns for Null Reference Antenna..... | 4-4 |
| 9. Test Case Results..... | D-3 |

PART I. THEORY

1. INTRODUCTION

A mathematical model has been developed for predicting the performance of image-type glide slope arrays in the presence of certain types of terrain irregularities. The basic theory is developed in the following section and then numerical results are presented, illustrating the performance of different glide slope array: for several terrain configurations.

2. THEORY

The vertical antenna pattern of an image-type glide slope array is determined by the interference between the direct and ground-reflected radiation. The ground-reflected radiation is of course generated by the charges and currents induced in the ground plane by the incident radiation from the glide slope array. For simplicity, we will assume that the ground is perfectly conducting. For a perfect conductor, the surface current density \vec{K} is given by:

$$\vec{K} = \hat{n} \times \vec{H}, \quad (1)$$

where \hat{n} is the unit normal vector pointing out of the ground and \vec{H} is the total magnetic field:

$$\vec{H} = \vec{H}_i + \vec{H}_s, \quad (2)$$

where \vec{H}_i is the incident and \vec{H}_s is the scattered magnetic field.

In terms of the surface current density \vec{K} , the ground-reflected or scattered magnetic field \vec{H}_s at a receiver above the ground is given by the following surface integral:

$$\vec{H}_s(\vec{r}_1) = \frac{1}{4\pi} \int_S \vec{K}(\vec{r}) \times \vec{\nabla} G(\vec{r}_1, \vec{r}) ds \quad (3)$$

The position vectors \vec{r}_1 and \vec{r} denote, respectively, the position vector of the receiver and the position vector of a source point on the ground plane S relative to some arbitrarily chosen origin of coordinates. The two-point Green's Function $G(\vec{r}_1, \vec{r})$ is given by:

$$G(\vec{r}_1, \vec{r}) = \frac{e^{ik|\vec{r}_1 - \vec{r}|}}{|\vec{r}_1 - \vec{r}|}, \quad (4)$$

where $k = 2\pi/\lambda$ and λ is the wavelength of the incident radiation.

We will adopt the physical optics model for the surface current density \vec{K} . Specifically, we will assume that on those portions of the ground plane not directly illuminated by the glide slope array (shadowed regions), \vec{K} is identically zero and that on those portions of the ground which are illuminated, \vec{K} is given by twice the tangential component of the incident magnetic field

$$\vec{K} \equiv 0 \text{ on } S_-; \quad (5)$$

$$\vec{K} = 2(\vec{H} \times \vec{H}_i) \text{ on } S_+, \quad (6)$$

where S_- and S_+ denote, respectively, the unilluminated and illuminated portions of the ground plane S . The physical optics approximation for the current distribution should be reasonably accurate when the characteristic dimensions of the terrain irregularities are large compared with the wavelength λ . Substituting equations (5) and (6) into equation (3), we obtain the following approximate expression for the ground-reflected magnetic field at the receiver point \vec{r}_1 :

$$\vec{H}_s(\vec{r}_1) = \frac{1}{2\pi} \int_{S_+} [\vec{H}(\vec{r}) \times \vec{H}_i(\vec{r})] \times \vec{\nabla} G(\vec{r}_1, \vec{r}) ds. \quad (7)$$

The numerical evaluation of the integral in Equation (7) for a ground plane exhibiting arbitrary terrain variations is, in general, a prohibitively time-consuming operation. Consequently, we will confine our attention to terrains which vary only along one coordinate axis. Specifically, we will treat ground planes which exhibit irregularities which do not vary in the direction perpendicular to the centerline of the runway. The touchdown point on the centerline of the runway opposite the glide slope array will be chosen as the origin of coordinates. The z -axis is chosen to be the vertical axis passing through the origin O and pointing out of the ground while the x - and y -axes lie in a horizontal plane whose normal parallels the z -axis. The x -axis points along the centerline of the runway while the y -axis is perpendicular to the centerline. The terrain irregularities are assumed to vary only with x .

That is to say, the equation of the surface of the ground is of the form $z = f(x)$ and is independent of variations in y . To put it another way, the local outward normal to the ground, \hat{n} , has only x and z components.

We will now consider the problem of a horizontal dipole mounted above such a ground plane and oriented parallel to the y -axis, the invariant axis of the terrain irregularities. The geometry of a typical problem is illustrated in Figure 1. The y -axis points into the page and the entire ground plane can be generated by projecting the cross section depicted in Figure 1 from $-\infty$ to $+\infty$ in the y -direction.

To calculate the scattered field \vec{H}_s , generated by a given terrain contour, the ground plane is first divided into a number of connected planar sections which extend from $-\infty$ to $+\infty$ in the y -direction. The side view of such a section is represented by the darkened segment of the contour depicted in Figure 1. The points (x_{01}, z_{01}) and (x_{02}, z_{02}) represent the end points of the section. The length L of a given segment

$$L = \sqrt{(x_{02} - x_{01})^2 + (z_{02} - z_{01})^2}$$

is so chosen that the unit normal \hat{n} is essentially constant for $z_{01} \leq z \leq z_{02}$ and $x_{01} \leq x \leq x_{02}$. Once the contour has been segmented into these planar sections, Equation (7) can be applied to each section and the total scattered field \vec{H}_s can be obtained by summing the contributions from all the sections. We will therefore concentrate upon obtaining an expression for the contribution to the total scattered field \vec{H}_s from a typical planar segment such as the one depicted in Figure 1. It will be assumed that only those segments which are in front of the receiver ($-\infty < x \leq x_1$) contribute to \vec{H}_s . The terrain behind the dipole ($-\infty < x \leq 0$) is assumed to be perfectly flat. The exact nature of terrain behind the antenna is not really critical since, in practice, the dipoles which make up glide slope arrays are screened to eliminate the back course.

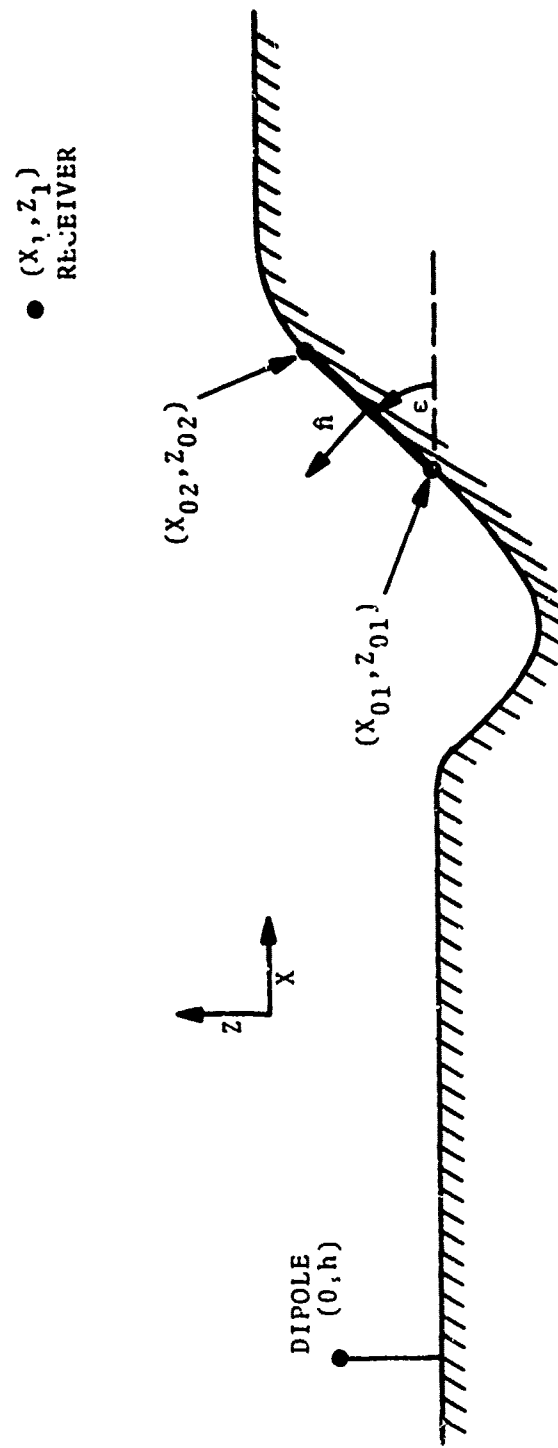


Figure 1. Geometry of a Typical One-Dimensional Ground Reflection Problem

Let \vec{h}_s denote the contribution to the total scattered field from the planar section shown in Figure 1:

$$\vec{h}_s(\vec{r}_1) = \frac{1}{2\pi} \int [\hat{n} \times \vec{H}_i(\vec{r})] \times \vec{\nabla} G(\vec{r}_1, \vec{r}) ds \quad (8)$$

where the integral is carried out over the surface of the segment (cf. Eq. (7)). Let \hat{e}_x , \hat{e}_y , and \hat{e}_z denote, respectively, the unit vectors in the x, y, and z directions. In terms of these vectors, the unit normal \hat{n} is given by:

$$\hat{n} = -\sin \epsilon \hat{e}_x + \cos \epsilon \hat{e}_z, \quad (9)$$

where ϵ is the angle between the planar section and the x-axis (cf. Fig. 1). The (x,z) coordinates of the transmitting dipole and the receiver are denoted, respectively, by (0,h) and (x_1, z_1). For simplicity, we will assume that the receiver is on the centerline of the runway so that $y_1 = 0$. The y-displacement of the dipole will be denoted by y_a . Glide slope arrays are generally located several hundred feet from the centerline of the runway.

The incident magnetic field $\vec{H}_i(\vec{r})$ produced by the transmitting dipole is given in terms of the volume current density \vec{J} in the dipole by the following formula:

$$\vec{H}_i(\vec{r}) = \frac{1}{4\pi} \int (\vec{J}(\vec{r}') \times \vec{\nabla}' G(\vec{r}, \vec{r}')) dv', \quad (10)$$

where $\vec{\nabla}'$ operates on the primed coordinates. Although the actual dipoles which make up glide slope arrays are half-wave-length bent dipoles, we will treat the case of a point dipole with the following volume current distribution:

$$\vec{J}(\vec{r}') = J_0 \hat{e}_y \delta(x') \delta(y' - y_a) \delta(z' - h). \quad (11)$$

This simplifying assumption expedites the evaluation of the integrals (10) and (8) and should not be too restrictive since we are only interested in the vertical radiation pattern formed by the direct and ground reflected radiation. In Equation (11), J_0 is some constant, the δ -functions are the Dirac delta functions, and, as previously noted, y_a and h denote, respectively, the displacement of the dipole from the centerline of the runway and the height of the antenna above ground.

Substituting Equation (11) into Equation (10) and integrating, we obtain the following expression for the incident magnetic field $H_i(r)$:

$$\vec{H}_i(\vec{r}) = i \frac{k J_0}{4\pi} \frac{e^{ikD}}{D} f(D) [x \hat{e}_z - (z-h) \hat{e}_x], \quad (12)$$

where $\vec{r} = x \hat{e}_x + y \hat{e}_y + z \hat{e}_z$ and D is the distance from the antenna to the field point \vec{r} :

$$D = [x^2 + (y-y_a)^2 + (z-h)^2]^{1/2}. \quad (13)$$

The function $f(D)$ is given by

$$f(D) = \frac{1}{D} + \frac{i}{kD^2}. \quad (14)$$

It will be noted from the form of $f(D)$ that we are retaining the near field as well as the far field contributions to \vec{H}_i .

Equations (9) and (12) can now be substituted into Equation (8), and the magnetic field \vec{H}_s at the receiver point $\vec{r}_1 = x_1 \hat{e}_x + z_1 \hat{e}_z$, due to the single planar section of terrain, evaluated. We will assume that the receiver is in the far field of the terrain segment so that $\vec{\nabla} G(\vec{r}_1, \vec{r})$ can be written as follows:

$$\vec{\nabla} G(\vec{r}_1, \vec{r}) \approx -ik \frac{(\vec{r}_1 - \vec{r}) e^{ik|\vec{r}_1 - \vec{r}|}}{|\vec{r}_1 - \vec{r}|^2}. \quad (15)$$

Actually, only the z -component of \vec{H}_s need be calculated since the receiving antenna responds primarily to this component (equivalently, the horizontal component of the electric field). The z -component of \vec{H}_s will be denoted by h_{sz} . Substituting Equations (9), (12), and (15) into Equation (8), we obtain the following expression for h_{sz} at the receiver:

$$h_{sz}(\vec{r}_1) = -\frac{k^2 J_0}{8\pi^2} \int \frac{(x_1 - x)(x \sin \epsilon - (z-h) \cos \epsilon) f(D) e^{ik(D+R)}}{DR^2} ds, \quad (16)$$

where $R = [(x_1 - x)^2 + y^2 + (z_1 - z)^2]^{1/2}$ is the distance from a point

on the terrain segment to the receiver. The element of area ds is equal to $dydn$, where η is a variable ranging from 0 to L along the surface of the terrain segment perpendicular to the y -axis. The x - and z -coordinates of a point on the surface of the planar section can be expressed in terms of η as follows (cf. Fig. 1):

$$\begin{aligned} x &= x_{01} + \eta \cos \epsilon, \quad 0 \leq \eta \leq L, \\ z &= z_{01} + \eta \sin \epsilon, \quad 0 \leq \eta \leq L \end{aligned} \quad (17)$$

Substituting Equations (17) into Equation (16), we obtain

$$\begin{aligned} h_{sz}(\vec{r}_1) &= \frac{k^2 J_0}{8\pi^2} [(z_{01} - h) \cos \epsilon - x_{01} \sin \epsilon] \times \\ &\int_0^L \int_{-\infty}^{+\infty} \frac{(x_1 - x_{01} - \eta \cos \epsilon)^2}{DR^2} f(D) e^{ik(D+R)} dy d\eta, \end{aligned} \quad (18)$$

where D and R are expressed as functions of the variables y and η as follows:

$$D = [(x_{01} + \eta \cos \epsilon)^2 + (y - y_a)^2 + (z_{01} - h + \eta \sin \epsilon)^2]^{1/2}, \quad (19)$$

$$R = [(x_1 - x_{01} - \eta \cos \epsilon)^2 + y^2 + (z_1 - z_{01} - \eta \sin \epsilon)^2]^{1/2}. \quad (20)$$

The integration with respect to y ($-\infty < y < +\infty$) can be performed approximately using the method of stationary phase leaving only an integral with respect to η to be evaluated numerically:

$$h_{sz}(\vec{r}_1) = \frac{k^2 J_0}{8\pi^2} [(z_{01} - h) \cos \epsilon - x_{01} \sin \epsilon] \lambda^{1/2} e^{i\pi/4} I, \quad (21)$$

where

$$I = \int_0^L e^{ikF(\eta)} G(\eta) d\eta, \quad (22)$$

and F and G are defined as follows:

$$A = [(x_1 - x_{01} - r \cos \epsilon)^2 + (z_1 - z_{01} - \eta \sin \epsilon)^2]^{1/2}.$$

$$B = [(x_{01} + \eta \cos \epsilon)^2 + (z_{01} - h + \eta \sin \epsilon)^2]^{1/2},$$

$$C = \left[1 + \frac{y_a^2}{(A+B)^2}\right]^{1/2}, \quad D = CB, \quad R = CA,$$

$$S = \frac{1}{C^3} \left[\frac{1}{A} + \frac{1}{B} \right],$$

$$F(\eta) = C(A + B),$$

$$G(\eta) = \frac{f(D) [x_1 - x_{01} - \eta \cos \epsilon]}{DR^2 S^{1/2}}. \quad (23)$$

The contribution to the total scattered field \tilde{H}_s from the region behind the antenna ($-\infty < x \leq 0$) can be calculated approximately using asymptotic methods. As noted previously, the terrain behind the glide slope array is assumed to be perfectly flat ($\epsilon=0$, $z=0$ for $-\infty < x \leq 0$). From Equation (16), the contribution to H_{sz} from this back course region, which will be denoted by \tilde{h}_{sz} , can be written as follows:

$$\tilde{h}_{sz}(\vec{r}_1) = \frac{-k^2 h J_0}{8\pi^2} \int_{-\infty}^0 \int_{-\infty}^{+\infty} (x_1 - x) \frac{f(D)}{DR^2} e^{ik(D+R)} dy dx, \quad (24)$$

where

$$D = [x^2 + (y - y_a)^2 + h^2]^{1/2}, \quad (25)$$

and

$$R = [(x_1 - x)^2 + y^2 + z_1^2]^{1/2}. \quad (26)$$

As before, the y -integration is performed by the method of stationary phase leaving an integral of the following form:

$$\tilde{h}_{sz}(\vec{r}_1) = \frac{-k^2 h J_0 \lambda^{1/2} e^{i\pi/4}}{8\pi^2} \int_{-\infty}^0 e^{ikF_1(x)} G_1(x) dx, \quad (27)$$

where F_1 and G_1 are defined as follows:

$$A_1 = [(x_1 - x)^2 + z_1^2]^{1/2},$$

$$B_1 = [x^2 + h^2]^{1/2},$$

$$C_1 = 1 + \left[\frac{y_a^2}{(A_1 + B_1)^2} \right]^{1/2}, \quad D = CB_1, \quad R = CA_1,$$

$$S_1 = \frac{1}{C_1^3} \left[\frac{1}{A_1} + \frac{1}{B_1} \right]$$

$$G_1(x) = \frac{f(D)}{D} \frac{[x_1 - x]}{R^2 S_1^{1/2}}.$$

$$F_1(x) = C_1 (A_1 + B_1)$$

Integrals of the type in Equation (27) with rapidly varying phase functions and no stationary points in the range of integration (here $-\infty < x \leq 0$) can be approximated very accurately using asymptotic techniques. It turns out that the major contribution to the integral in (27) comes from the vicinity of $x = 0$ and that we can write to a very good approximation:

$$h_{sz}(\vec{r}_1) = \frac{ikhJ_0 \lambda^{1/2} e^{i\pi/4}}{8\pi^2} \frac{G_1(0)e^{ikF_1(0)}}{F_1'(0)}, \quad (28)$$

where $G_1(0)$, $F_1(0)$, and $F_1'(0)$ denote, respectively the values of G_1 , F_1 , and the first derivative of F_1 at $x = 0$. These quantities are defined below:

$$A_1(0) = [x_1^2 + z_1^2]^{1/2}$$

$$B_1(0) = h$$

$$C_1(0) = \left[1 + \frac{y_a^2}{(A_1(0) + B_1(0))^2} \right]^{1/2}$$

$$D(0) = C_1(0)B_1(0)$$

$$R(0) = C_1(0)A_1(0)$$

$$S_1(0) = \frac{1}{C_1^3(0)} \left[\frac{1}{A_1(0)} + \frac{1}{B_1(0)} \right]$$

$$\begin{aligned}
F_1(0) &= C_1(0) [A_1(0) + B_1(0)] \\
G_1(0) &= \frac{f(D(0))x_1}{D(0)R^2(0)S_1^{1/2}(0)} \\
F_1'(0) &= \frac{-[A_1(0)+B_1(0)]}{F_1(0)} \frac{x_1}{A_1(0)} .
\end{aligned} \tag{29}$$

Using Equation (28) to represent the contribution to the total scattered field from the region behind the antenna and applying Equation (21) to each illuminated terrain segment lying between the dipole and the receiver, we obtain the total z-component of the scattered magnetic field by summing all these contributions:

$$H_{sz} = \bar{h}_{sz} + \sum h_{sz} . \tag{30}$$

The procedure for calculating the difference in depth of modulation (DDM) at a given receiver location is quite straightforward. First, using the procedure outlined above, the complex field amplitudes at the receiver due to each element in the glide slope array are calculated. Let H_c , H_{150} , and H_{90} denote the total complex field amplitudes (direct plus scattered summed for all dipoles in the array) at the carrier frequency, the 150 Hz modulated frequency, and 90 Hz modulated frequency, respectively. In terms of these complex amplitudes, the difference in depth of modulation is given by:

$$D.D.M. = \operatorname{Re} \left(\frac{H_{150} - H_{90}}{H_c} \right) , \tag{31}$$

where Re denotes the real part of the complex number. Full scale deflection (150 microamperes) corresponds to a D.D.M. of .175 for the glide slope. Consequently, the C.D.I. (course deviation indication) is given by:

$$C.D.I. = 857.14 \operatorname{Re} \left(\frac{H_{150} - H_{90}}{H_c} \right) . \tag{32}$$

3. NUMERICAL RESULTS

3.1 INTRODUCTION

The formalism developed in the preceding section has been applied to a whole series of glide slope siting problems. All three main types of image glide slope arrays (null reference, sideband reference, capture effect) have been treated. Comparative results will be presented illustrating the performance of each array for a few terrain configurations suggested to us for study by the FAA.

The null reference array is the simplest of the image glide slope systems. It consists of two transmitting antennas whose heights are in the ratio of 2:1. The upper antenna is fed sideband only signal, the 150 Hz and the 90 Hz components being of equal amplitude but 180° out of phase. The lower antenna is fed both carrier and sideband. The carrier signal is nominally 40% modulated. The ratio of the sideband currents in the upper antenna to the sideband currents in the lower antenna is typically 0.3. The sideband ratio of 0.3 would nominally yield a 1.4° course width (full deflection 0.7° above or below the glide path). Let I_c , I_{150} , and I_{90} denote the current amplitudes fed to the antennas at the carrier frequency, the 150 Hz modulated frequency, and the 90 Hz modulated frequency, respectively. The null reference array parameters discussed above can be summarized as follows:

| <u>Carrier Antenna</u> | <u>Sideband Antenna</u> |
|------------------------|-------------------------|
| Height = h | Height = $2h$ |
| $I_c = 1$ | $I_c = 0$ |
| $I_{150} = 0.4$ | $I_{150} = 0.12$ |
| $I_{90} = 0.4$ | $I_{90} = -0.12$ |

Note that all current amplitudes have been normalized relative to the carrier current amplitude ($I_c = 1$).

The sideband reference array employs two transmitting dipoles whose heights are in the ratio of 3:1. If the lower antenna is positioned at 1/2 the height of the lower antenna of the null

reference array and if the upper antenna is positioned at 3/4 of the height of the upper antenna of the null reference array, the same glide angle is produced. Modulated carrier (40% modulated) is fed to the lower antenna. Both antennas are fed separate sideband signal. The separate sideband signals fed to the two antennas are equal in amplitude but are 180° out of phase. The amplitude ratio of the separate sideband signal to the carrier sideband signal is typically 0.3. This ratio produces a nominal course width of 1.4° as in the case of the null reference array. The sideband reference parameters are summarized below.

| <u>Lower Antenna</u> | <u>Upper Antenna</u> |
|----------------------|----------------------|
| Height = h | Height = 3h |
| $I_c = 1$ | $I_c = 0$ |
| $I_{150} = 0.28$ | $I_{150} = 0.12$ |
| $I_{90} = 0.52$ | $I_{90} = -0.12$ |

Note that the I_{150} and I_{90} current amplitudes given above for the lower antenna represent the sums of the carrier sideband and separate sideband signals ($I_{150} = .4 - .12 = .28$, $I_{90} = .4 + .12 = .52$). All current amplitudes have been normalized relative to the carrier signal amplitude.

The capture effect glide slope array consists of three transmitting antennas whose heights are in the ratios of 1:2:3. If the lower and middle antennas are set at the same heights as the null reference antennas, the same glide angle is produced. We will not treat the clearance signal which provides a strong fly up signal at low approach angles but has little effect upon the glide angle and course width. Concerning the primary signal, modulated carrier is fed to both the lower and the middle antennas. The modulated carrier fed to the middle antenna has half the amplitude and is 180° out of phase with the modulated carrier fed to the lower antenna. The carrier signals are nominally 40% modulated. In addition, all three antennas are fed separate sideband signal. The separate sideband signals fed to the lower and upper antennas have half the amplitude and are 180° out of phase with the separate sideband signal fed to

the middle antenna. The ratio of the separate sideband signal fed to the middle antenna to the carrier sideband signal in the lower antenna is typically 0.3. This ratio yields nominally a course width of 1.4° as in the case of the null reference array. The capture effect array parameters are summarized below.

| <u>Lower Antenna</u> | <u>Middle Antenna</u> |
|----------------------|-----------------------|
| Height = h | Height = 2h |
| $I_c = 1$ | $I_c = -0.5$ |
| $I_{150} = 0.34$ | $I_{150} = -0.08$ |
| $I_{90} = 0.46$ | $I_{90} = -0.32$ |
| <u>Upper Antenna</u> | |
| Height = 3h | |
| $I_c = 0$ | |
| $I_{150} = -0.06$ | |
| $I_{90} = 0.06$ | |

Note that the I_{150} and I_{90} current amplitudes given above represent the sums of the carrier sideband and separate sideband signals. Again, all values have been normalized relative to the carrier amplitude in the lower antenna.

It should be noted here that our computer program automatically offsets the elements of each glide slope array to correct for the effects of proximity phase lag. The y coordinates of the elements are adjusted so that all dipoles are at the same slant distance from the touchdown point on the runway directly opposite the array. For each array, one element is held fixed while the other elements are offset relative to the fixed one. For the null reference and sideband reference arrays, the lower element is held fixed while for the capture array, the middle element is held fixed. The amount of the offset for each dipole can be calculated approximately in the following manner. Let y_a and h denote, respectively, the y-coordinate and height of the fixed antenna element. The y-displacement, c, of any other element in the array relative to the fixed one is given approximately by:

$$\epsilon = \frac{h^2 - H^2}{2y_a} \quad (33)$$

where H is the height of the element which is to be offset.

For the present study, the wavelength λ was set at 3 feet. All arrays were positioned 400 feet from the centerline of the runway. The heights of the array elements were set at 14.33 feet and 28.66 feet (approximately 5λ and 10λ) for the null reference array, 7.17 feet and 21.5 feet (approximately 2.5λ and 7.5λ) for the sideband reference array, and 14.33 feet, 28.66 feet, and 42.99 feet (approximately 5λ , 10λ , and 15λ) for the capture effect array. If the ground plane were perfectly flat, a glide angle of 3° would be produced by all three arrays.

Two types of data will be presented. CDI as a function of horizontal distance from touchdown will be plotted for an aircraft in level flight at an altitude of 1200 feet as measured from the base of the antenna array ($z_1 = 1200$ ft.). This horizontal flight data is useful for studying course linearity. In addition, CDI as a function of horizontal distance from touchdown will be plotted for an aircraft flying the nominal 3° glide path. On the graphs to be presented, positive CDI indicates that the 150 Hz modulation is dominant (fly up indication) while negative CDI indicates that the 90 Hz modulation is dominant (fly down indication).

3.2 FLAT TERRAIN

Figures 2 and 2A show the level flight and nominal glide path CDI for the null reference array assuming a perfectly flat ground plane. The data was generated by summing the contributions to the scattered field from the first 5000 feet of ground plane. The results for all three arrays are essentially identical in this case so that we will present only the null reference data. The dashed lines in the figures represent the ideal results which are based upon simple image theory assuming a flat, infinite ground plane. The ideal results and the predictions of our model are clearly in close agreement. Obviously, 5000 feet of flat ground are quite sufficient to produce an excellent course. The small discrepancies between the ideal results and the predictions of our

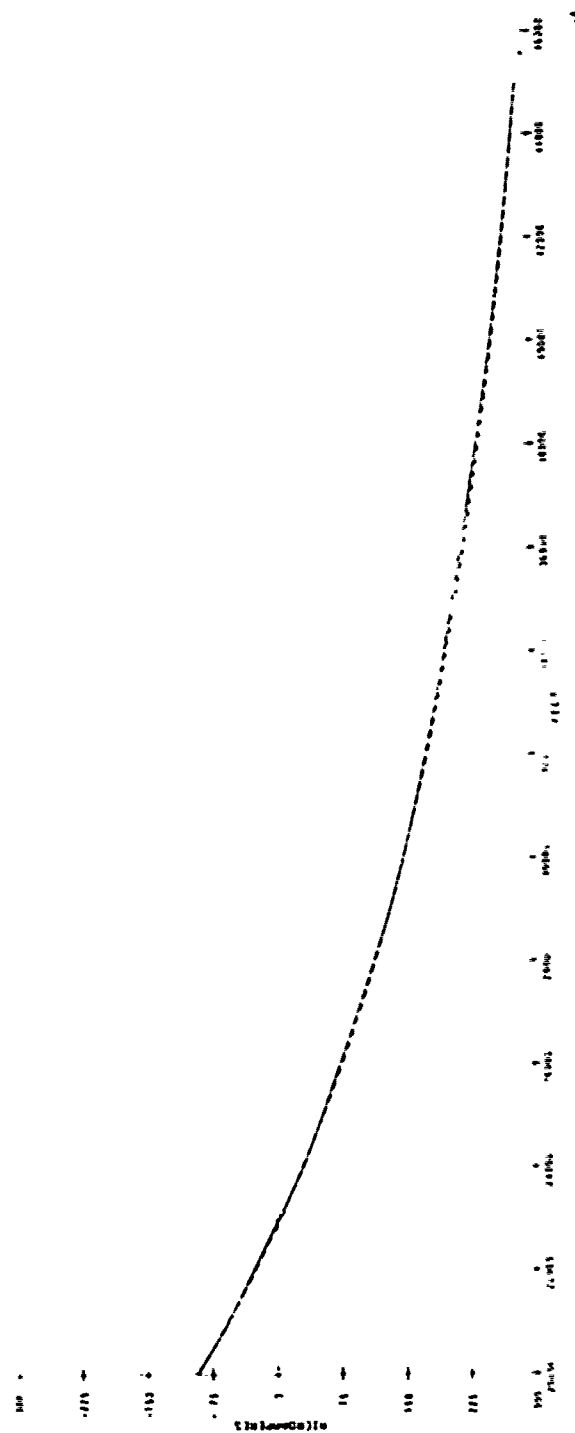


Figure 2. Null Reference Array, Level Run Flight, Flat Terrain

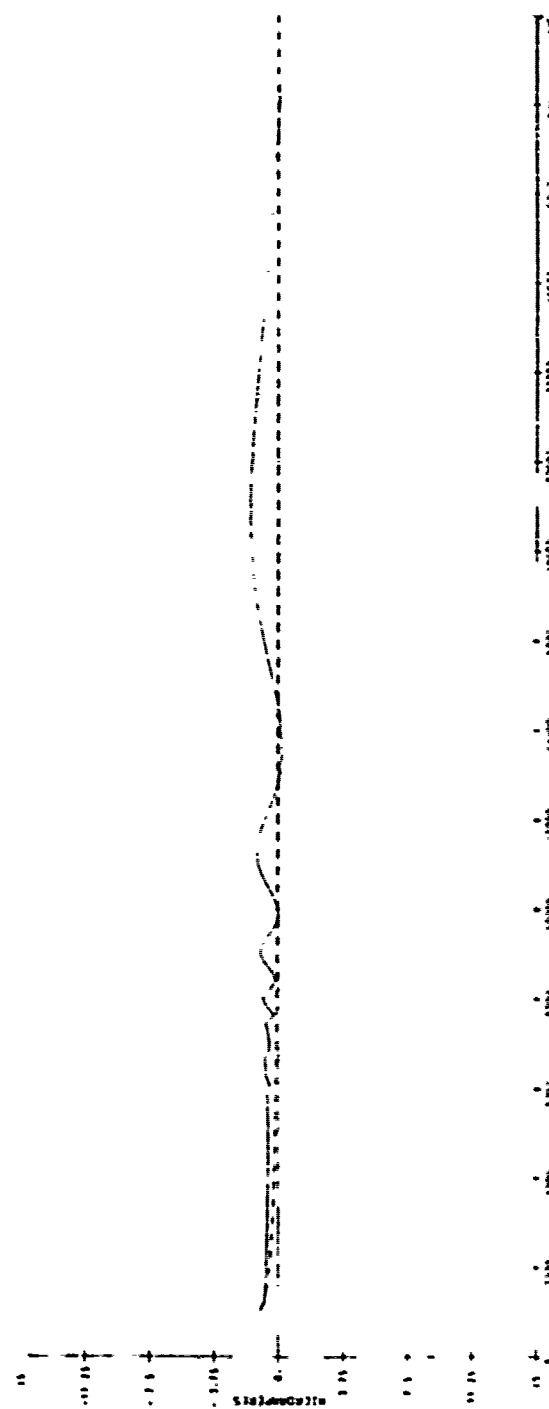


Figure 2A. Null Reference Array, Flyability Run, Flat Terrain

model which are most apparent in Figure 2A result from the truncation of the ground. These deviations however amount to, at most, approximately 2 microamps. Figure 2A shows a perfect flare or hyperbola being flown as would appear in a standard radio theodolite flight inspection run. (Had a straight line glide path at 3° been flown, the CDI would have assumed larger and larger positive values (fly up indication) as the receiver approached the touchdown point due to the fact that the straight line glide path is actually only asymptotic to and actually below the true zero DDM trajectory which is a hyperbola.)

3.3 TERRAIN DISCONTINUITY

The next series of graphs (Figs. 3A, 3B, 3C, 3D, 3E, 3F) give the predictions of our model for a terrain which slopes downward away from the array for 1200 feet at an angle of 0.6° from the horizontal and then levels off for an additional 3800 feet at which point we truncate the ground plane (see Fig. 3). The dashed lines represent the ideal image theory predictions based upon the infinite, flat ground plane. The results for all three arrays (null reference, sideband reference, and capture effect) are very similar. The courses undergo a downward shift of 0.6° relative to the horizontal.

Referring to the level run flight data (Figs. 3A, 3B, 3C), it will be noted that the zero crossings occur at approximately 29,500 feet from touchdown. For a receiver at a height of 1200 feet as measured from the base of the antenna array ($z_1 = 1200$ ft.), the zero crossing at 29,500 feet would indicate a glide angle of approximately 2.33° relative to the horizontal (the x-y plane). The nominal glide angle is 3° .

The flyability runs (Figs. 3D, 3E, 3F) also reflect this downward shift. Flying the nominal 3° glide path, the data shows a nearly constant fly down indication of between 111 and 140 microamperes. Assuming a course width of 1.4° (0.7° above or below the glide path corresponding to full scale deflection of 150 microamperes), fly down signals in this range indicate that the receiver is about 0.6° above the true glide angle.

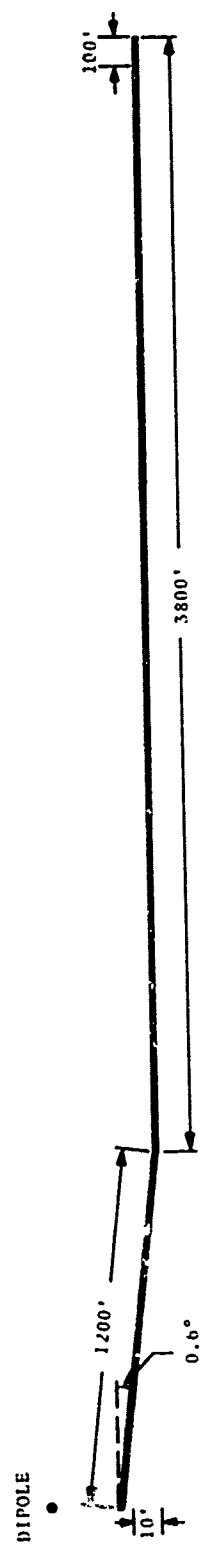
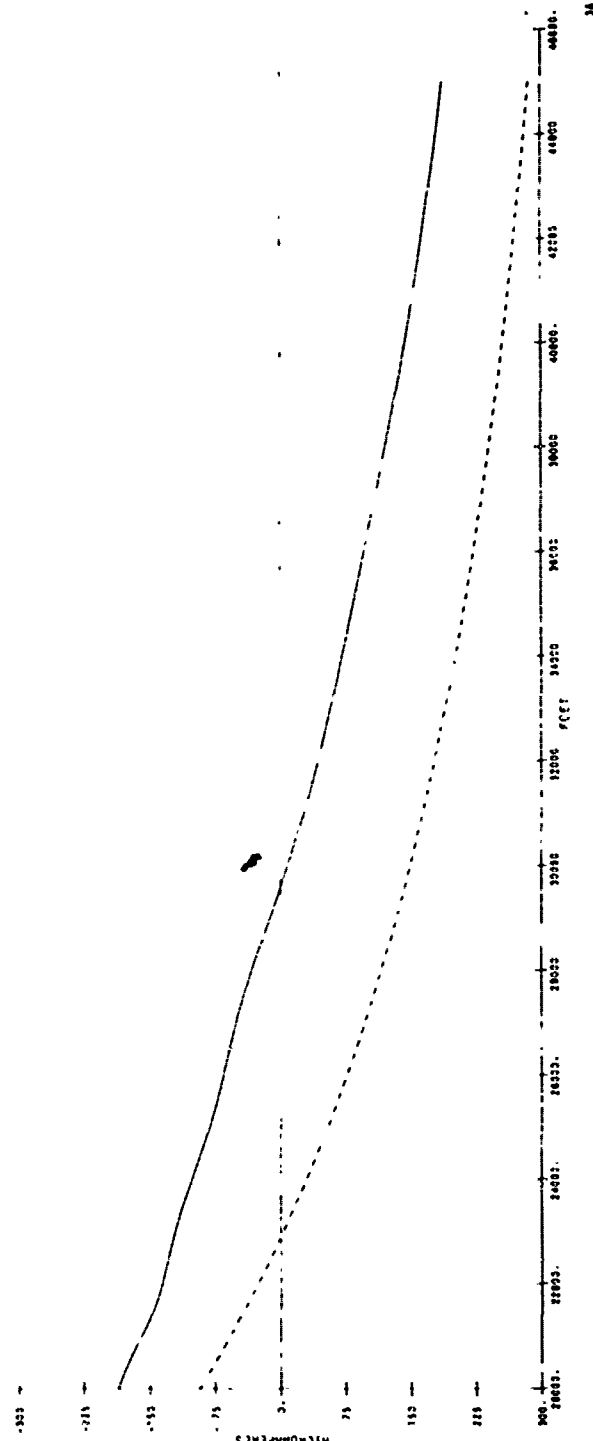


Figure 3. Terrain Discontinuity



34

Figure 3A. Null Reference Array, Level Run Flight, Terrain Discontinuity

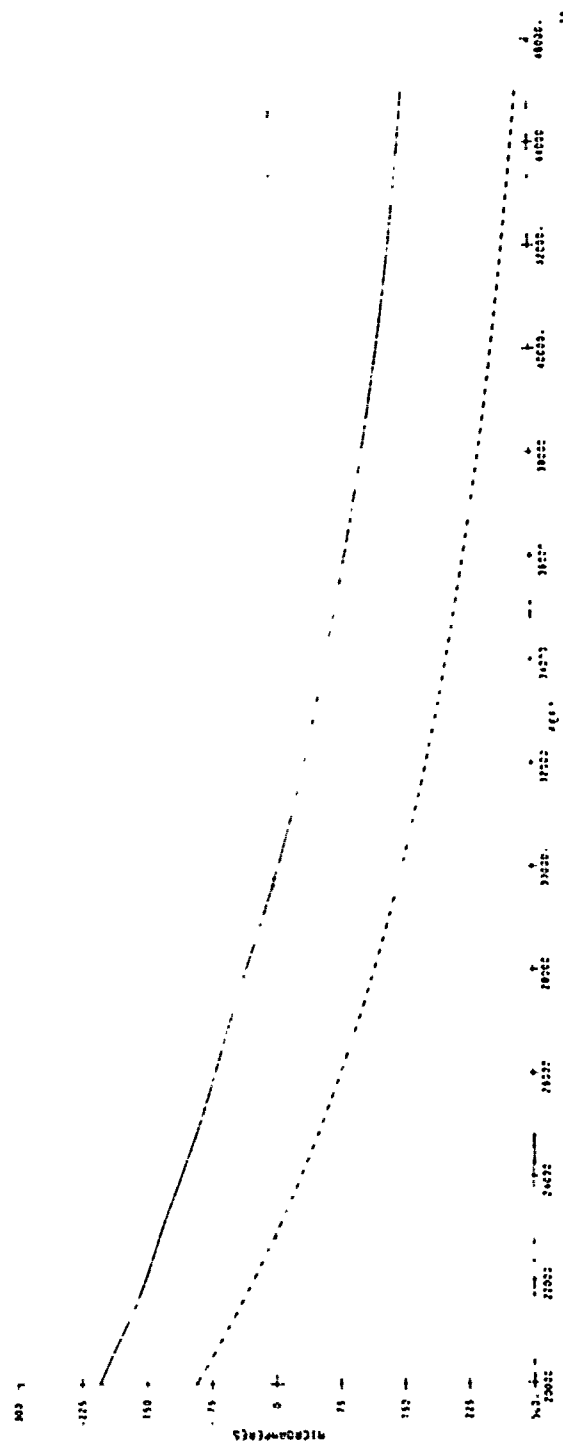


Figure 3B. Sideband Reference Array, Level Run. Flight, Terrain Discontinuity



Figure 3C. Capture Effect Array, Level Run Flight, Terrain Discontinuity

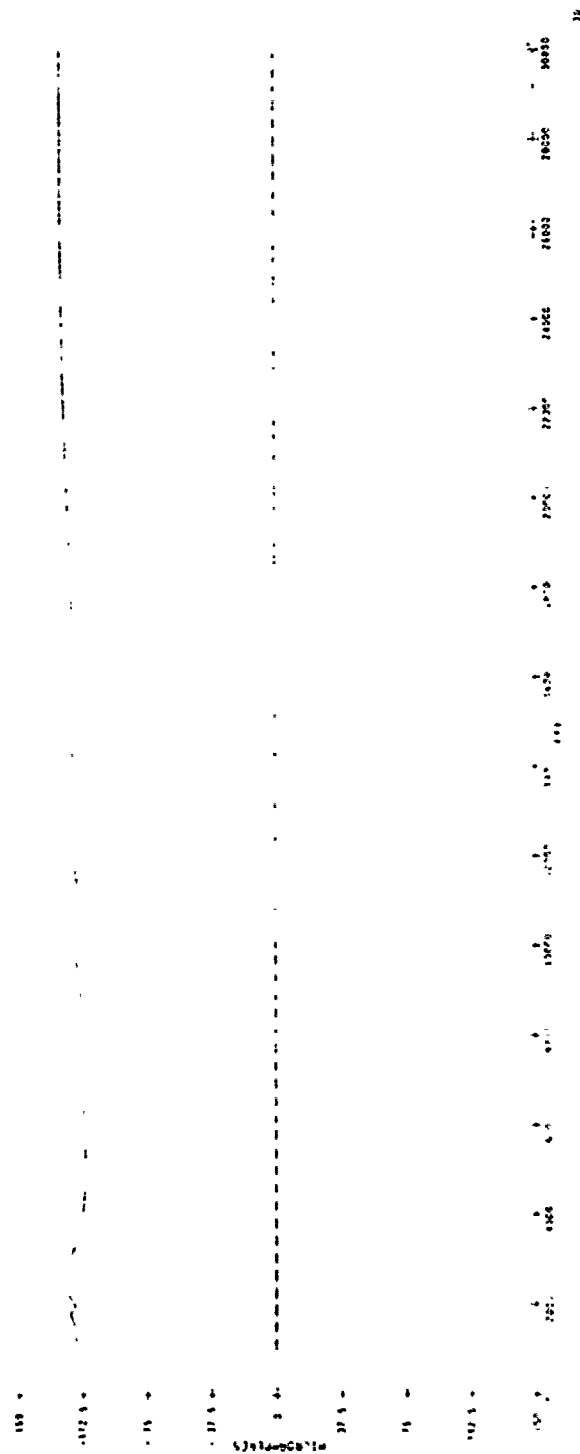


Figure 3D. Null Reference Array, Flyability Run, Terrain Discontinuity

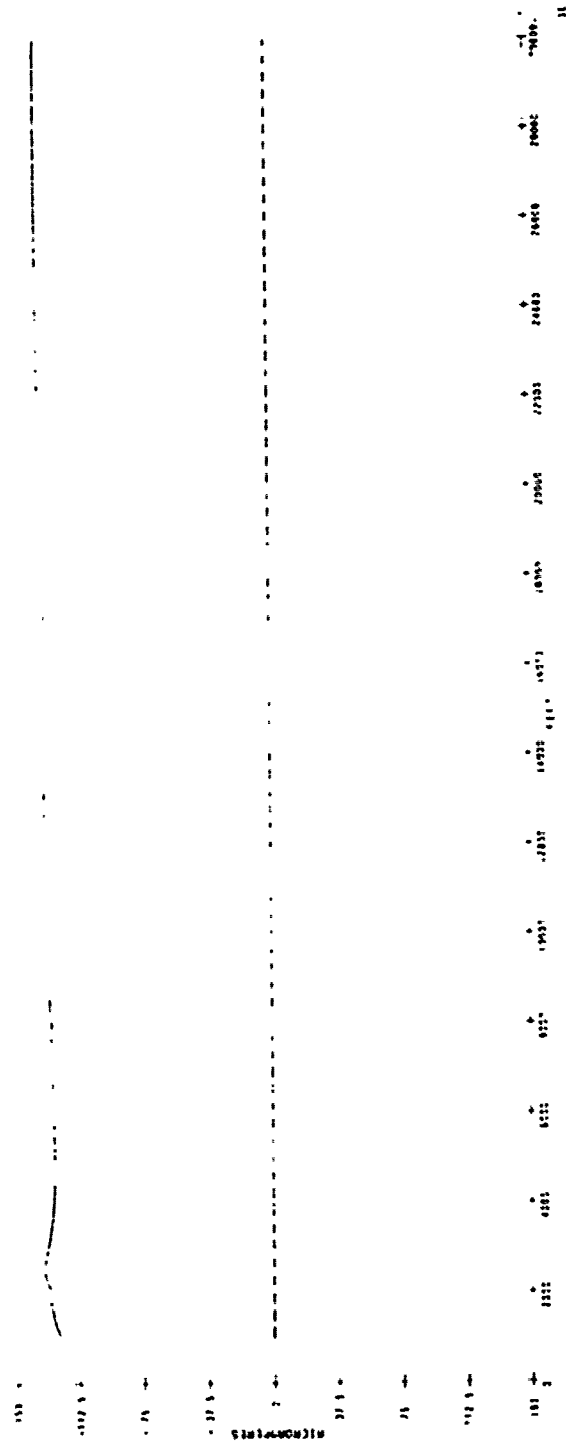


Figure 3E. Sideband Reference Array, Flyability Run, Terrain Discontinuity



Figure 3F. Capture Effect Array, Flyability Run, Terrain Discontinuity

3.3.1 Adjusted Antenna Element Heights

In order to correct for this downward shift of the glide path angle, the antenna array elements have been repositioned downwards to give a 3° glide path angle. This glide path angle is determined as the arithmetical mean over the distance between the middle marker (3500 feet from the threshold) and four miles from the threshold along the runway centerline extended.

The null reference, sideband reference and capture effect antenna element re-positioning are shown in Table 1.

TABLE 1.

| | <u>Original Positions (feet)</u> | | | <u>New Positions (feet)</u> | | |
|----------------|----------------------------------|---------------|----------------|-----------------------------|---------------|----------------|
| | <u>Lowest</u> | <u>Middle</u> | <u>Highest</u> | <u>Lowest</u> | <u>Middle</u> | <u>Highest</u> |
| Null Reference | 14.33 | | 28.66 | 11.99 | | 23.97 |
| S.B. Reference | 7.17 | | 21.5 | 5.88 | | 17.64 |
| Capture Effect | 14.33 | 28.66 | 42.99 | 11.66 | 23.32 | 34.97 |

The level flight results with these new antenna element positioning are shown in Figures 3G, 3H, and 3I. The crossovers occur very nearly at the nominal glide angle of 3° (which for the 1200 foot high horizontal flight corresponds to approximately 22,900 feet on the abscissa of the graph).

The flyability run results with this new positioning are shown in Figures 3J, 3K, and 3L. For all three antennas, the CDI has been reduced to just a few microamperes by the above repositioning of the antenna element heights.

3.4 20-FOOT DROP OFF

The next series of graphs (Figs. 4A, 4B, 4C, 4D, 4E, 4F) show the results for a terrain which extends flat for 1200 feet in front of the array and then drops off 20 feet to a lower plateau which then extends outward an additional 3800 feet (see Fig. 4). From Figures 4A and 4D, it can be seen that the null reference course tends to be elevated in the presence of such a terrain.



Figure 3G. Adjusted Null Reference Array, Level Run Flight, Terrain Discontinuity

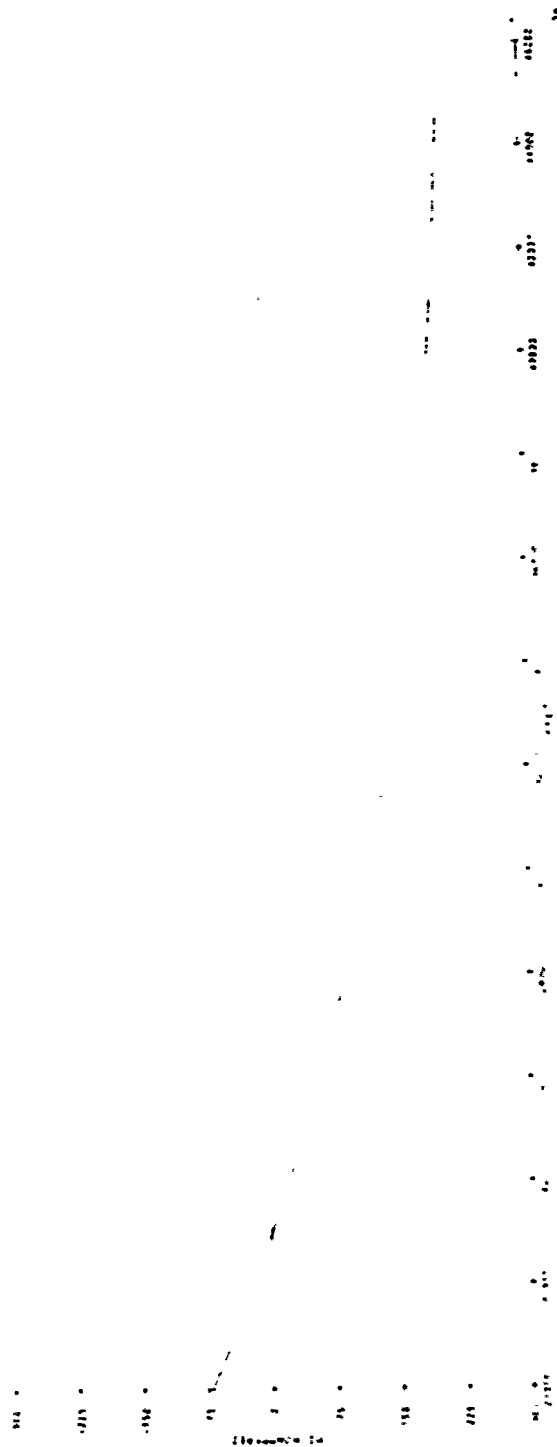


Figure 3H. Adjusted Sideband Reference Array, Level Run Flight, Terrain Discontinuity



Figure 31. Adjusted Capture Effect Array, Level Run Flight, Terrain Discontinuity



Figure 3J. Adjusted Null Reference Array, Flyability Run, Terrain Discontinuity



Figure 3L. Adjusted Capture Effect Array, Flyability Run, Terrain Discontinuity

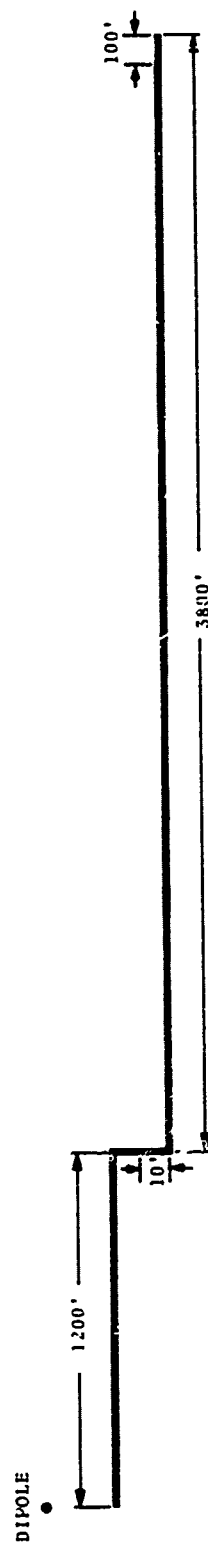


Figure 4. 20-Foot Dropoff

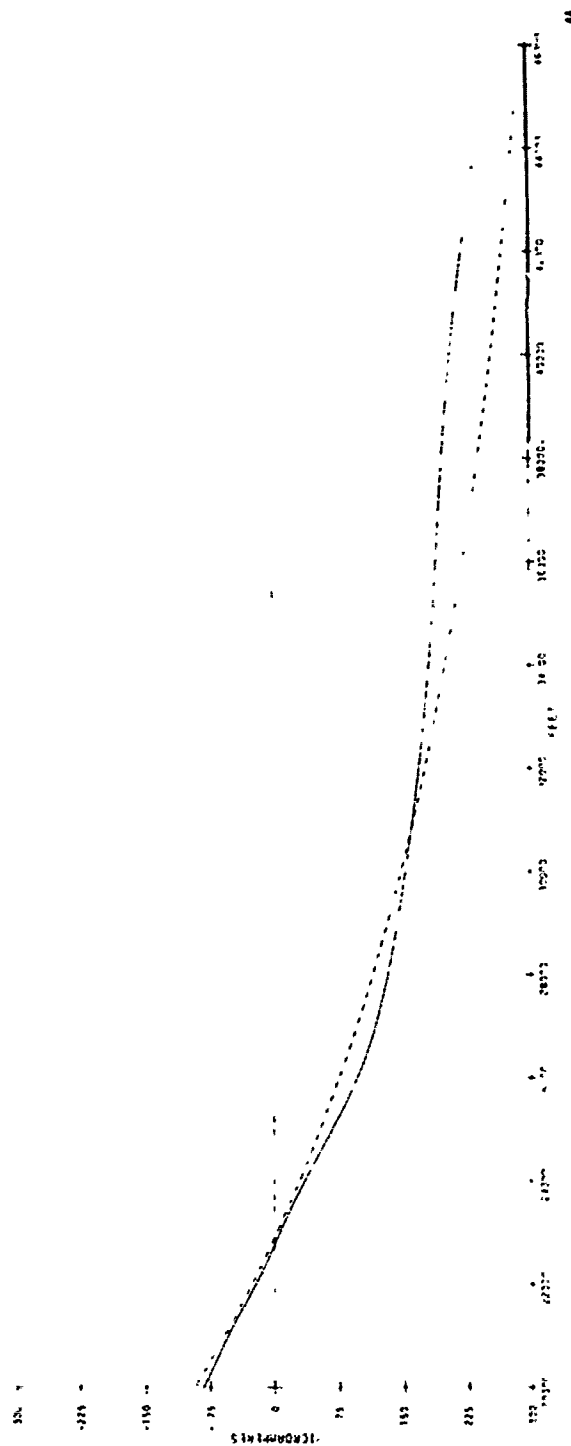


Figure 4A. Null Reference Array, Level Run Flight, 20-Foot Dropoff



Figure 4B. Sideband Reference Array, Level Run Flight, 20-Foot Dropoff

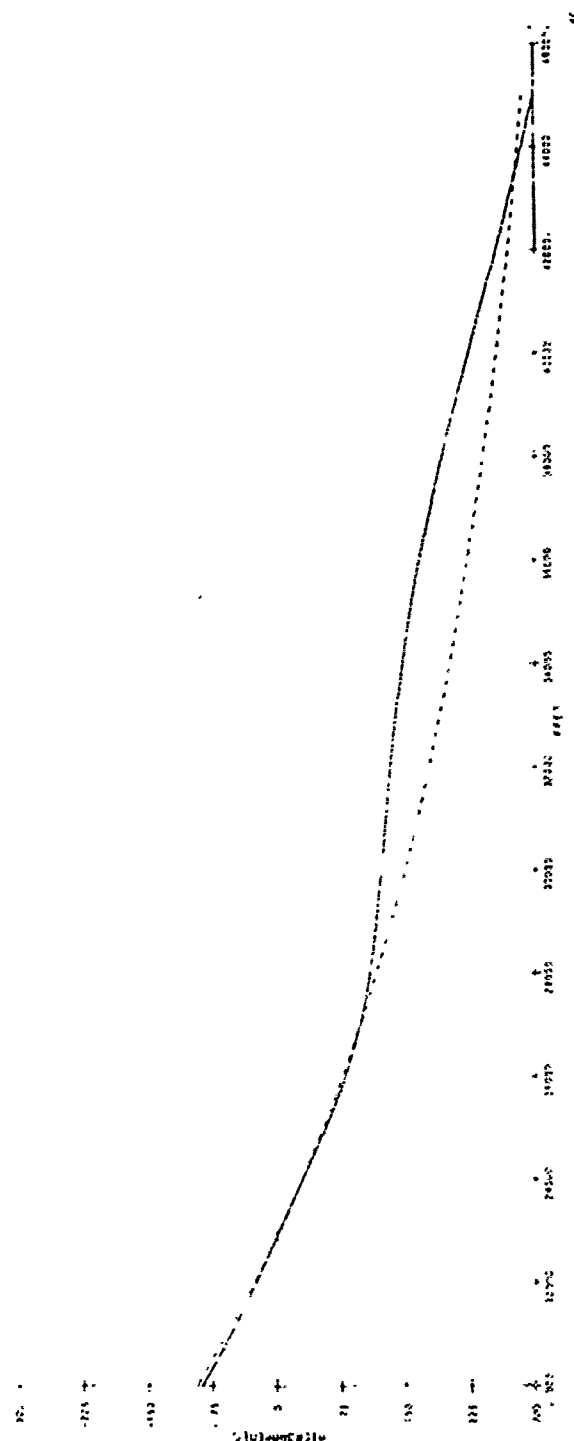


Figure 4C. Capture Effect Array, Level Run Flight, 20-Foot Dropoff

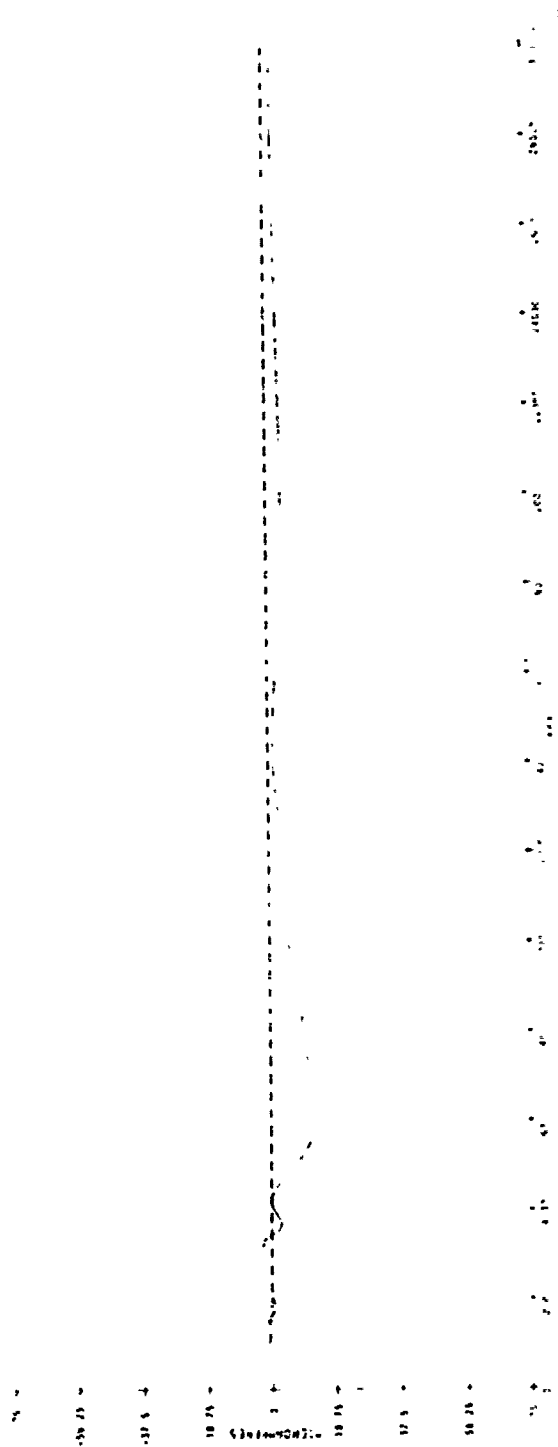


Figure 4D. Null Reference Array, Flyability Run, 20-Foot Dropoff

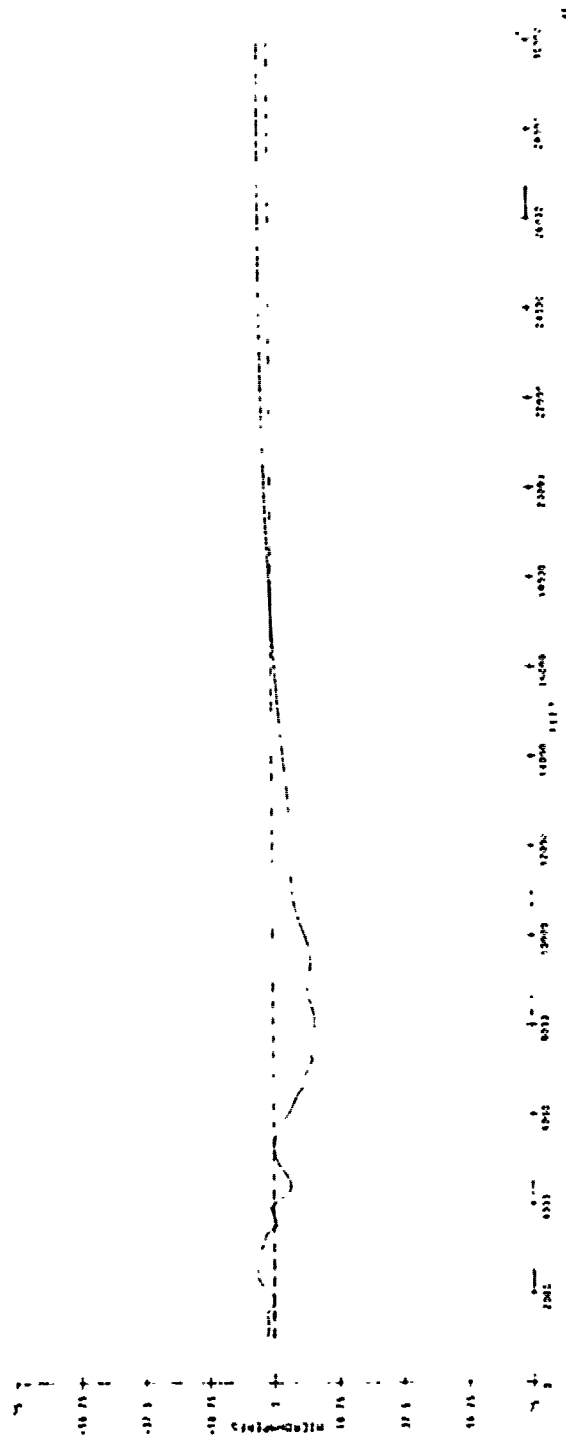


Figure 4E. Sideband Reference Array, Flyability Run, 20-Foot Dropoff

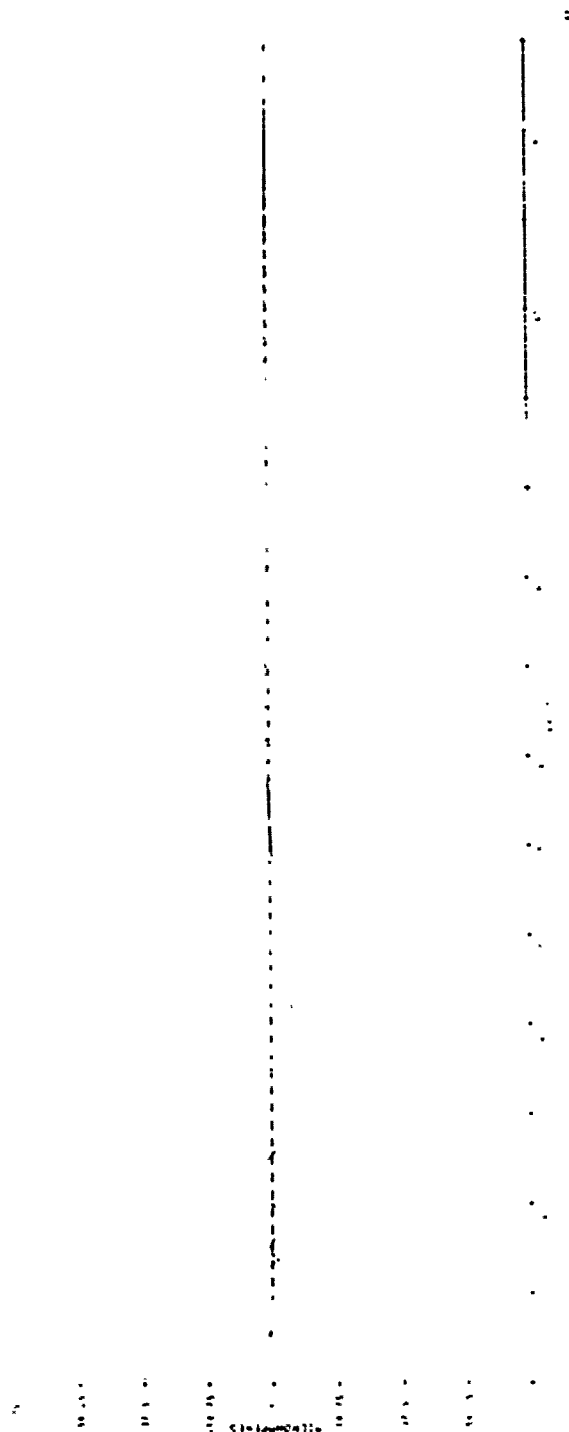


Figure 4F. Capture Effect Array, Feasibility Run, 20-Foot Dropoff

The horizontal flight curve is shifted relative to the ideal curve yielding, over much of the course, stronger fly up signals, weaker fly down signals, and a zero crossing slightly closer to touchdown (an elevated glide path) than are predicted by image theory assuming a flat infinite ground plane.

The nominal flyability run (Fig. 4D) shows a consistent fly up indication over most of the course ranging between 6 and 13 microamperes except between the middle marker and threshold where a fly down signal of -6 microamperes occurs.

The sideband reference data are depicted in Figures 4B and 4E. Note in Figure 4B that the sideband reference zero crossing point is unaffected by the presence of the dropoff. Inside the zero crossing point, the predicted CDI is somewhat weaker than is predicted by image theory while beyond the zero crossing point the predicted CDI is somewhat stronger than is predicted by image theory, at least in the relevant course region (CDI < 150 microamperes).

The flyability run (Fig. 4E) exhibits alternate fly down and fly up indications with peak values ranging from -5 to +12 microamperes.

The capture effect results are shown in Figures 4C and 4F. The level run flight exhibits relatively close agreement between the predicted CDI and the ideal image theory predictions except in the region beyond approximately 27,000 feet where the predicted fly up indication is considerably weaker than is predicted by image theory.

The nominal flyability run exhibits excursions ranging from -4 to 7 microamperes. All these deviations from ideal performance result from reflections from the lower plateau which tend to disrupt the nominal space modulation pattern.

3.4.1 Adjusted Antenna Element Heights

A 3° glide path angle, obtained as the arithmetic mean over the distance between the middle marker and four miles out, was next flown. The 3° glide path angle was obtained by re-positioning

the antenna element heights as shown in Table 2.

TABLE 2.

| | <u>Original Positions (feet)</u> | | | <u>New Positions (feet)</u> | | |
|----------------|----------------------------------|---------------|----------------|-----------------------------|---------------|----------------|
| | <u>Lowest</u> | <u>Middle</u> | <u>Highest</u> | <u>Lowest</u> | <u>Middle</u> | <u>Highest</u> |
| Null Reference | 14.33 | | 28.66 | 14.45 | | 28.89 |
| S.B. Reference | 7.17 | | 21.5 | 7.21 | | 21.62 |
| Capture Effect | 14.33 | 28.66 | 42.99 | 14.35 | 28.72 | 43.08 |

The level flight results with this new antenna element positioning are shown in Figures 4G, 4H, and 4I. These new results are only slightly different from the original as might be expected with only a slight change in the antenna element heights.

The flyability run results are shown in Figures 4J, 4K, and 4L. The null reference flyability run, Figure 4J exhibits a mostly fly up indication with a peak value of 8 microamperes. Near the middle marker region there is a fly down indication with a peak value of -11 microamperes.

The sideband reference and capture effect antennas (Figures 4K and 4L, respectively) behave similarly, with peak values ranging from -9 to +8 microamperes for the sideband antenna and ranging from -6 to +6 microamperes for the capture effect antenna.

3.5 DROPOFF AND UPGRADE

The next terrain configuration to be discussed is depicted in Figure 5. The terrain consists of 1200 feet of flat ground ending in a 40 foot drop followed by an upgrade rising 58 feet in 1900 feet and finally terminating with 1900 feet of flat ground. This terrain configuration as well as the others previously discussed was suggested to us for study by the FAA. The null reference data are shown in Figures 5A and 5D. The level run flight results (Fig. 5A) show considerable deviation from the ideal. The zero crossing point is shifted by nearly 2000 feet toward touchdown (equivalent to an elevation of the glide path to 3.19°). Course

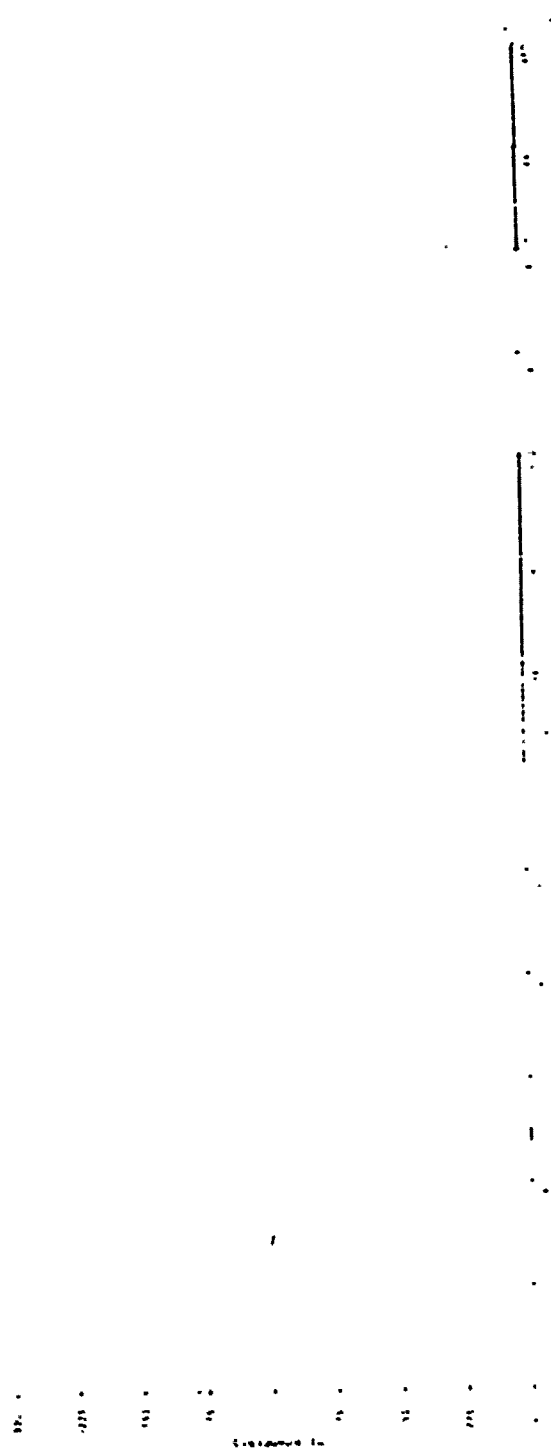


Figure 4G. Adjusted Null Reference Array, Level Run Flight, 20-Foot Dropoff



Figure 4H. Adjusted Sideband Reference Array, Level Run Flight, 20-Foot Dropoff



Figure 41. Adjusted Capture Effect Array, Level Run Flight, 20-Foot Dropoff

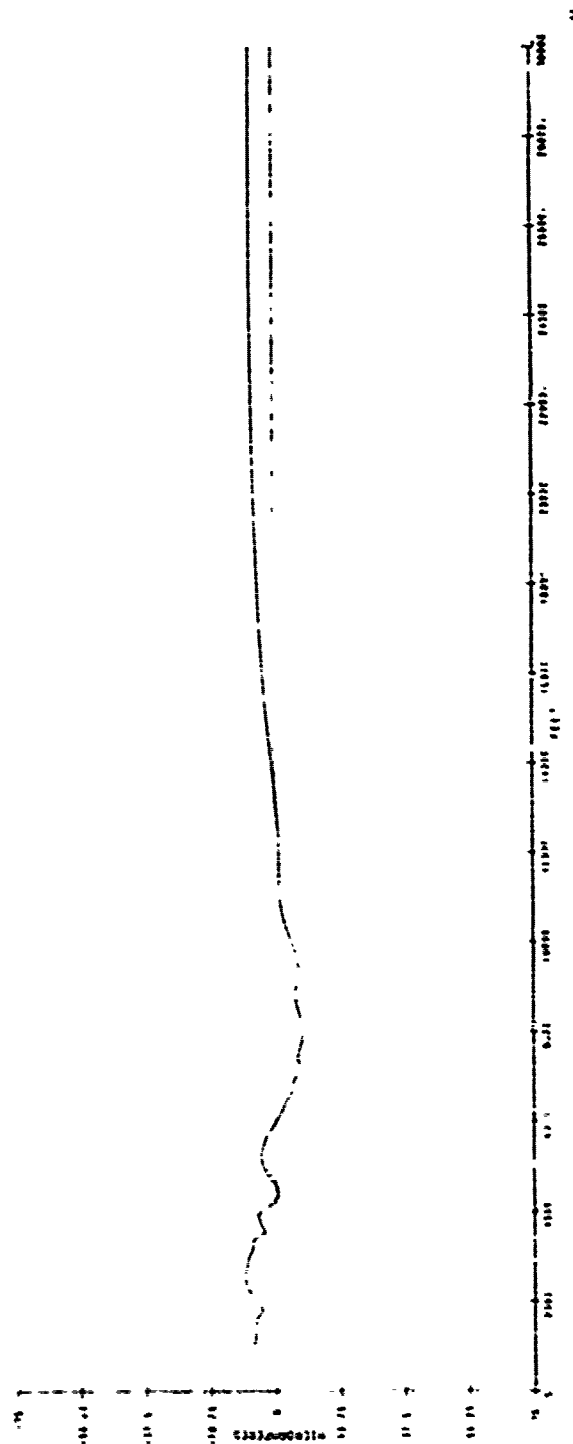


Figure 4K. Adjusted Sideband Reference Array, Flyability Run, 20-Foot Dropoff

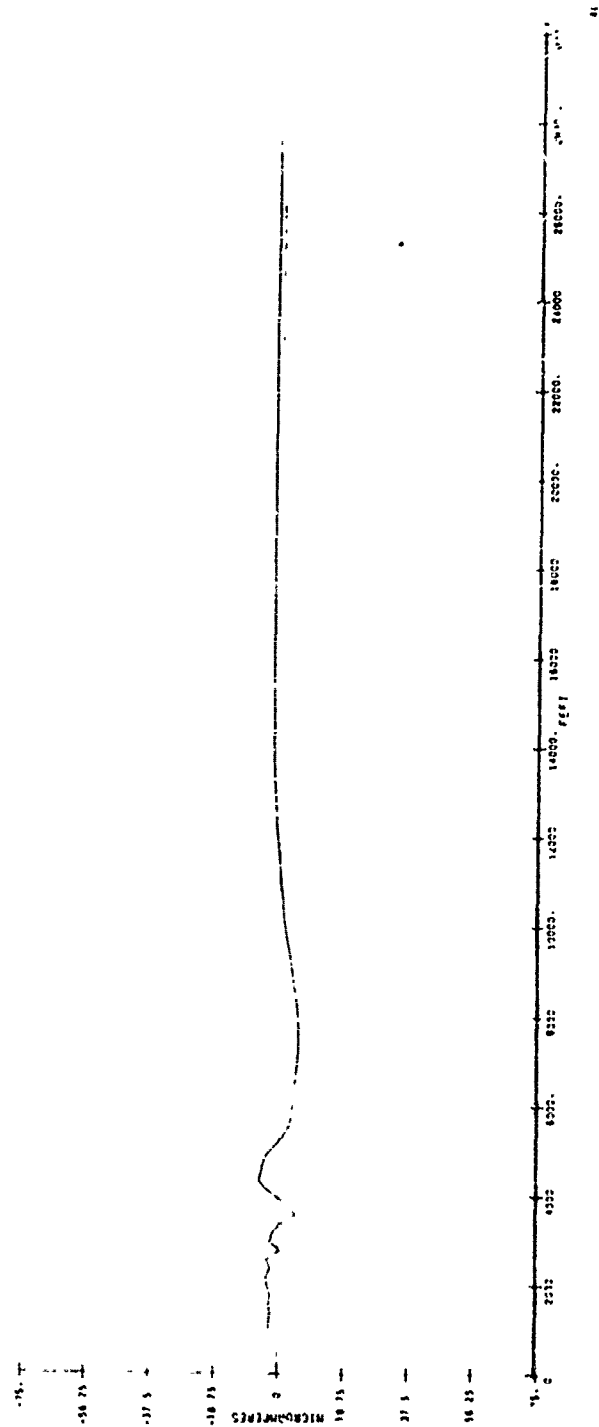


Figure 4L. Adjusted Capture Effect Array, Flyability Kun, 20-Foot Dropoff

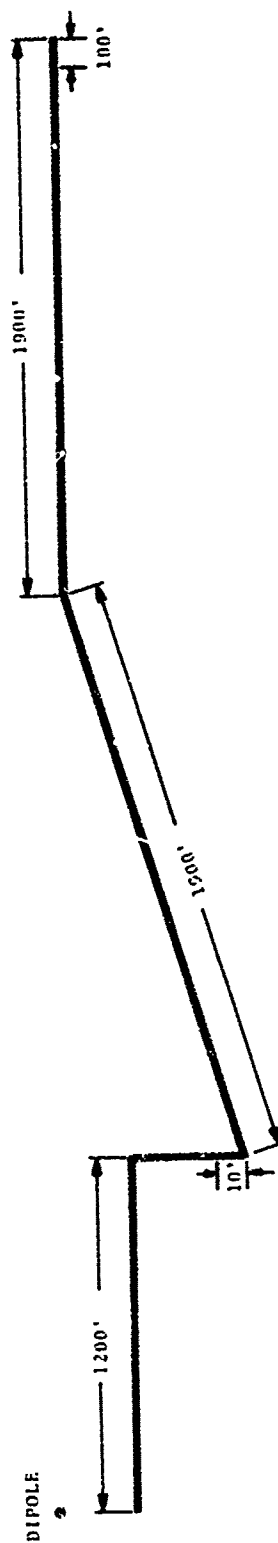


Figure 5. Dropoff and Upgrade

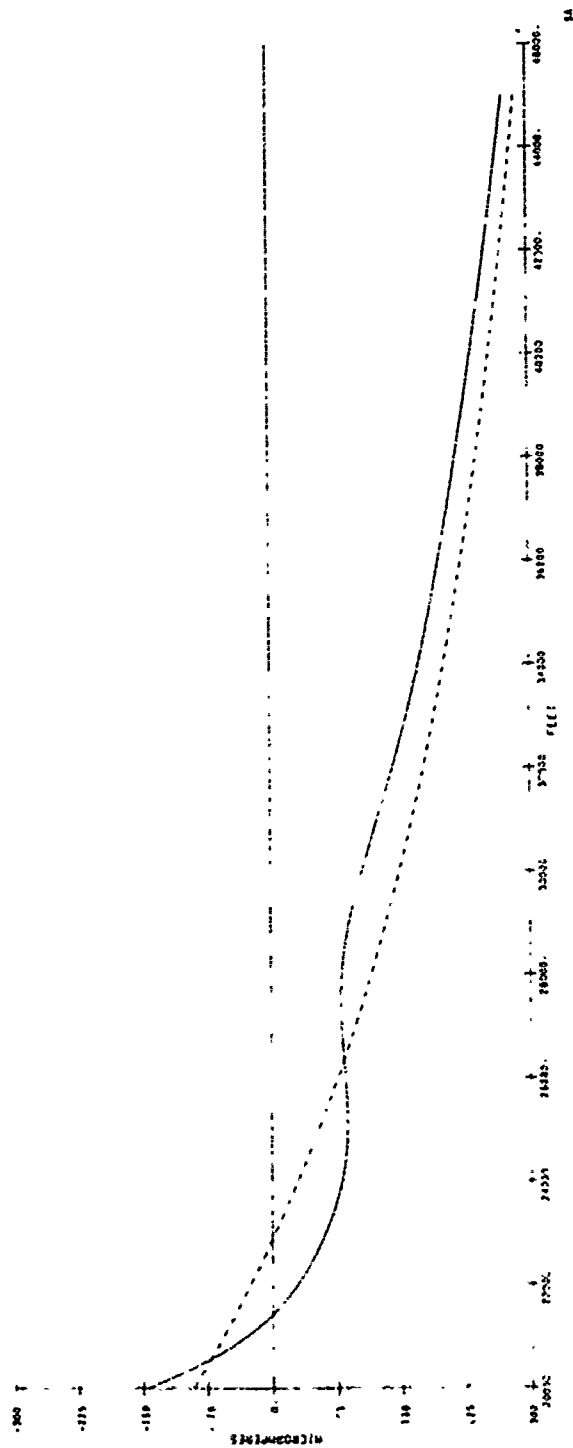


Figure 5A. Null Reference Array, Level Run Flight, Dropoff and Upgrade

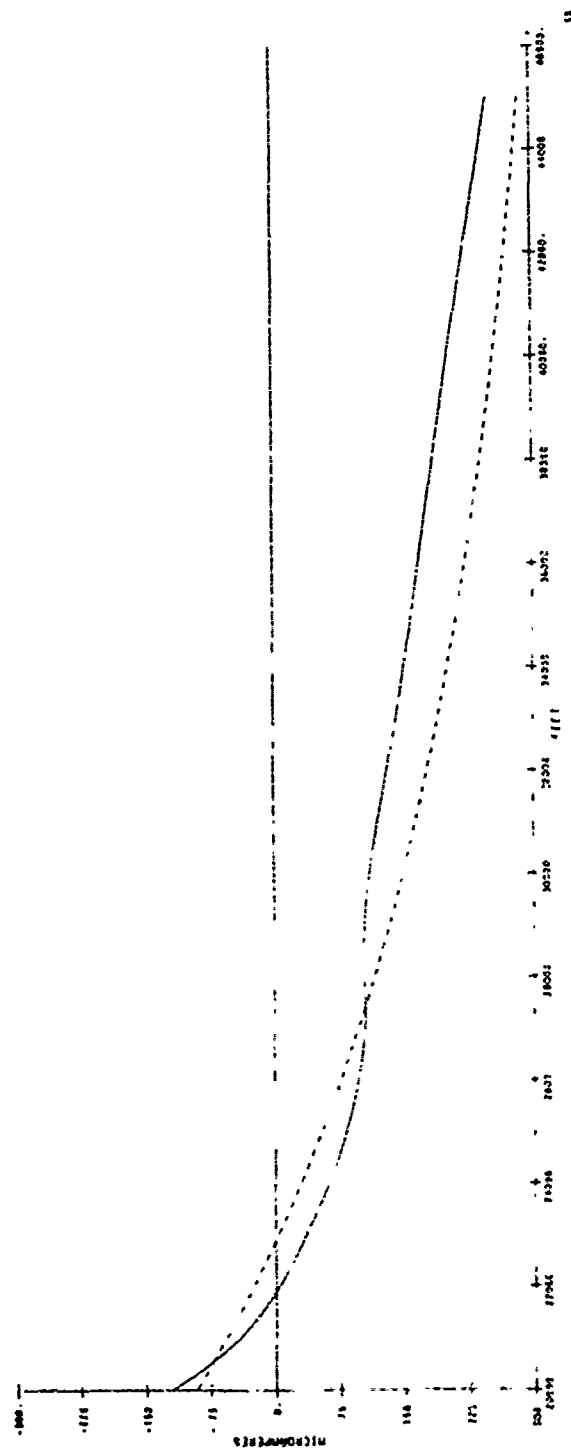


Figure 5B. Sideband Reference Array, Level Run Flight, Dropoff and Upgrade

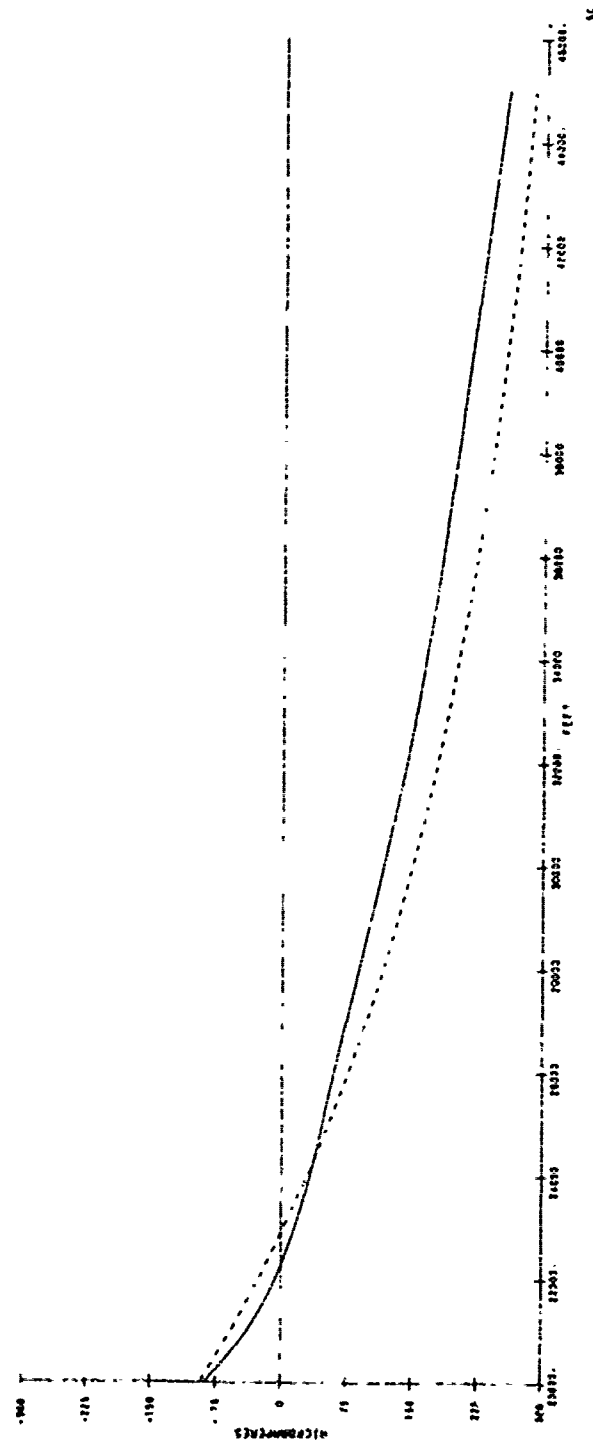


Figure 5C. Capture Effect Array, Level Run Flight, Dropoff and Upgrade

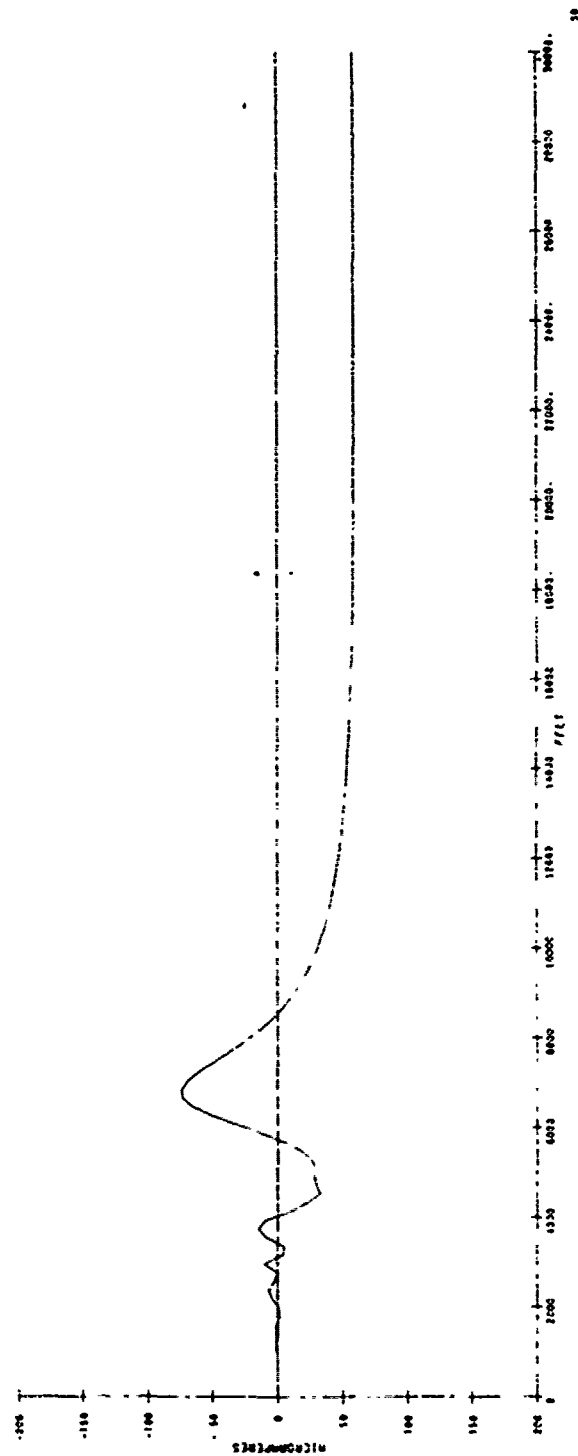


Figure 5D. Null Reference Array, Flyability Run, Dropoff and Upgrade

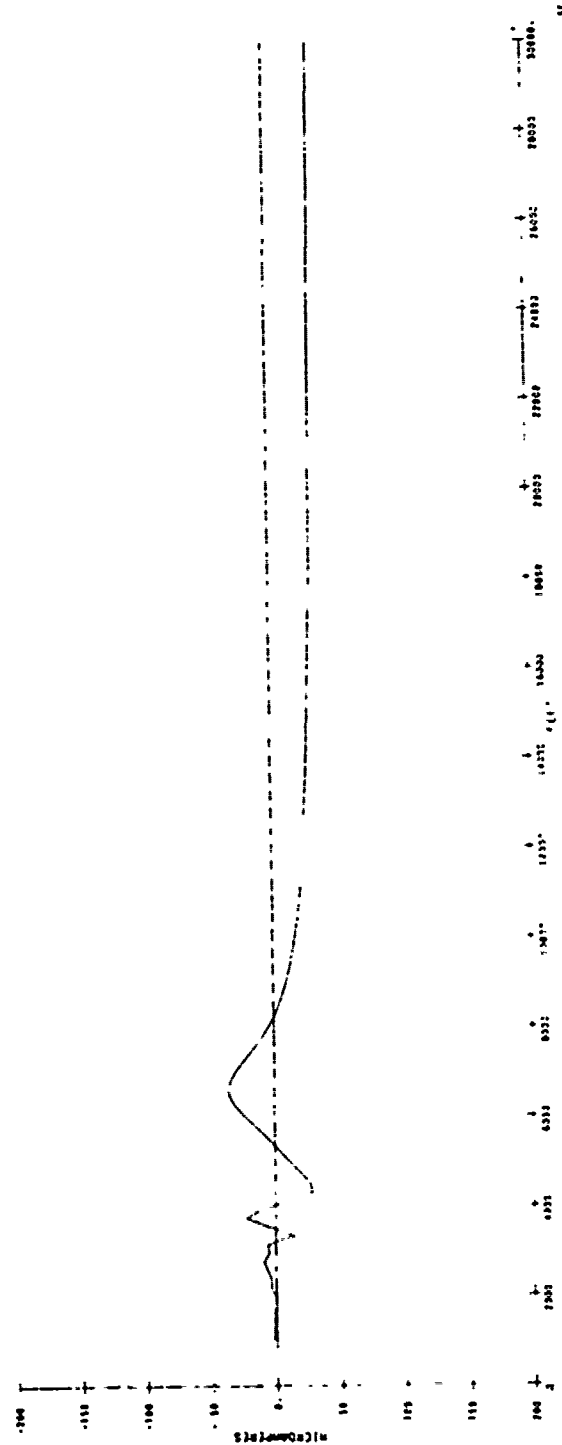


Figure 5E. Sideband Reference Array, Flyability Run, Dropoff and Upgrade

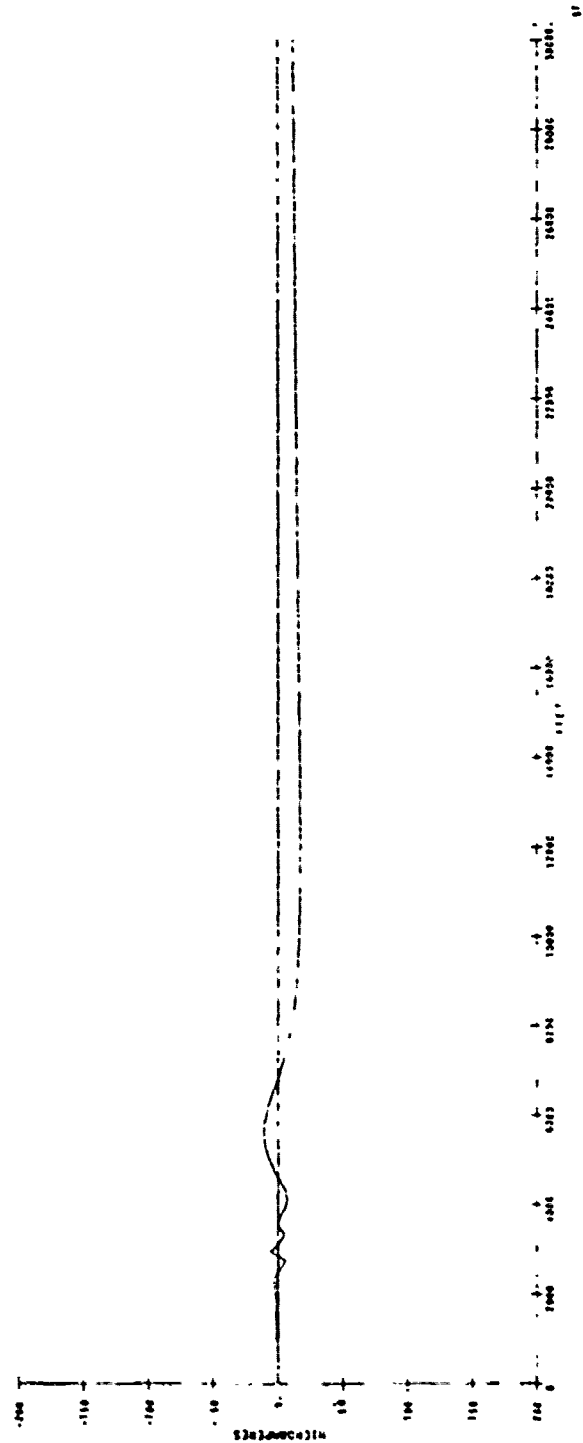


Figure 5F. Capture Effect Array, Flyability Run, Dropoff and Upgrade

linearity is greatly distorted. Note that the curve is almost level from 25,000 feet out to 29,000 feet.

The nominal flyability results (Fig. 5D) reveal a strong fly up indication of about 60 microamperes over much of the course and an even stronger fly down signal at about 7000 feet from touchdown of about -70 microamperes.

The sideband reference results (Figs. 5B and 5E) are qualitatively very similar to the null reference results but, quantitatively, the distortions are not as severe. It will be noted in Figure 5E that the excursions are about ± 35 microamperes in magnitude as compared with 60 and -70 microamperes in the case of the null reference array.

The capture effect results (Figs. 5C and 5F) show the least distortion. In Figure 5C, it can be seen that the zero crossing point undergoes a relatively modest displacement, the nominal glide path results (Fig. 5E) exhibits excursions ranging from -11 to 17 microamperes, a decided improvement over the null reference and sideband reference arrays.

3.5.1 Adjusted Antenna Element Heights

In an attempt to improve the flyability of this course, the antenna element heights were adjusted to give a mean 3° glide path angle over the distance between the middle marker and four miles out. The new antenna element heights are shown in Table 3

TABLE 3.

| | <u>Original Positions (feet)</u> | | | <u>New Positions (feet)</u> | | |
|----------------|----------------------------------|---------------|----------------|-----------------------------|---------------|----------------|
| | <u>Lowest</u> | <u>Middle</u> | <u>Highest</u> | <u>Lowest</u> | <u>Middle</u> | <u>Highest</u> |
| Null Reference | 14.33 | | 28.66 | 15.02 | | 30.04 |
| S.B. Reference | 7.17 | | 21.5 | 7.35 | | 22.04 |
| Capture Effect | 14.33 | 28.66 | 42.99 | 14.59 | 29.18 | 43.77 |

The level flight results with this new positioning are shown in Figures 5G, 5H, and 5I. The flyability results are shown in Figures 5J, 5K, and 5L.

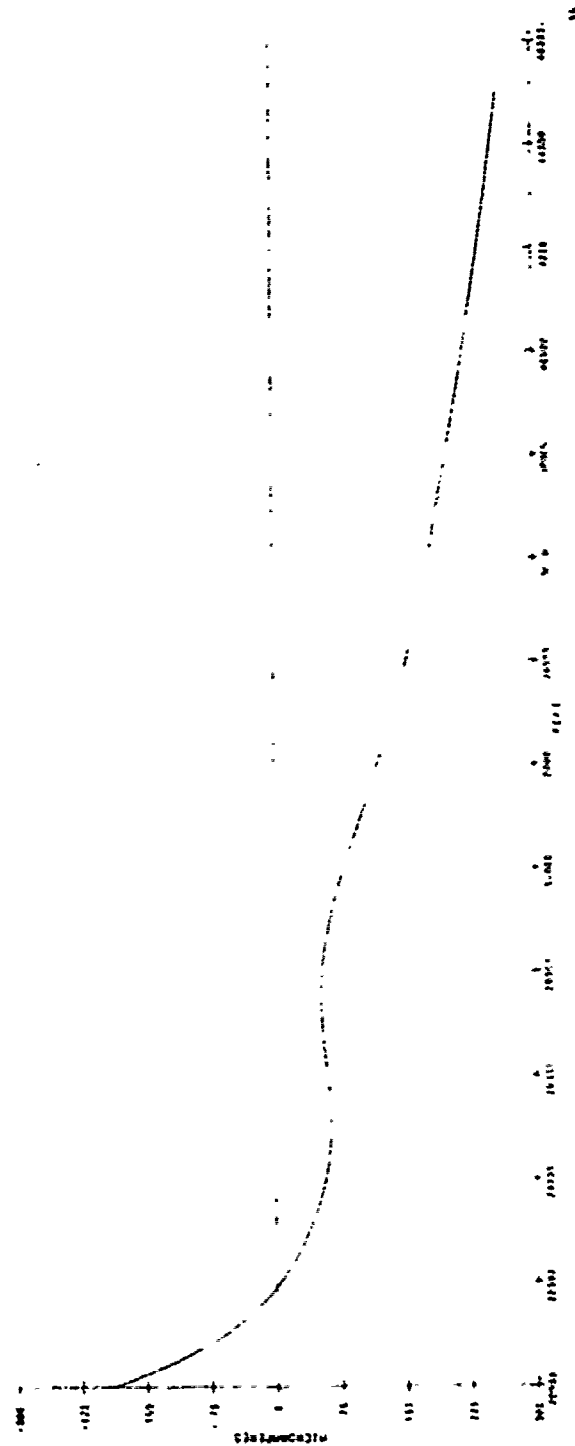


Figure 5G. Adjusted Null Reference Array, Level Run Flight, Dropoff and Upgrade

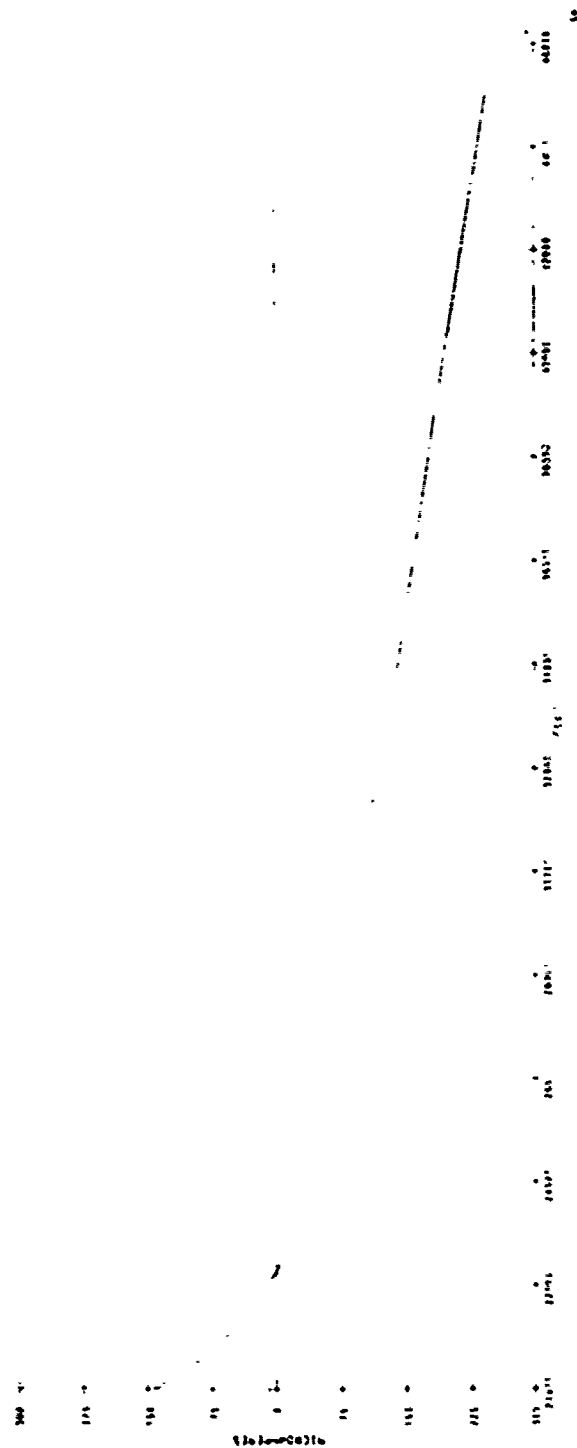


Figure 5H. Adjusted Sideband Reference Array, Level Run Flight, Dropoff and Upgrade

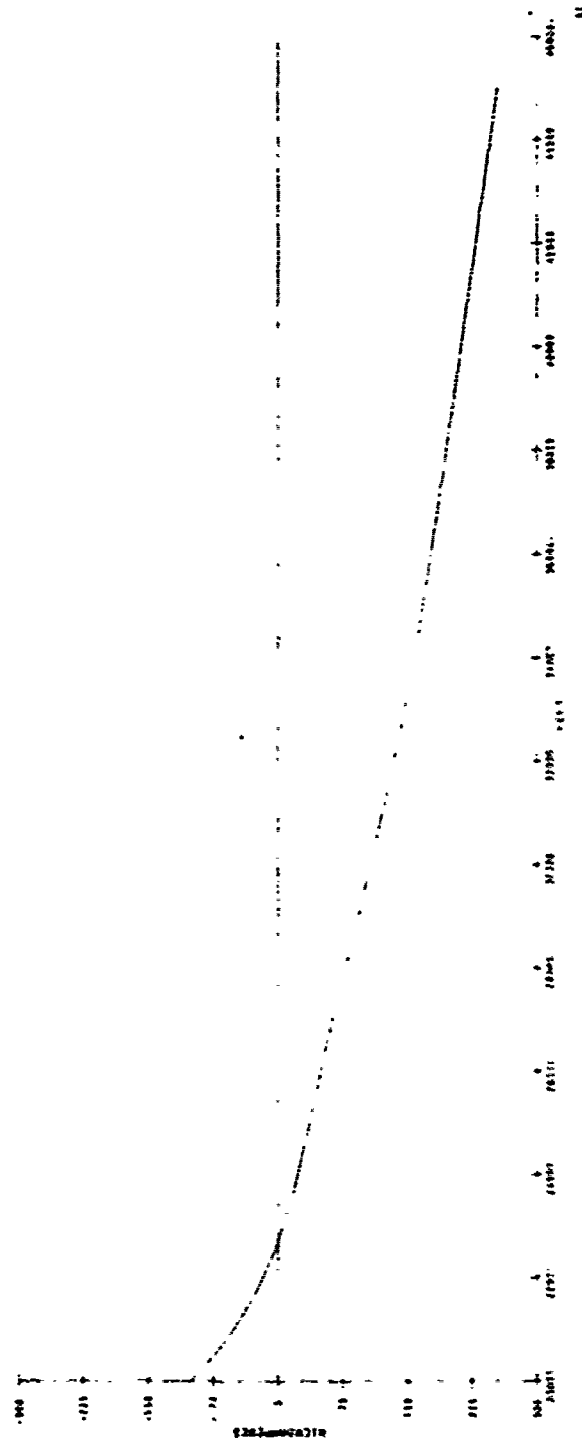


Figure 51. Adjusted Capture Effect Array, Level Run Flight, Dropoff and Upgrade



Figure 5J. Adjusted Null Reference Array, Flyability Run, Dropoff and Upgrade

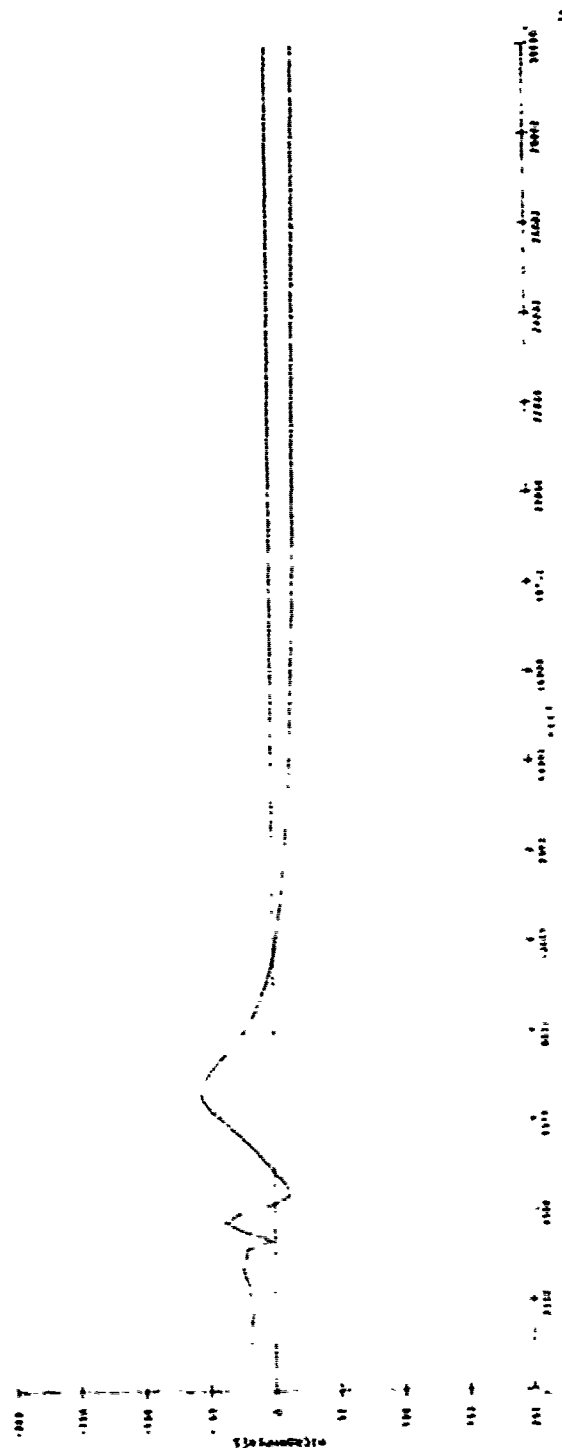


Figure 5K. Adjusted Sideband Reference Array, Flyability Run, Dropoff and Upgrade

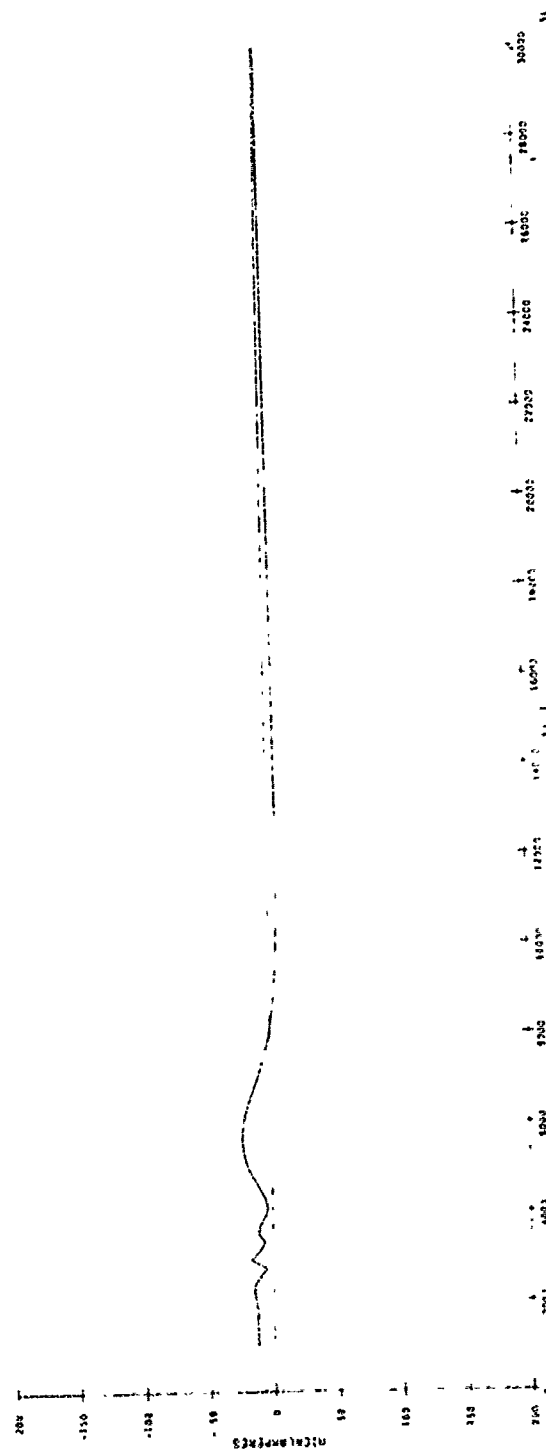


Figure 5L. Adjusted Capture Effect Array, Flyability Run, Dropoff and Upgrade

Re-positioning of the antenna element heights for this type of terrain to obtain a mean 3° glide path angle does not improve the course though the cross overs (Figures 5G, 5H, and 5I) do occur somewhat closer to the required 3° glide angle. As can be seen on comparing Figure 5J, 5K, and 5L with the uncorrected values shown in Figures 5B, 5E, and 5F, the flyability of the course has not improved by this re-positioning. The peak-to-peak values are now -115 to 21 microamperes for the null reference antenna; -57 to 21 microamperes for the sideband reference antenna; and -22 to 7 microamperes for the capture effect antenna. While the fly up indications have in all cases been reduced, the fly down indications have all gone up. This is because the re-positioning of the antenna element heights simply shifts the CDI pattern either up or down. This type of correction is very useful when a uniform shift of the CDI pattern occurs, for example, when the terrain has an up or down slope, as was the case depicted in Figure 3. Adjusting the antenna element heights there for a mean 3° glide path angle shifted the whole pattern back toward zero CDI. However, for the terrain depicted in Figure 5, which produced both up and downward CDI shifts (as shown in Figures 5D, 5E, and 5F), the simple translation of the CDI pattern that was produced by adjusting the antenna element heights for a mean 3° glide path angle, cannot yield zero CDI over the whole course. By reducing the fly up indications, the fly down indications, in fact, became stronger.

We do emphasize again, however, that for this terrain the sideband reference antenna produced a much improved course over the null reference, and that the capture effect antenna a much improved course over the sideband reference antenna.

3.6 UPGRADE, DROPOFF AND UPGRADE

The next terrain configuration to be discussed is depicted in Figure 6. The terrain consists of 1000 feet of ground sloping up at $3/4^\circ$ ending in a 20 foot drop which is then followed by 500 feet of flat ground followed by 3500 feet of ground again sloping up at $3/4^\circ$. The results are shown in Figures 6A, 6B, 6C, 6D, 6E, and 6F.

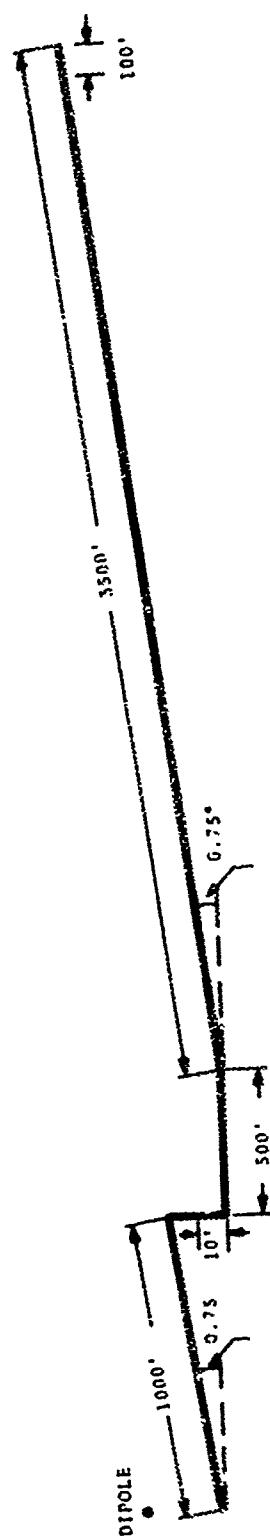


Figure 6. Upgrade, Dropoff and Upgrade

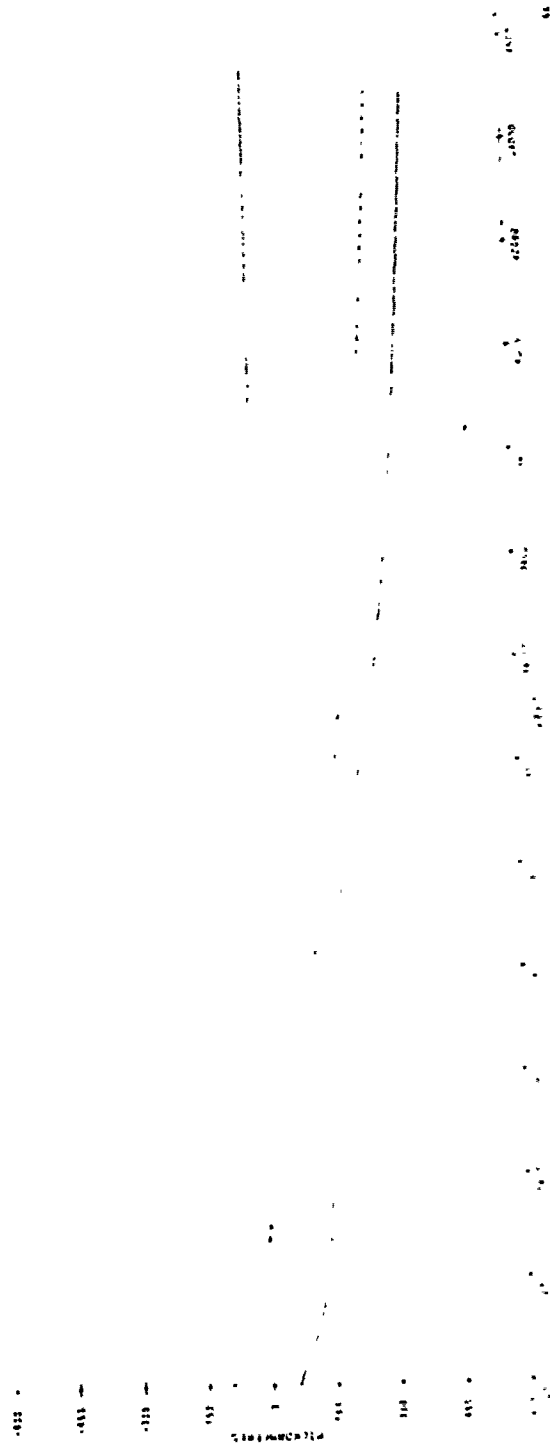


Figure 6A. Null Reference Array, Level Run Flight, Upgrade, Dropoff and Upgrade

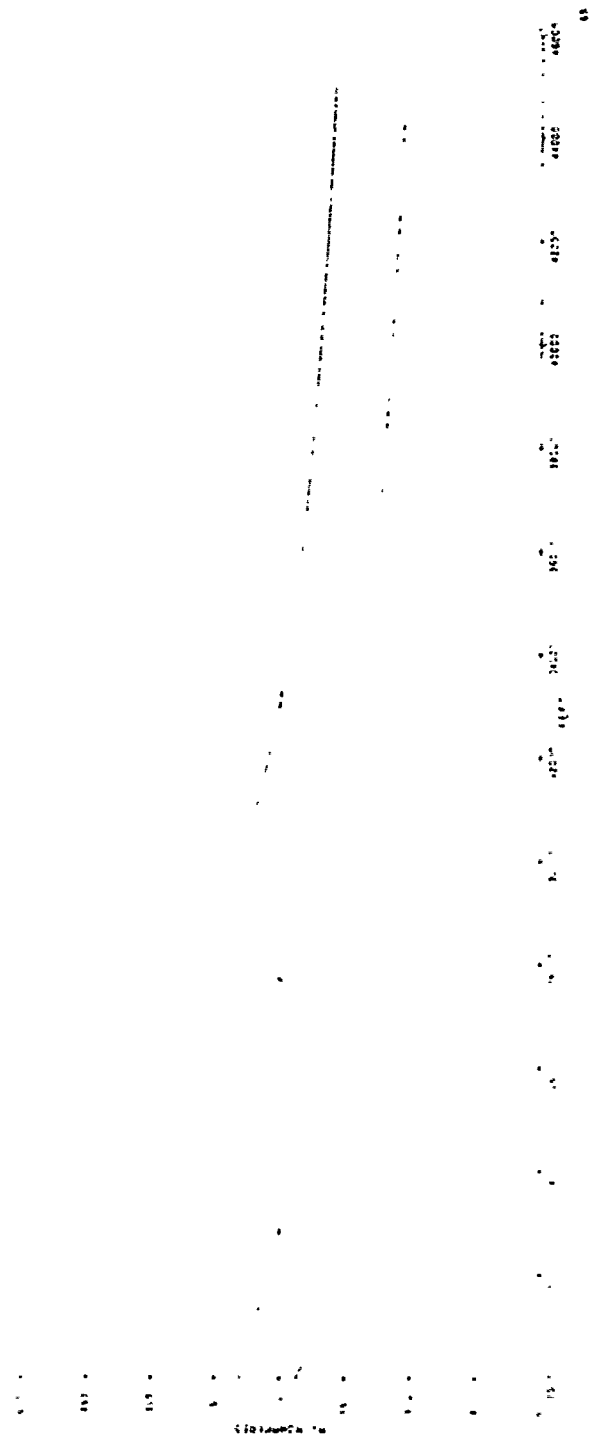


Figure 6B. Sideband Reference Array, Level Run Flight, Upgrade, 'Dropoff and Upgrade

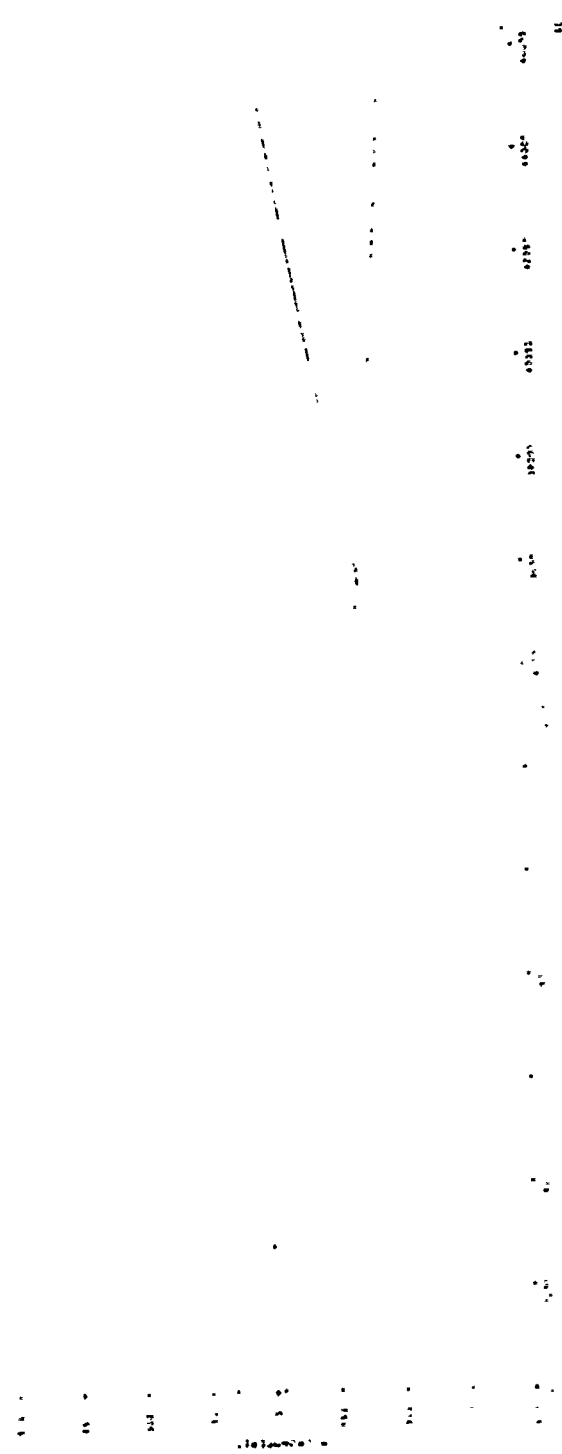


Figure 6C. Capture Effect Array, Level Run Flight, Upgrade, Dropoff and Upgrade

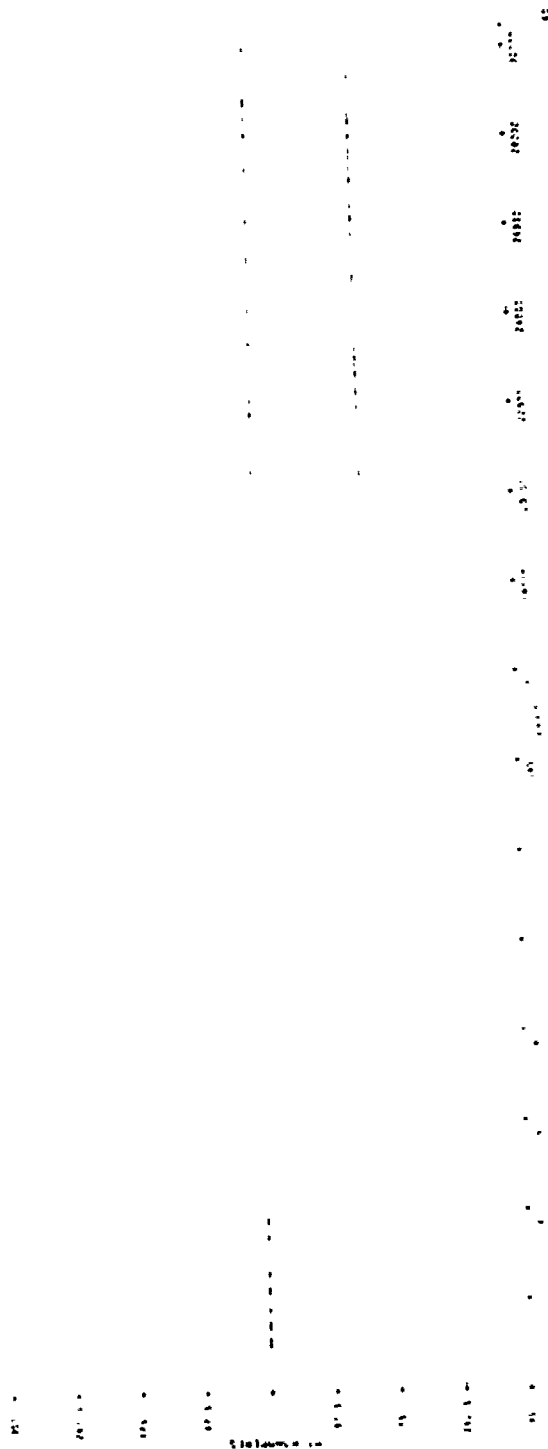


Figure 6D. Null Reference Array. Flyability Run, Upgrade, Dropoff and Upgrade

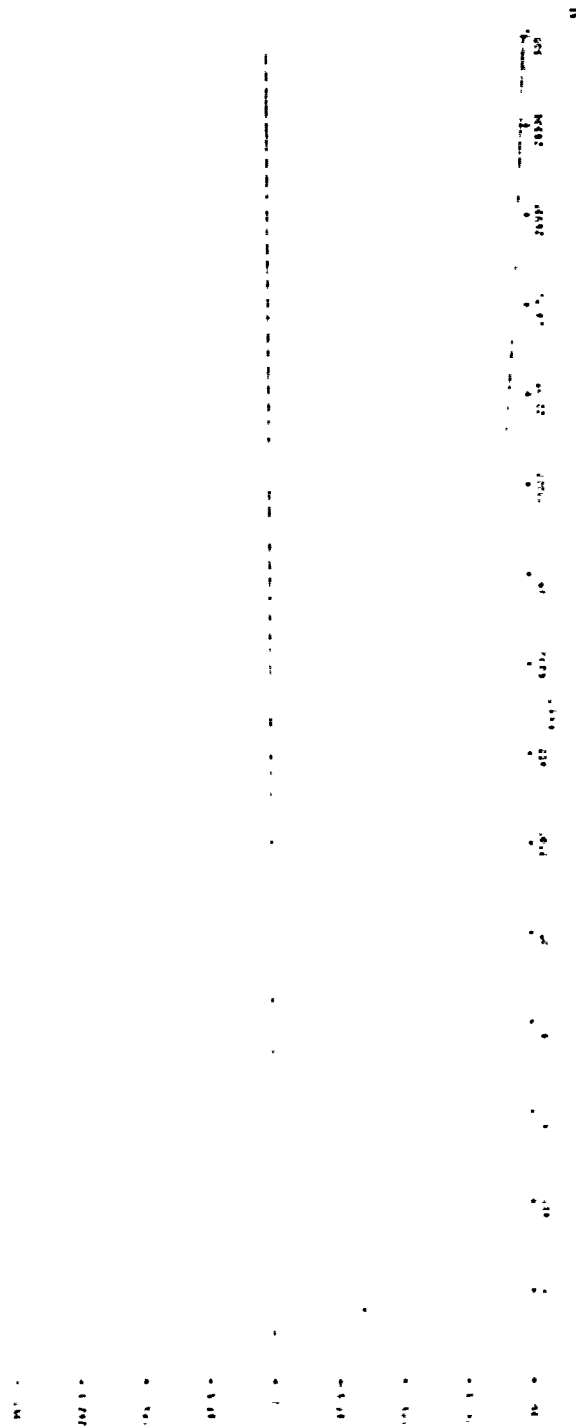


Figure 6E. Sideband Reference Array, Flyability Run, Upgrade, Dropoff and Upgrade



Figure 6F. Capture Effect Array, Flyability Run, Upgrade, Dropoff and Upgrade

Looking at the level flight runs first, Figures 6A, 6B, and 6C, we see that the null reference antenna data exhibits no zero cross over in the range considered (though there is a probable zero cross over at an elevated glide path angle of 3.7° ; in contrast to this the sideband reference antenna has two zero cross overs in the same range, one at about 2.1° and the other at approximately 2.5° (and another probable zero crossover at about 3.7°) to produce a highly non linear distorted course; the capture effect antenna appears to have two zero cross overs one at 1.5° and another at 3.6° .

The flyability results are shown in Figures 6D, 6E, and 6F. The null reference data (Figure 6D) reveals a strong fly up signal of about 155 microamperes which is equivalent to almost $3/4^\circ$, which is just the angle at which the two separate pieces of ground slope upwards (see Figure 6). Clearly, to the null reference antenna, this type of terrain appears as a simple upslope.

Interestingly, the sideband reference results (Figure 6E) for this type of terrain are even poorer than the preceding for the null reference antenna.

The best performance is exhibited by the capture effect antenna whose results are depicted in Figure 6F. There is a fly up signal over the flight path whose peak-to-peak excursions range from 46 microamperes to 90 microamperes, about half that of the null reference antenna. The terrain does not appear as a simple $3/4^\circ$ upslope to the capture effect antenna which would have then produced the same 155 microampere excursion as it did for the null reference antenna (see for example, the results for the simple upslope pictured in Figure 3).

3.6.1 Adjusted Antenna Element Heights

Figures 6G, 6H, 6I, 6J, 6K, and 6L exhibit the results for the terrain of Figure 6 after the antenna element heights have been adjusted to provide a 3° glide path. This 3° glide path angle was determined as the arithmetic mean over the distance between the middle marker and four miles from the threshold. The adjusted heights of the elements are given in Table 4.



Figure 6G. Adjusted Null Reference Array, Level Run Flight, Upgrade, Dropoff and Upgrade



Figure 6H. Adjusted Sideband Reference Array, Level Run Flight, Upgrade, propoff and Upgrade

1000
 800
 600
 400
 200
 0

1000

1000

1000

1000

1000

1000

1000

1000

1000

1000

1000

1000

1000

1000

1000

1000

1000

Figure 61. Adjusted Capture Effect Array, Level Run Flight, Upgrade, Dropoff and Upgrade

Figure 6.1. Adjusted Null Reference Array. Flyability Run, Upgrade
Dropoff and Upgrade

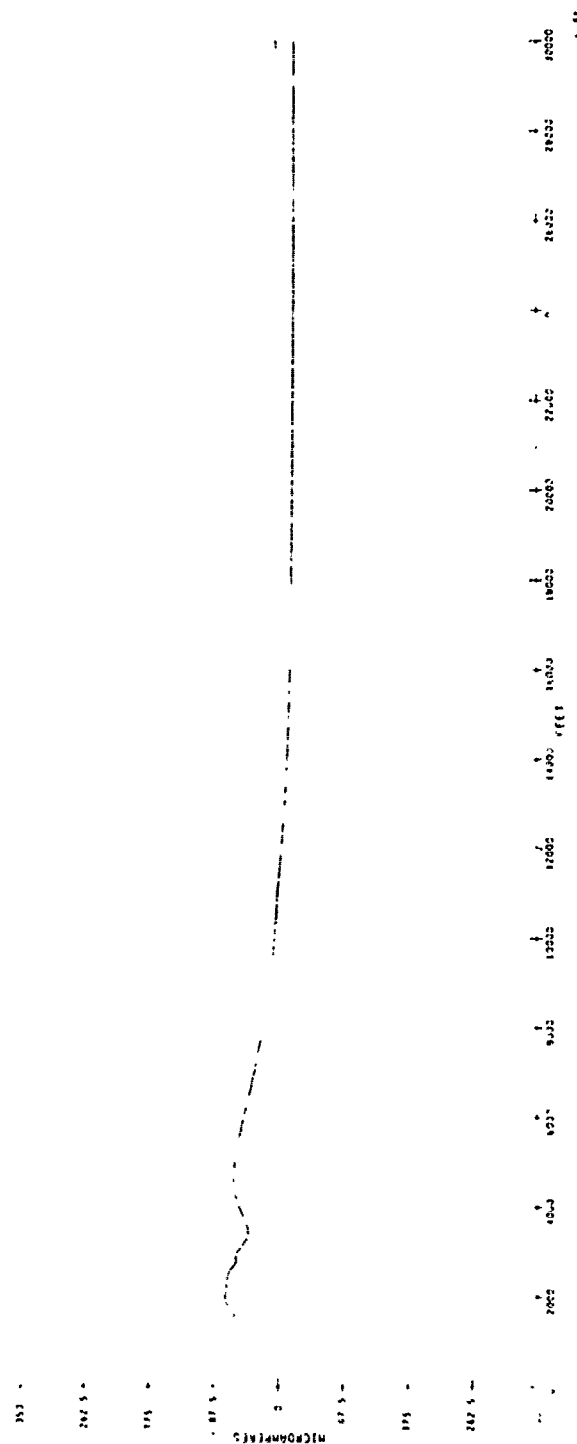


Figure 6K. Adjusted Sideband Reference Array, Flyability Run, Upgrade, Dropoff and Upgrade



Figure 6L. Adjusted Capture Effect Array, Flyability Run, Upgrade, Dropoff and Upgrade

TABLE 4.

| | <u>Original Positions (feet)</u> | | | <u>New Positions (feet)</u> | | |
|----------------|----------------------------------|---------------|----------------|-----------------------------|---------------|----------------|
| | <u>Lowest</u> | <u>Middle</u> | <u>Highest</u> | <u>Lowest</u> | <u>Middle</u> | <u>Highest</u> |
| Null Reference | 14.33 | | 28.66 | 19.28 | | 38.55 |
| S.B. Reference | 7.17 | | 21.5 | 9.87 | | 29.61 |
| Capture Effect | 14.33 | 28.66 | 42.99 | 16.48 | 32.97 | 49.45 |

The level flight results with these re-adjusted antenna element heights are shown in Figures 6G, 6H, and 6I. These level flight results still show considerable deviation from the ideal; with course linearity, in all three cases, distorted, though the null reference antenna data (Figure 6G), does exhibit the correct zero cross over at 3° .

The sideband reference level flight results (Figure 6H) exhibits no less than three zero cross over points within the range considered here (20,000' to 46,000'). Two of these zero crossings (one at about 3° and the other at about 2°) are in the right direction, which therefore could present a serious problem to the pilot. These results indicate that it is possible to fly a zero CDI course at the incorrect glide angle using a sideband reference antenna over this terrain.

The level flight values produced by the capture effect system are shown in Figure 6J. The zero crossing here is at approximately 2.8° .

The flyability of the course has been dramatically improved in all three cases with the new re-positioned antenna element heights. The null reference antenna results, shown in Figure 6J, has excursions between -20 microamperes and +9 microamperes (compared to 155 microamperes before re-positioning). This is considerably better than the sideband reference results (Figure 6K) which could not be corrected to give less than peak-to-peak microampere excursions of -73 to +25, and even somewhat better than the capture effect antenna results (Figure 6L) which show excursions

of between -19 and +25 microamperes after re-positioning of the antenna element heights.

It is interesting that for this type of terrain, consisting of two upslopes and a discontinuity, it has still been possible to correct the null reference antenna to produce results at least as good as those produced by the capture effect antenna. This will be the case, in general, whenever the terrain consists of simple up or downslopes.

3.7 HILL TERRAIN

The final terrain configuration to be discussed is depicted in Figure 7. The terrain consists of 3000 feet of flat terrain followed by an upgrade of 5° extending for another 2000 feet. The null reference data are shown in Figures 7A and 7D. The level flight results (Figure 7A) show a zero crossing point which is shifted about 1000 feet toward touchdown, equivalent to an elevation of the glidepath to 3.12° .

The flyability results (Figure 7D) reveal a strong fly up indication of 67 microamperes over the course from 30,000 feet to about 9000 feet from touchdown. This is followed by several very strong fly down indications, the highest of which occurs approximately 5500 feet from touchdown with a peak value of -182 microamperes.

The sideband reference results are shown in Figures 7B and 7E. The level flight data (Figure 7B) shows a cross over precisely at the 3° glide path angle, though an additional false cross over occurs at 1.6° (about 43,000 feet from touchdown for the 1200 foot high level flight). The flyability data (Figure 7E) reveals an almost distortion-free course until about 18,000 feet from touchdown. However, as the aircraft approaches closer, a gradually increasing fly up signal is received which peaks at 87 microamperes at about 8500 feet from touchdown. This is followed by even stronger fly down signals, the largest of which peaks at -165 microamperes about 5500 feet from touchdown.

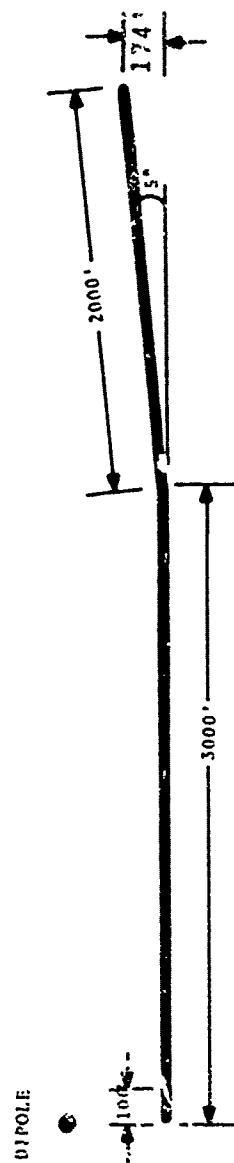


Figure 7. Hill (5° Upgrade)

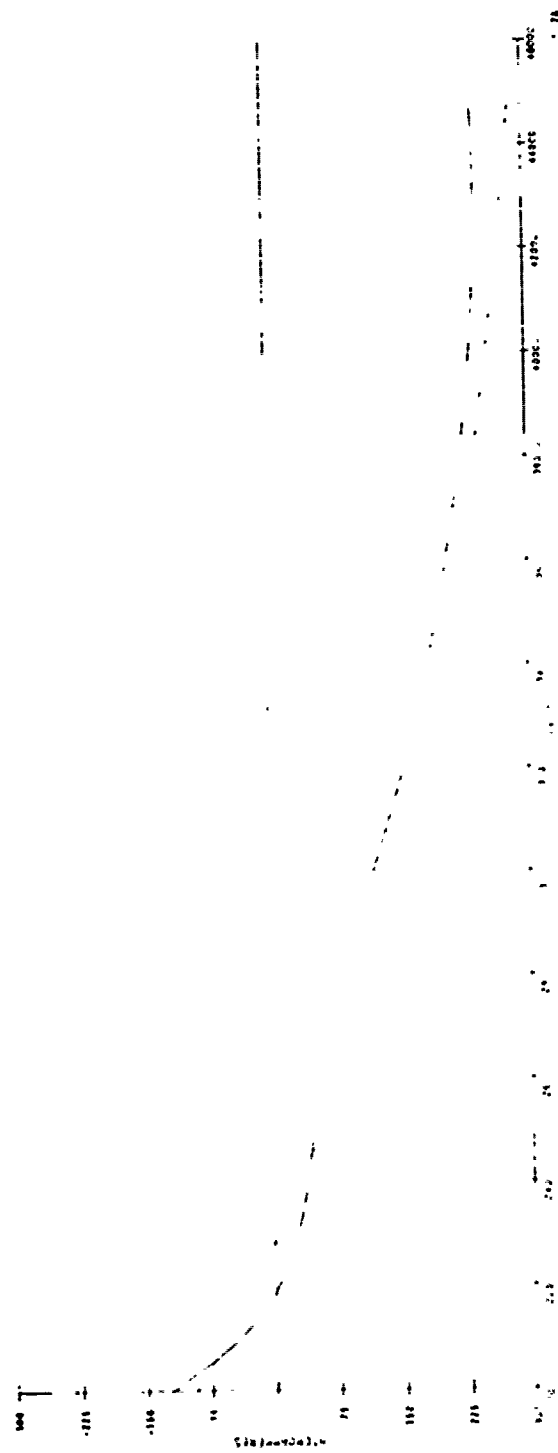


Figure 7A. Null Reference Array, Level Run Flight, Hill



Figure 7B. Sideband Reference Array, Level Run Flight, Hill



Figure 7C. Capture Effect Array, Level Run Flight, Hill

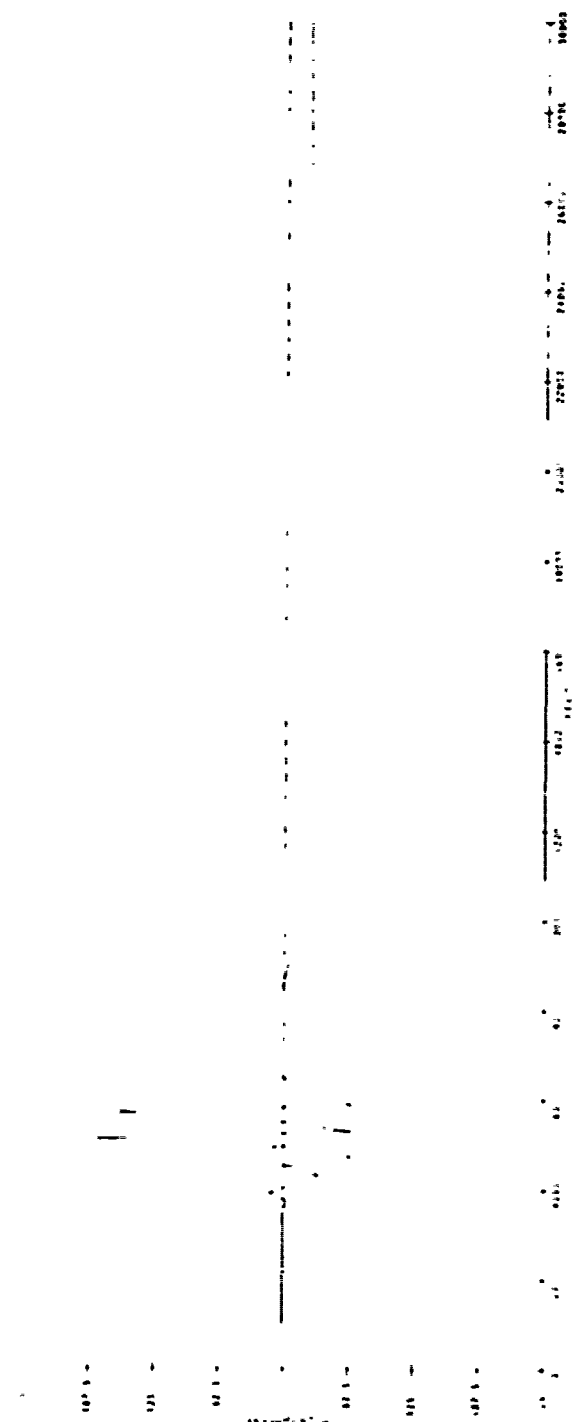


Figure 7D. Null Reference Array, Flyability Run, Hill

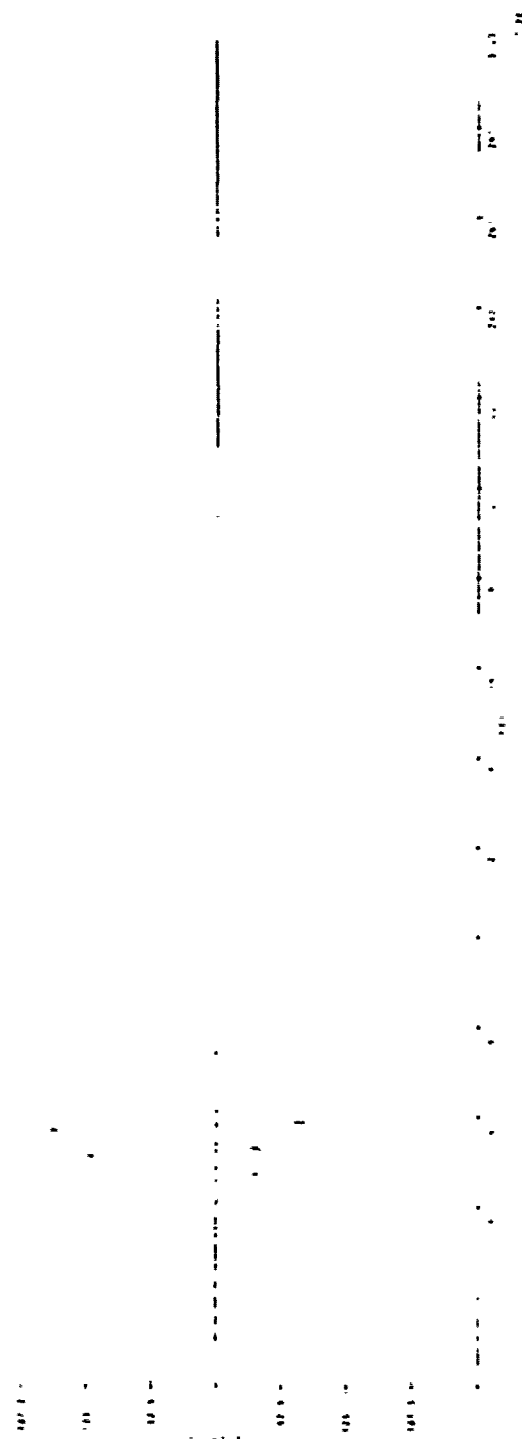


Figure 7E. Sideband Reference Array, Flyability Run, Hill

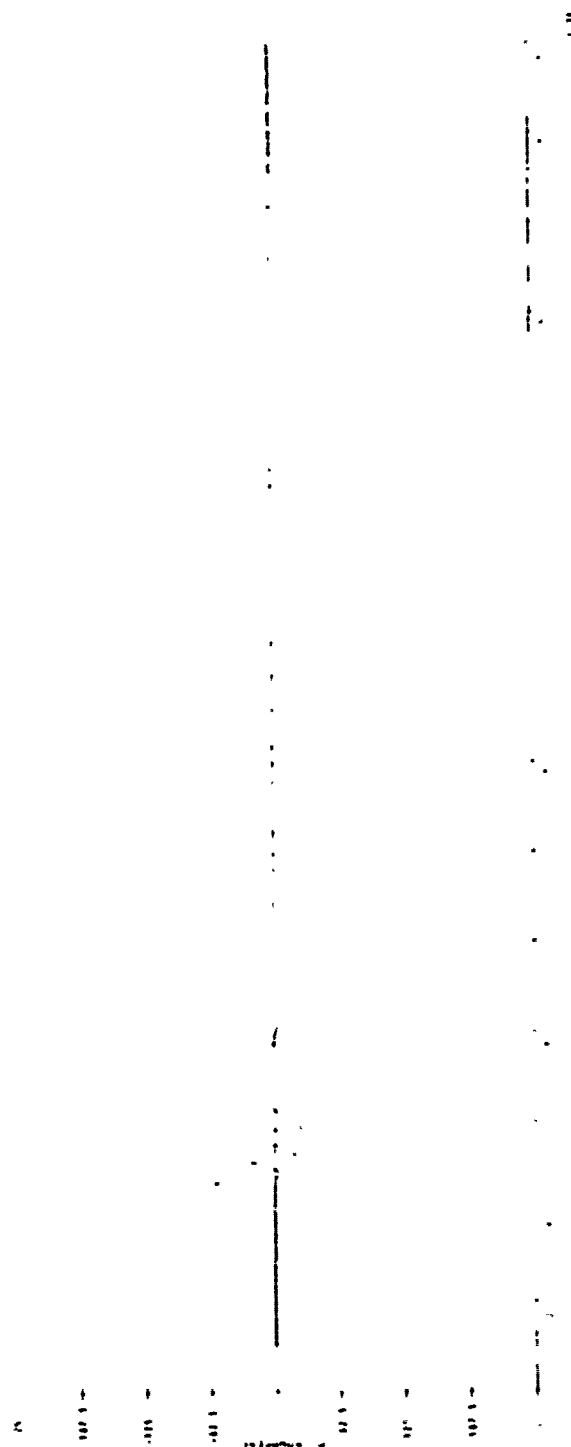


Figure 7F. Capture Effect Array, Flyability Run, Hill

The capture effect antenna system results are shown in Figures 7C and 7F. The level flight data (Figure 7C) exhibits a zero cross over which is very nearly at the correct 3° glide path angle, though here too, as in the sideband reference data, there appears to be a false cross over (at about 1.46°). The nominal glide path results (Figure 7F) show that the capture effect antenna system offers a decided improvement over the two previous antenna systems. There is a near zero CDI over most of the course, never exceeding 27 microamperes, from 30,000 feet until 8000 feet from touchdown. This mild fly up signal is followed by several fly down signals which, however, never exceed -45 microamperes (which is only about a quarter that of the other two systems). Clearly, for this type of terrain, characterized by flat ground followed by a mildly steep hill, only the capture effect system can produce an acceptable course structure. This is true even after the antenna element heights are adjusted to form a mean 3° glide path angle.

3.7.1 Adjusted Antenna Element Heights

This mean glide path angle was formed by re-positioning the antenna element heights as shown in Table 5:

TABLE 5.

| | <u>Original Positions (feet)</u> | | | <u>New Positions (feet)</u> | | |
|----------------|----------------------------------|---------------|----------------|-----------------------------|---------------|----------------|
| | <u>Lowest</u> | <u>Middle</u> | <u>Highest</u> | <u>Lowest</u> | <u>Middle</u> | <u>Highest</u> |
| Null Reference | 14.33 | | 28.66 | 14.64 | | 29.28 |
| S.B. Reference | 7.17 | | 21.5 | 7.22 | | 21.7 |
| Capture Effect | 14.33 | 28.66 | 42.99 | 14.35 | 28.71 | 43.07 |

The results with this re-positioning of the antenna element heights are shown in Figures 7G, 7H, 7I, 7J, 7K, and 7L. The level flight data, Figures 7G, 7H, and 7I, are similar to the previous level flight data, which was to be expected with the modest change in the antenna element heights needed to obtain a mean 3° glide path angle.

"
"
"
"
"
"
"
"
"

"
"
"
"
"
"
"
"
"

Figure 7G. Adjusted Null Reference Array, Level Run Flight, Hill

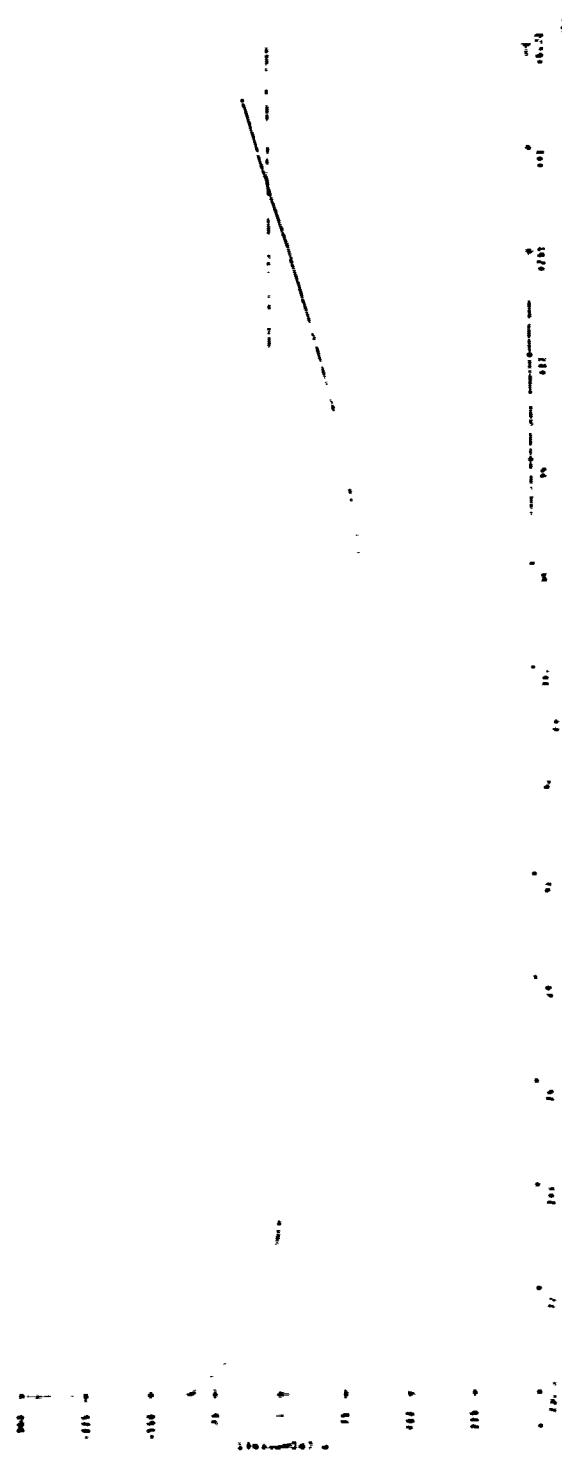


Figure 7H. Adjusted Sideband Reference Array, Level Run Flight, H11

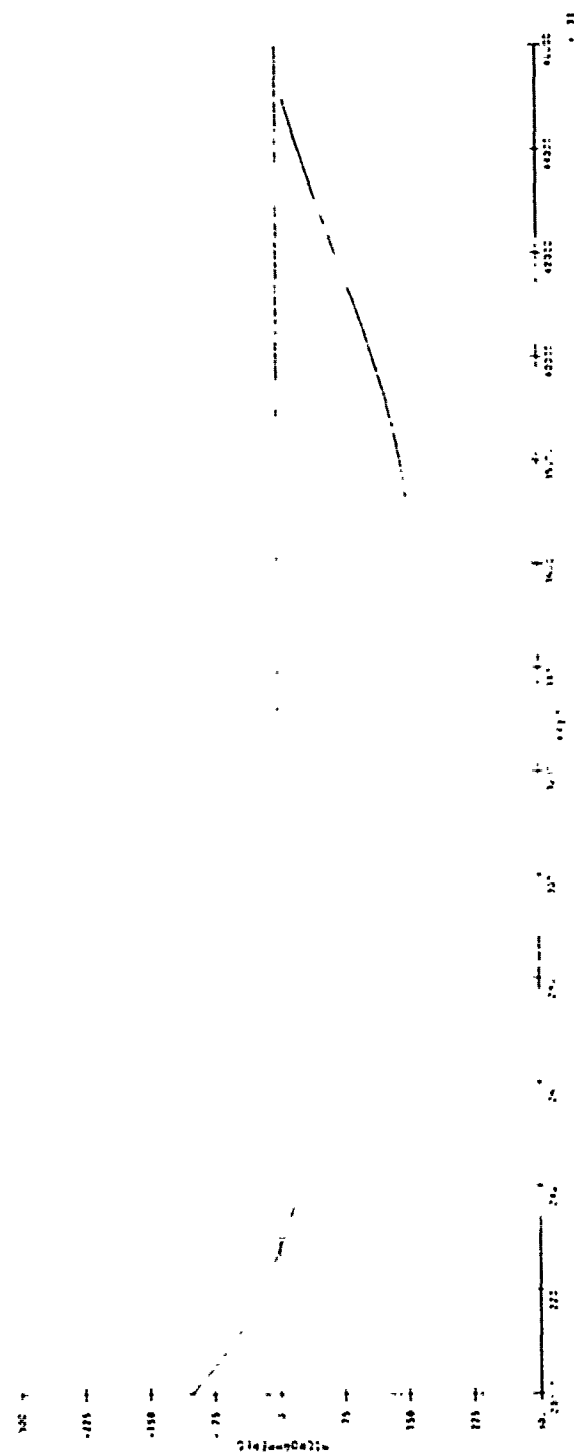


Figure 71. Adjusted Capture Effect Array, Level Run Flight, Hill

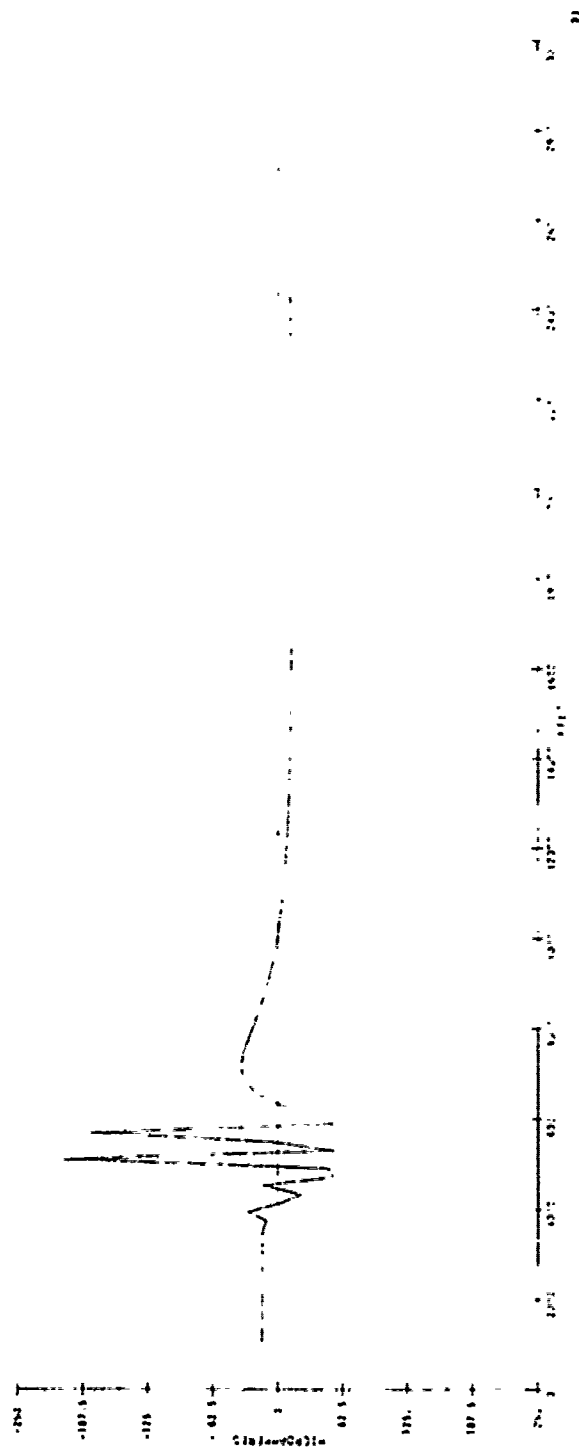


Figure 7J. Adjusted Null Reference Array, Flyability Run, Hill

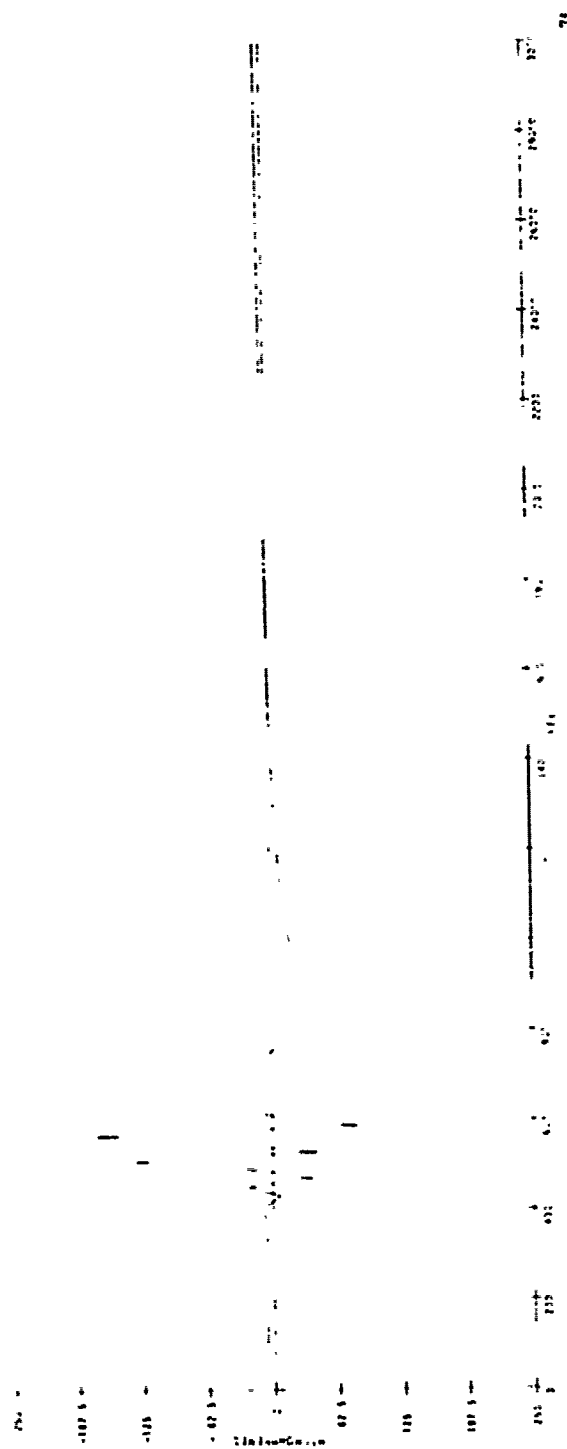


Figure 7K. Adjusted Sideband Reference Array, Flyability Run, Hill

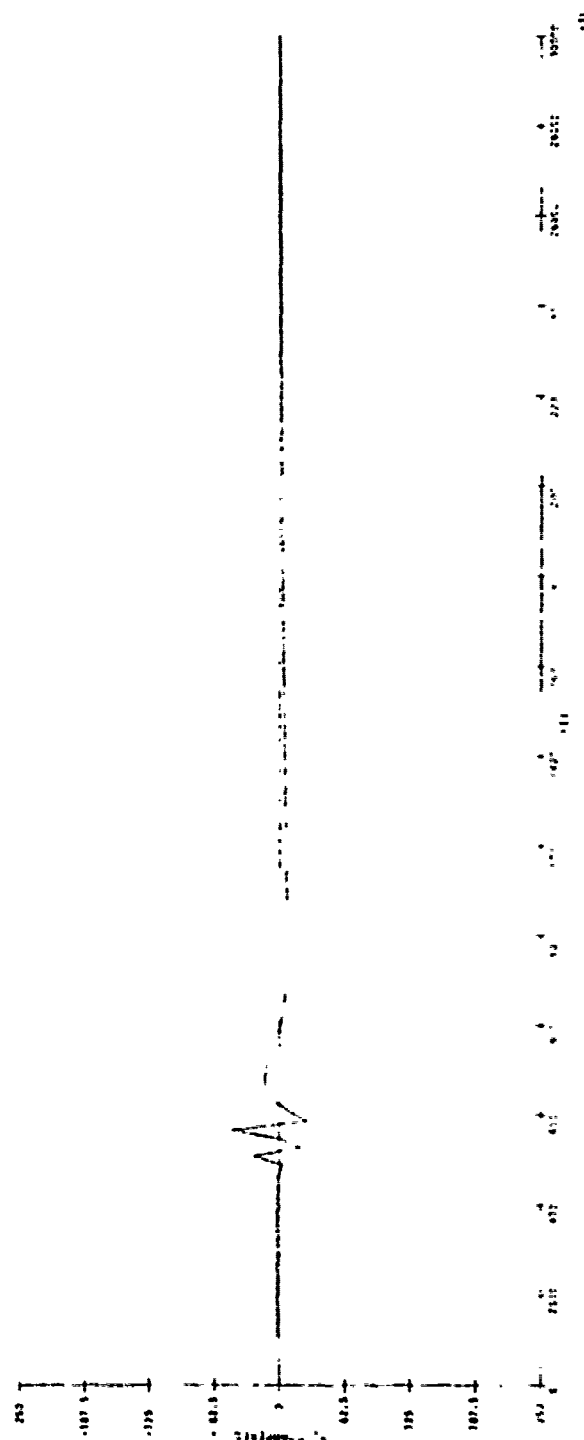


Figure 7L. Adjusted Capture Effect Array, Flyability Run, Hill

The flyability data are shown in Figures 7J, 7K, and 7L. With the null reference antenna (Figure 7J) there is less of a fly up indication after antenna adjustment than before (an almost uniform 56 microamperes as compared to 67 microamperes before the re-positioning) but larger fly down peaks (-208 microamperes as compared to -182 microamperes). Similarly, for the sideband reference antenna: the fly up signal decreased from a maximum of 87 microamperes to a maximum of 82 microamperes, but the fly down signal increased from -165 microamperes to -171 microamperes maximum. The course structure using the capture effect system remains essentially the same as before re-positioning.

As also found for the case of the terrain depicted in Figure 5, a simple re-positioning of the antenna element heights to obtain a mean 3° glide path angle over the distance between the middle marker and four miles out does not improve the course structure for the terrain of Figure 7. As before, here too, the original course structure showed both fly up and fly down excursions. In correcting the one, the other becomes worse. The only system capable of producing an acceptable course structure for this "hill" type terrain is the capture effect system.

PART II. USER'S MANUAL*

1. INTRODUCTION: DEFINITION OF INSTRUMENT LANDING SYSTEM

The ILSGLD program has been written to simulate certain terrain conditions which affect the glide slope portion of the Instrument Landing System. The ILS is used to provide signals for the safe navigation of landing aircraft during periods of low cloud cover and other conditions of restricted visual range. Separate systems are used to communicate vertical and horizontal information; the vertical system is called the "glide slope".

This system operates by the transmission of an RF carrier, amplitude modulated by two audio frequencies, beamed to approaching airborne receivers. In an instrumented aircraft, the glide slope receiver serves to demodulate the RF signal, amplify and isolate the corresponding audio signals and derive a signal to drive the ILS vertical display in the cockpit. The pilot, by reading the display, can determine if he is on course, above or below the glide path. These signals must be strong enough to cover a radius of 15 miles around the antenna.

The directional information is determined by the relative strengths of the transmitted sideband signals. The audio frequency modulations, which are fixed at 90 Hz and 150 Hz, are radiated in different angular patterns with respect to the intended glidepath. The "course" is defined as the locus of points where the amplitudes of the two modulations are equal. The display of a difference of the amplitudes (90 Hz and 150 Hz) of the sidebands is referred to as the Course Deviation Indication. Thus, the CDI is the pilot's indication as to what his altitude is relative to the glidepath. The CDI is measured in microamps. The actual course generated by any particular ILS installation will deviate from the ideal due to irregularities in the terrain. The deviation of the CDI, caused by these irregularities, from the ideal receiver reading at that point in space (e.g., on the glidepath a CDI reading other than 0) is the derogation effect.

*Part II is in actuality Section 4 of the report; accordingly, Chapters 1-5, Part II, are paginated as 4-1 through 4-16.

The glide slope system transmits an asymmetrical pattern by beaming a "carrier plus sideband" pattern and a "sideband only" pattern, the composite of which gives the desired effect.

2. ANTENNA PATTERNS

The proper angular variation of the transmitted 90 Hz and the 150 Hz modulation is achieved by the radiation of the two independent sideband patterns by the transmitting antennae. One pattern, the "carrier plus sidebands" (C+S) signal, is radiated in a symmetrical pattern; the other pattern, the "sidebands-only" (SO) signal, is radiated in an "anti-symmetrical" pattern relative to the prescribed glide angle (see Figure 8.)

The C+S signal is composed of a carrier wave and paired sideband waves at 90 Hz and 150 Hz. The sideband amplitudes are equal and represent a 40% modulation of the carrier wave (or a "depth of modulation" of 0.4) at both frequencies. The SO wave is a carrier wave that is equally modulated at 90 Hz and 150 Hz to the extent that it retains no pure carrier component.

The spatial modulation pattern obtained by combining the symmetrical C+S pattern with the "anti-symmetrical" SO pattern is illustrated in Figure 8. At a given receiver point the total signal is the C+S carrier plus the combined sideband amplitudes of the C+S and SO patterns. The sideband amplitudes are phased so that above the glide path the 90 Hz amplitudes add and the 150 Hz amplitudes subtract, while below the glide path, the 90 Hz amplitudes subtract and the 150 Hz amplitudes add.

Any angular deviation of the airplane's receiver from the correct course results in a "Difference in Depth of Modulation" (DDM) between the 150 Hz and 90 Hz signals. Since the strength of C+S and SO signals fall off at the same rate with distance from the transmitting antenna, the DDM is independent of range.

The antenna patterns are generated by using arrays of one or more elements in combination with the ground as reflector. The effect of an ideal ground plane on a single element is as though there was an "image" element located below the ground and radiating equal power to the real element but with opposite phase. In a glide slope array there will be two or more elements radiating different signals to give the desired combined antenna pattern.

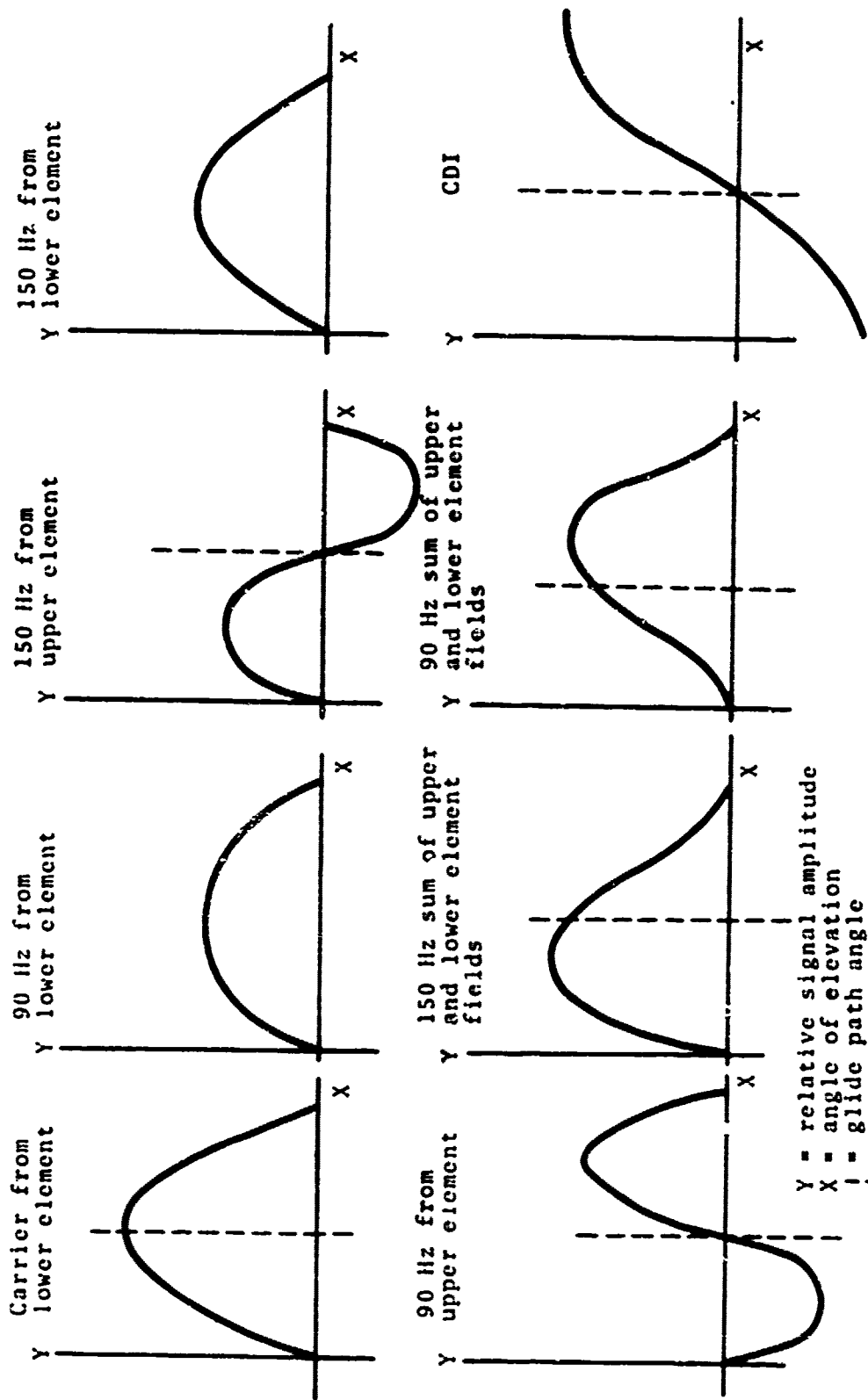


Figure 8. Antenna Patterns for Null Reference Antenna

(Note that this means that a glide slope array is defined by giving, for each element, its location and complex amplitude of the carrier and sidebands.) However, the real ground is not an ideal plane. This has the effect of distorting the element patterns and results in a derogation of the glide slope system performance.

3. SIMULATION DESCRIPTION OF ILSGLD

The ILSGLD simulation program allows the user to study the effects of various ground shapes and antenna types. Using this program, the user may determine what antenna systems will give acceptable performance with a particular ground configuration or what ground shapes cause problems with various antennae.

The program uses a ground description, an antenna description, and a set of spatial coordinates of the receiver location as input. The program calculates and outputs for each receiver location, the CDI at that point both from the "real" ground and from an "ideal" (perfectly conducting and flat) ground plane. In addition, the effects of the electrical and mechanical inertia are included and "dynamic CDI's" are also output for both cases.

The inputs for ILSGLD are data files prepared by the program FMAKE. The outputs from ILSGLD are in data files which are used as input to a third program GLDPLT. GLDPLT produces graphical outputs of the various CDI's. The description and usage of these programs are described in succeeding sections.

The ILSGLD simulation makes certain simplifying assumptions. These include:

- a. perfectly reflecting ground surface
- b. far field scattering - all scattering from points on the ground surface is assumed independent of all other points, thus multiple reflections and near field interactions are ignored
- c. noise free environment
- d. relative field strengths - the absolute field strengths involved are not calculated. Thus, while the CDI's can be calculated in microamperes, the absolute electric field intensities are not ascertained
- e. idealized receiver model
- f. geometrical shadowing - the shadowing of one portion of

the ground on another is done by straight ray approximations assuming a total cutoff with no diffraction.

g. antenna elements are assumed to be simple dipoles.

3.1 METHOD OF SIMULATION

An antenna element is described by giving its x-, y- and z-coordinates and the complex amplitudes of its radiated amplitude at the three frequencies (carrier, 150 Hz, and 90 Hz sidebands). The ground is broken up into strips; these strips have an infinite width and a finite length. The infinite extent is parallel to the y-axis, that is at a right angle to the runway centerline. Thus, a ground strip is described by giving the x- and z-coordinates of the leading and trailing edges of the strip. A receiver location is described by giving its time, x-, y- and z-coordinates.

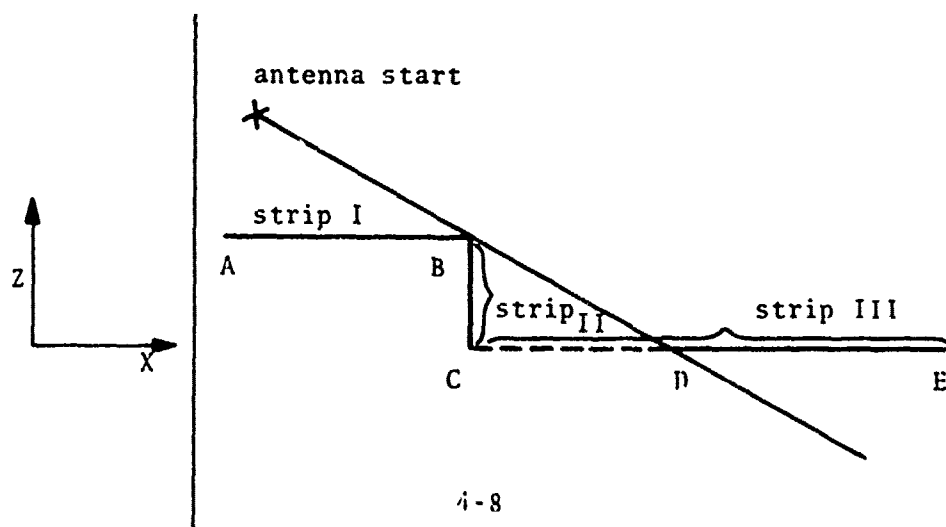
The basic part of the simulation consists of calculating the field at a receiver location. This field is caused by the power radiated from an element and reflected from a strip. A detailed description of the method of calculation has been given previously (Part I). The receiver field can be expressed as a complex gain factor times the radiated antenna field. This gain factor is expressed as a double integral over the strip. The integration along the infinite extent (y-axis direction) was approximated by using the stationary phase method. The resulting single integral is solved by a modified trapezoid rule. The trapezoid rule is used with the spacing between sample points adjusted for the derivative of the integrand.

Thus, for a given receiver location, the program takes an antenna element and calculates the "gain factor" for each ground strip, multiplies by the radiated power, and sums the three complex field intensities for all ground strips. The direct field of the element at the receiver is then added. This process is repeated for all elements, giving the total field at the receiver. Using an idealized receiver model the voltages at the output of the receiver are calculated and the CDI derived. This is then repeated for the next receiver location by summing the fields over all the

elements and over all the strips. For comparison purposes, the "ideal" ground plane field is also calculated and summed separately. The CDI's due to actual and idealized ground conditions may then be compared. Finally, a second pair of CDI's are derived by using a first order difference equation with the instrument time constant and the time difference from the last point, thus simulating the "inertia" of the ILS glide slope receiver and display (so called "dynamic" CDI).

At each receiver point, an output record is generated in file STRIP.DAT consisting of the x-, y-, z-, and time coordinates of the receive plus the four CDI's.

If the terrain is sufficiently irregular, part of the energy radiated toward a point on the ground may be intercepted by another piece of the ground closer to the antenna. This shadowing is complex including, as it does, diffraction as well as reflection. This is approximated in the simulation by using ray optics; that is, the shadow is assumed to have no diffraction at the edges and a zero field amplitude inside the shadow. The program does this by assuming the ground is continuous, i.e. the far edge of one strip is the near edge of the next, and keeping track of the "furthest" (in angular sense) edge. If part (or all) of the next strip is "below" that edge then that part (or all) will not be included in the trapezoid integration. For example in the sketch below



all of strip I, none of strip II and that part of strip III between D and E will be included in the integration.

For the receiver antenna a "semi" directional antenna is assumed; that is, only the incident fields from the front half-sphere around the receiver are included. This is as though an omni-directional antenna was used but blocked by the fuselage from receiving signals from the direction of the tail. This is done in the program by stopping the summation of fields over the ground strips at a point directly below the receiver.

The back half-plane is assumed to be an ideal flat horizontal reflector of infinite extent. The field from this is included by adding the "gain factor" for this as an initial strip to that calculated by integrating over the "real" strips.

3.2 OPERATION

ILSGLD assumes the ground description is a file called GRND.DAT, and that the receiver locations are in a file called PATH.DAT. The user starts the program and then inputs the name of the file containing the antenna description. The simulation will be run, and the output will be found in file STRIP.DAT.

3.3 CONCLUSION

ILSGLD represents an initial effort at glide slope landing system simulation. It has been exercised with simple test cases. Two possible areas for future work include:

1. terrain variation perpendicular to runway centerline direction - the ground does not usually have a constant profile along the y-direction as is presently assumed;
2. varying conductivity - the physical ground surface is not necessarily the "surface" as seen by the radio frequency fields as is presently assumed.

4. FMAKE PROGRAM DESCRIPTION

FMAKE is a file generation program used to create input files for ILSGLD. It is designed to be used interactively. The user starts by running the program. The program will respond by typing:

INPUT SWITCH:

The user then types in a single character switch, followed by a <CR>, for the file he wishes to generate. The program will then respond with a request for the input required for that file. If a blank is used as the input switch the program will terminate. If any character other than the ones explained below are used an error message will be given. After each file is generated, the program will return to the switch input point thus allowing the user to generate the data files for many simulation runs in one sitting.

(N.B. All units are in feet unless otherwise stated)

4.1 SWITCH: Y

The program will type:

INPUT YO, LAMBDA:

The user then inputs in free field format the y-offset (i.e. the y-coordinate) of the antenna elements and the wave length of the carrier, followed by a <CR>. The y-offset is the distance from the base of the antenna to the centerline of the runway. As this information is required for both the antenna description and the flight path it is input with a separate switch to avoid repetition.

4.2 SWITCH: G

This is used to input the ground description. The program will respond with:

INPUT GROUND FILE NAME:

The user then inputs a five(5) character name for the ground description file, followed by a <CR>. ILSGLD requires the ground

file to be called GRND.DAT (The .DAT extension is a system default). FMAKE allows the user to generate several ground files with different names at one sitting. Then by using system renaming commands a single batch job may be set up that will run many simulations without further user interactions.

The program will then type:

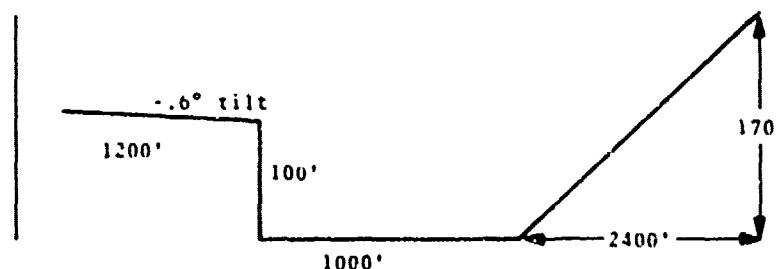
INPUT GROUND LABEL

The user then inputs up to 40 characters to be used as a label for this ground description. This label is carried in the ground description file and will be placed in the output file by ILSGLD. This allows the GLDPLT program to label the plots with the ground description. This is necessary if a batch job generates plots from more than one simulation.

The program will then type:

INPUT GROUND SEGMENTS. STARTING FROM ANTENNA, GIVE CONSECUTIVELY EITHER X AND Z INCREMENTS, OR THE LENGTH AND ANGLE FROM HORIZONTAL IN DEGREES, SEPARATED BY A ZERO. HIT CARRIAGE RETURN FOR END OF DATA, OR IF THERE ARE NO MORE STRIPS.

The user inputs ground strip end points in either Cartesian or polar increments using two or three fields respectively. These are input in floating free field format followed by a <CR>. The first point is taken relative to the origin and is the near edge of the closest strip to the antenna. The second point is the far edge of the first strip and the near edge of the second strip. This second point is relative to the first. This will continue for additional strips until a <CR> is hit with no data, at which point the program will return to the switch input. For example to input this profile:



The input would be

0.,0.
1200., 0., -.6
0., -100.
2400., 170.

There is a maximum of 20 strips allowed in both FMAKE and ILSGLD. This is determined by array sizes and could be changed if desired.

4.3 SWITCH: P

This is used to generate a flight path file. The program will respond:

INPUT FLIGHT PATH FILE NAME:

The user then inputs a five(5) character file name (the name must be exactly 5 characters). ILSGLD requires the flight path to be in a file called PATH.DAT (for explanation of multiple files see SWITCH:G). The program will then type:

INPUT FLIGHT PATH TITLE:

The user then inputs a title, using up to 40 characters, for the flight path. This is used as a label on the plots output by GLDPLT. The program will then type:

INPUT FLIGHT PATH TYPE:

The user has a choice of two flight path types, linear or hyperbolic. For a linear flight path, type a <CR>; for a hyperbolic path type a 'G' followed by a <CR>. When it is a linear flight the program will respond:

INPUT X0, Y0, Z0:

The user then inputs the x-, y-, and z-coordinates of the first receiver point in free field floating point format followed by a <CR>. The program will respond:

INPUT XF, YF, ZF:

The user then inputs the final receiver location in the same way. The program then types:

INPUT # OF POINTS, VELOCITY, TIME CONSTANT:

The user then inputs the total number of receiver locations desired in integer free field format, followed by the velocity of the aircraft in feet/sec. in floating point free field and the time constant in seconds (usually 0.4) used for the "inertia" of the receiver in dynamic simulation. The program will then generate the data file and return to the SWITCH POINT.

The actual ideal surface of zero CDI is a hyperboloid of two sheets whose axis of rotation is parallel to the z-axis and passes through the antenna. For comparison purposes it is convenient to have the aircraft travel along this surface and see how the real CDI deviated from 0. If the glide path is used for linear flight in the near field (between threshold and antenna) large CDI's will occur because of the hyperbolic shape. The program will allow the user to generate a hyperbola which is the intersection of the 0 CDI surface and the plane containing the runway centerline parallel to the z-axis. To do this the user types a 'G' for the flight path type. The program will respond:

INPUT X0, XF, H:

The user inputs these in floating point free field format followed by a <CR>. X0 is the x-coordinate of the initial receiver point (Y0 is zero and Z0 is specified by the hyperboloid), XF is the x-coordinate of the final receiver point. H is the height of the main carrier element in the antenna array. The program will then respond:

INPUT # OF POINTS, VELOCITY, TIME CONSTANT

These are input as above. The program will generate the file and return to the switch point.

4.4 SWITCH: A

This switch is used to generate the antenna description file. The program will respond:

INPUT ANTENNA FILE NAME:

The user inputs the 5 character file name. The program will type:

INPUT ANTENNA DESCRIPTION:

The user inputs a <40 character antenna description to be used as a plot label. The program will then type:

INPUT ELEMENT VALUES:

The user then types in, in free field floating format, a maximum of 8 fields followed by a <CR>. The fields have the following usage:

| <u>field #</u> | <u>usage</u> |
|----------------|---|
| 1 | x-coordinate of element (usually 0) |
| 2 | z-coordinate of element (height) |
| 3 | real amplitude of carrier |
| 4 | imaginary amplitude of carrier |
| 5 | real amplitude of 150 Hz side band |
| 6 | imaginary amplitude of 150 Hz side band |
| 7 | real amplitude of 90 Hz side band |
| 8 | imaginary amplitude of 90 Hz side band |

This element inputting is repeated for each element. After the last element is input an extra carriage return is typed. No y-coordinate is input for the elements. This is because nominally all the elements have the same y offset (the value input as Y0 under switch:Y). However, a small offset correction is applied for near field correction. An explanation of this correction may be found in part I (see discussion preceeding Eq. (33)). This is automatically done by the program. As the first element input is assumed to have the correct offset, it will always have a value of Y0. Thus the main carrier element should be input first, for example, a null reference antenna was input as follows:

INPUT SWITCH: Y

INPUT Y0, LAMBDA: 300., 3.

INPUT SWITCH: A

INPUT ANTENNA FILE NAME: NULL

INPUT ANTENNA DESCRIPTION

NULL REFERENCE ANTENNA

INPUT ELEMENT VALUES

0., 15., 1., 0., .4, 0., .4, 0.

0., 30., 0., 0., -.12, 0., .12, 0.

5. GLDPLT PROGRAM DESCRIPTION

GLDPLT is a plotting output program to graph the CDI information from ILSGLD. The user runs GLDPLT which then types:

INPUT FILE NAME AND AXIS TYPE:

The user then types in a 5 character (left-justified and blank filled to 5 characters) and two integer fields in free field format. The first integer is the switch for x-axis type and the second integer is the switch for the y-axis. The y-switch has two values, 1 and 2, the x-switch has three 1, 2, and 3; any other values will terminate the program.

The switches have the following usage:

| | |
|------------|---|
| y-switch=1 | this plots the static CDI values |
| y-switch=2 | this plots the dynamic CDI values |
| x-switch=1 | this uses the altitude angle, in degrees measured from the origin of the receiver point as x-coordinate |
| x-switch=2 | this uses the x-coordinate of the receiver as the x-axis |
| x-switch=3 | uses the time in seconds, at the receiver point, as the x-coordinate. |

After the input, a plot is generated and the program returns to the input and asks for the data for the next plot. The user can give the same file name to plot the data differently, or a new file name can be given. This would be done when multiple runs were done before plotting; the output file from each simulation run carrying its own name.

APPENDIX A
LISTING OF ILSGLD

```

1      DIMENSION ILABL(6)
2      DIMENSION IPTDAT(33)
3      COMMON /PLT/ BPP,BIHH,BIHX,BIFT,BILT,BYHH,BYHX,BYFT,BYLT,
4      IRIZ,BIZ,BIFT,BILT,BYHH,BYHX,BYFT,BYLT,
5      JAS,BIZ,BIFT,BILT,BYHH,BYHX,BYFT,BYLT,
6      JADIZ,BDIZ,BDIF,BDIL,
7      QADH,ADH,ADBF,ADBL
8      EQUIVALENCE (IPTDAT(1),*P)
9      IMPLICIT COMPLEX (C)
10     DIMENSION X(20),Y(20),Z(20)
11     DIMENSION CF1(20),CF2(20),CF3(20)
12     IMPLICIT DOUBLE PRECISION (D)
13     COMMON /REC/PI,BY,BZ,BY,BZ,BZ,BZ
14     REAL LAMBDA
15     COMMON /GROUND/ K,X1(20),Z1(20),X2(0/20),Z2(0/20),ILL
16     COMMON /ANT/AL,AY,AZ,LAMBDA,DAF,DPI
17     COMMON /VAL/ NR,NI
18
19     C
20     C      THIS VALUE OF T=0 PI IS INITIALIZED THIS WAY TO AVOID USING
21     C BLOCK DATA
22     DPI=0.2831853071709664769
23
24     C
25     C      THIS OPENS THE OUTPUT FILE
26     CALL OFILE(1,'STRIP')
27
28     C
29     C      THIS IS A DUMMY RECORD. AFTER THE RUN IS FINISHED THE OUTPUT
30     C FILE WILL BE REWOUND AND THE ACTUAL RECORD WILL BE WRITTEN
31     WRITE(1) IPTDAT
32
33     C
34     C      THIS SUBROUTINE OPENS THE FLIGHT PATH FILE AND RETURNS WITH
35     C THE FLIGHT PATH PLOT LABEL (ILABL) AND TIME CONSTANT (TAU)
36     C THE FILE WAS SET UP WITH JOVPAK SO THIS SUBROUTINE AND INPUT ARE
37     C USED TO FACILITATE MODIFICATIONS
38     CALL IF(ILABL,TAU)
39     1000 FORMAT(A5)
40     WRITE(1,1000) ILABL
41
42     C
43     C      THIS SECTION INITIALIZES SOME CONSTANTS
44     *NP=0
45
46     C
47     C      THIS SECTION INPUTS THE GROUND STRIPS DESCRIPTIONS
48     CALL IFILE(20,'GRND')
49     READ(20,1000) ILABL
50     WRITE(1,1000) ILABL
51     READ(20) K,X1,Z1,X2,Z2
52     CALL RELEAS (20)
53
54     C
55     C      THIS SECTION INPUTS THE ANTENNA FILE NAME TO BEUSED
56     C AND THEN INPUTS THE ANTENNA ELEMENT DESCRIPTIONS
57     WRITE(3,2001)
58     2001 FORMAT(' INPUT ANTENNA FILE NAME:'.*)
59     READ(3,2000) ILBL
60     2000 FORMAT(A5)

```



```

94      CALL IFILE(20,ILBL)
95      READ(20,1000) ILBL
96      WRITE(1,1000) ILBL
97      READ(20) LAMBDA,NEL,(X(I),Y(I),Z(I),CF1(I),CF2(I),CF3(I),I=1,NEL)
98      CALL DELZAS (20)
99      SORTEL=1./SORT(2,-LAMBDA)
100     TEMP=LAMBDA
101     DAX=0.01/DOLE(LAMBDA)
102     DAX=0.01(DAX)
103
104     C
105     C      THIS IS THE MAIN LOOP FOR THE SIMULATION. THE RECEIVER
106     C LOCATION IS READ IN BY INPUT. THE DATA IS IN COMMON 'REC'
107     C THE INPUT BEING DONE BY JOURN1. IF THERE ARE NO MORE RECEIVED
108     C POINTS THE SUBROUTINE RETURNS TO 202.
109     201 CALL INPUT(0200)
110
111     C
112     C      THIS SECTION INITIALIZES THE COMPLEX AMPLITUDES FOR
113     C THE RECEIVED FIELDS AS FOLLOWS:
114     C      CFB1 CARRIER WITH 'REAL' GROUND
115     C      CFB2 150 MH SIDEBAND WITH 'REAL' GROUND
116     C      CFB3 90MH SIDEBAND WITH 'REAL' GROUND
117     C      CFB1 CARRIER WITH 'IDEAL' FLAT GROUND PLANE
118     C      CFB2 150MH WITH 'IDEAL' GROUND
119     C      CFB3 90 MH WITH 'IDEAL' GROUND
120     CFB1=(0.,0.)
121     CFB2=(0.,0.)
122     CFB3=(0.,0.)
123     CFB1=(0.,0.)
124     CFB2=(0.,0.)
125     CFB3=(0.,0.)
126     D2=0.001*(PI*0.01*0.01)
127
128     C
129     C      THIS LOOP IS OVER THE ELEMENTS OF THE ANTENNA
130     C THE COMPLEX FIELDS ARE SUMMED IN CFB1,CFB2 ETC.
131     DO 3 IEL=1,NEL
132
133     C
134     C      THESE ARE THE LOCATION COORDINATES OF THE ANTENNA ELEMENTS
135     C AND CONSTANTS USED IN THE STRIP INTEGRATION
136     AX=X(IEL)
137     AY=Y(IEL)
138     AZ=Z(IEL)
139     DELX=AX-AX
140     DELY=AY-AY
141     DELZ=AZ-AZ
142     DDELX=DELX*DELX+DELY*DELY+DELZ*DELZ
143     DDELX=GL(DDELX)
144     DDELX=DDELX
145     ILC=0/DPI
146
147     C
148     C      THIS SECTION INITIALIZES ND AND NI TO INCLUDE THE
149     C SE=1-INFINITE REAL GROUND PLANE
150     TEMP2=0.01*DOLE(FLD(IEL))*0.01
151     TEMP=ND2*AZ

```

```

107      F1=SQRT(TEMP*TEMP*AT*AT)
108      F2=-RX*TEMP/(R1*F1)
109      TC=SQRT(1.+AT*AT/(TEMP*TEMP))
110      TS=TC*AX
111      R1=TS*TC
112      S=SQRT((1./R2+1./R1)/(TC*TC*TC))
113      G=RX/(TS*TS*0.0108)
114      TEMP=AX*F1
115      SF=SBIN(TEMP)
116      FC=CCOS(TEMP)
117      TEMP=AX*G/SAK/F2
118      C
119      C      NR AND NI ARE THE REAL AND IMAGINARY PARTS OF THE COMPLEX
120      C "GAIN" FACTOR OF THE GROUND SURFACE SCATTERING TO THE RECEIVER
121      C LOCATION
122      NR=TEMP*(SF*FC/(SAK*TS))
123      NI=TEMP*(FC*SF/(SAK*TS))
124      C
125      C      THIS SUBROUTINE JUMPS THE "GAIN" FACTOR FOR EACH STRIP OF
126      C THE GROUND SURFACE
127      CALL SCAT
128      C
129      C      THIS SECTION INCLUDES THE EFFECT OF THE DIRECT RADIATION FROM
130      C THE ANTENNA ELEMENT AT THE RECEIVER
131      NR=NR+SQRT3L
132      NI=NI+SQRT3L
133      TEMP=CXLI/(R0R)
134      SF=SBIN(TEMP)
135      FC=CCOS(TEMP)
136      C
137      C      CTEMP IS THE COMPLEX GAIN FACTOR INCLUDING ALL RADIATION FROM
138      C THIS ELEMENT
139      CTEMP=CXPLI(-TEMP*SF*NR-NI,TEMP*FC*NR+NI)
140      C
141      C      THIS SECTION ACCUMULATES THE FIELDS OF THE VARIOUS FREQUENCIES
142      CFS1=CFS1+CTEMP*CF1(IEL)
143      CFS2=CFS2+CTEMP*CF2(IEL)
144      CFS3=CFS3+CTEMP*CF3(IEL)
145      ALPH=SAK*2.*X2/P
146      CTEMP=TEMP*.5/LAMBDA*CXPLI(-SF,FC)*
147      ICXPLI((1.-COS(ALPH)),SIN(ALPH))
148      CFS1=CFS1+CTEMP*CF1(IEL)
149      CFS2=CFS2+CTEMP*CF2(IEL)
150      CFS3=CFS3+CTEMP*CF3(IEL)
151      CONTINUE
152      C
153      C      AFTER THE FIELDS HAVE BEEN ACCUMULATED FOR ALL THE ELEMENTS
154      C THE CDI'S ARE CALCULATED
155      C      ACOR CDI FOR THE GROUND SURFACE
156      C      ACDI CDI FOR "IDEAL" GROUND PLANE
157      ACOR=0.97,14*REAL((CFS3-CFS1)/CFS1)
158      ACDI=0.97,14*REAL((CFS3-CFS2)/CFS1)
159      C

```

```

165 C      NCP IS THE COUNT OF THE RECEIVED POINTS
166 NCP=0
167 IF(NCP .NE. 1) GO TO 4
168 C
169 C      THIS SECTION INITIALIZES THE MAXIMUM AND MINIMUM VALUES
170 C OF THE VARIOUS RANGE AND DOMAIN VARIABLES. THESE ARE
171 C USED IN THE PLOTTING PROGRAM TO SCALE THE PLOTS. AFTER THE
172 C RUN IS FINISHED THEY WILL BE OUTPUT IN PLACE OF THE
173 C INITIAL DUMMY DECODE
174 ADDIACDI
175 ADDIACDI
176 TCRNT
177 ADIACDI
178 ADIACDI
179 ADIACDI
180 ADIACDI
181 ADIACDI
182 ADIACDI
183 ADIACDI
184 ADIACDI
185 ADIACDI
186 ADIACDI
187 ADIACDI
188 ADIACDI
189 ADIACDI
190 ADIACDI
191 ADIACDI
192 ADIACDI
193 ADIACDI
194 ADIACDI
195 ADIACDI
196 C
197 C      THIS SECTION UPDATES THE MAXIMUM AND MINIMUM VALUES
198 C
199 C
200 C
201 C
202 C
203 C
204 C
205 C
206 C
207 C
208 C
209 C
210 C
211 C
212 C

```

```

213 IF(ACDI .GT. AIMX) AIMX=ACDI
214 IF(ACDI .LT. AIMN) AIMN=ACDI
215 IF(ACDR .GT. ARMX) ARMX=ACDR
216 IF(ACDR .LT. ARMN) ARMN=ACDR
217 COM=EXP((TO-RT)/TAU)
218
219
220
221

```

```

C THIS SECTION SIMULATE THE EFFECT OF THE ELECTRICAL AND
C MECHANICAL "INERTIA" OF THE ILS
C RECEIVER SYSTEM FOR DYNAMIC SIMULATION

```

```

222 TO=RT
223 ADDI=CON*(ACDI-ACDI)*ACDI
224 ADDR=CON*(ACDR-ACDR)*ACDR
225 IF(ADDI .LT. ADIN) ADIN=ADDI
226 IF(ADDR .GT. ADIX) ADIX=ADDR
227 ADIL=ADDI
228 ADRL=ADDR
229 IF(ADDR .GT. ADRX) ADRX=ADDR
230 ADRL=ADDR
231

```

```

C THIS IS THE OUTPUT OF THE REAL AND 'IDEAL' , STATIC
C AND DYNAMIC COI'S WITH THE RECEIVER COORDINATES
232 WRITE(1,2003) RX,RY,RT,ACDI,ACDR,ADDI,ADDR
233 FORMAT(8F)
234
235 GO TO 201

```

```

C THIS IS THE TERMINATION SECTION. THE INITIAL RECORD ON
C THE OUTPUT FILE IS WRITTEN AND THE PROGRAM TERMINATES.

```

```

200 CALL RELEAS (1)
201 CALL DEFINE FILE(1,25,1,'STRIP.DAT')
202 WRITE(1,1) IPTDAT
203 CALL RELEAS (1)
204 CALL EXIT
205 STOP
206 END

```

CONSTANTS

```

0 263622077325 1 15004205061 2 000000000001 3 516512244640 4 000000000000
5 000000000000 6 436451642100 7 000000000000 10 000000000000 11 212654443656
12 000000000000 13 516512244640 14 2721.1152100 15 000000000000

```

COMMON

```

NRP /PLXT /+0 RXRX /PLXT /+1 RXPX /PLXT /+2 RXFT /PLXT /+3
RXVH /PLXT /+5 RXVH /PLXT /+6 RXFT /PLXT /+7 RXFT /PLXT /+8
RXMX /PLXT /+12 RXFT /PLXT /+13 RXLT /PLXT /+14 RXMX /PLXT /+15
RXFT /PLXT /+17 RXLT /PLXT /+20 RXMX /PLXT /+21 RXMX /PLXT /+22
ALIT /PLXT /+24 ARMX /PLXT /+25 ARMX /PLXT /+26 ARFT /PLXT /+27
ADIX /PLXT /+31 ADIX /PLXT /+32 ADIL /PLXT /+33 ADIL /PLXT /+34
ADRX /PLXT /+36 ADRX /PLXT /+37 ADRL /PLXT /+40 RX /PLXT /+0
RZ /PLXT /+2 RT /PLXT /+3 RX /PLXT /+4 RX /PLXT /+5
21 /GROUND/+25 X2 /GROUND/+51 X2 /GROUND/+76 X2 /GROUND/+123
22 /ANT /+1 /ANT /+2 /ANT /+3 /ANT /+4 /ANT /+5
23 /ANT /+6 /ANT /+7 /ANT /+8 /ANT /+9 /ANT /+10 /ANT /+11
24 /ANT /+12 /ANT /+13 /ANT /+14 /ANT /+15 /ANT /+16 /ANT /+17
25 /ANT /+18 /ANT /+19 /ANT /+20 /ANT /+21 /ANT /+22 /ANT /+23
26 /ANT /+24 /ANT /+25 /ANT /+26 /ANT /+27 /ANT /+28 /ANT /+29
27 /ANT /+30 /ANT /+31 /ANT /+32 /ANT /+33 /ANT /+34 /ANT /+35
28 /ANT /+36 /ANT /+37 /ANT /+38 /ANT /+39 /ANT /+40 /ANT /+41
29 /ANT /+42 /ANT /+43 /ANT /+44 /ANT /+45 /ANT /+46 /ANT /+47
30 /ANT /+48 /ANT /+49 /ANT /+50 /ANT /+51 /ANT /+52 /ANT /+53
31 /ANT /+54 /ANT /+55 /ANT /+56 /ANT /+57 /ANT /+58 /ANT /+59
32 /ANT /+60 /ANT /+61 /ANT /+62 /ANT /+63 /ANT /+64 /ANT /+65
33 /ANT /+66 /ANT /+67 /ANT /+68 /ANT /+69 /ANT /+70 /ANT /+71
34 /ANT /+72 /ANT /+73 /ANT /+74 /ANT /+75 /ANT /+76 /ANT /+77
35 /ANT /+78 /ANT /+79 /ANT /+80 /ANT /+81 /ANT /+82 /ANT /+83
36 /ANT /+84 /ANT /+85 /ANT /+86 /ANT /+87 /ANT /+88 /ANT /+89
37 /ANT /+90 /ANT /+91 /ANT /+92 /ANT /+93 /ANT /+94 /ANT /+95
38 /ANT /+96 /ANT /+97 /ANT /+98 /ANT /+99 /ANT /+100

```

001 100

| | | | | | | | | | | | | | |
|--------|-----|-----|-----|-----|-----|-----|-----|-----|-----|-----|-----|-----|-----|
| ACDI | 156 | 169 | 172 | 173 | 174 | 182 | 192 | 193 | 203 | 213 | 214 | 223 | 234 |
| ACDR | 157 | 170 | 175 | 176 | 177 | 183 | 194 | 195 | 204 | 215 | 216 | 224 | 234 |
| ADDI | 169 | 223 | 225 | 226 | 227 | 234 | | | | | | | |
| ADDP | 170 | 224 | 228 | 229 | 230 | 236 | | | | | | | |
| ADIF | 3 | 174 | | | | | | | | | | | |
| ADIC | 3 | 227 | | | | | | | | | | | |
| ADIM | 3 | 173 | 225 | | | | | | | | | | |
| ADIX | 3 | 172 | 226 | | | | | | | | | | |
| ADRP | 3 | 177 | | | | | | | | | | | |
| ADRL | 3 | 230 | | | | | | | | | | | |
| ADRV | 3 | 176 | 220 | | | | | | | | | | |
| ADRX | 3 | 175 | 229 | | | | | | | | | | |
| ADTX | 3 | 182 | | | | | | | | | | | |
| AIPT | 3 | 203 | 214 | | | | | | | | | | |
| AIPT | 3 | 193 | 213 | | | | | | | | | | |
| AIMH | 3 | 192 | | | | | | | | | | | |
| AIMX | 3 | 192 | | | | | | | | | | | |
| ALPH | 145 | 146 | | | | | | | | | | | |
| AMT | 14 | | | | | | | | | | | | |
| AMT | 14 | | | | | | | | | | | | |
| ARFT | 3 | 183 | | | | | | | | | | | |
| ARLT | 3 | 204 | | | | | | | | | | | |
| ARLT | 3 | 195 | 216 | | | | | | | | | | |
| ARMH | 3 | 195 | 215 | | | | | | | | | | |
| ARMX | 3 | 194 | | | | | | | | | | | |
| AX | 16 | 92 | 93 | 107 | 109 | 112 | 117 | 145 | | | | | |
| AZ | 16 | 94 | 97 | 106 | 110 | | | | | | | | |
| CF1 | 11 | 57 | 142 | 148 | | | | | | | | | |
| CF2 | 11 | 57 | 141 | 149 | | | | | | | | | |
| CF3 | 11 | 57 | 144 | 150 | | | | | | | | | |
| CFR1 | 78 | 148 | 157 | | | | | | | | | | |
| CFR2 | 79 | 149 | 157 | | | | | | | | | | |
| CFR3 | 80 | 150 | 157 | | | | | | | | | | |
| CFR4 | 81 | 142 | 158 | | | | | | | | | | |
| CFR5 | 82 | 143 | 158 | | | | | | | | | | |
| CFR6 | 83 | 144 | 156 | | | | | | | | | | |
| CFR7 | 83 | 144 | 156 | | | | | | | | | | |
| CFR8 | 139 | 146 | | | | | | | | | | | |
| CON | 217 | 272 | 224 | | | | | | | | | | |
| COS | 116 | 135 | 146 | | | | | | | | | | |
| CTEP | 139 | 142 | 143 | 144 | 146 | 149 | 150 | | | | | | |
| CTEP | 139 | 142 | 143 | 144 | 146 | 149 | 150 | | | | | | |
| OAK | 16 | 61 | 62 | 100 | 117 | 122 | 123 | | | | | | |
| OBLZ | 31 | 105 | | | | | | | | | | | |
| DEFINE | 241 | | | | | | | | | | | | |
| DELX | 95 | 98 | 133 | | | | | | | | | | |
| DELT | 96 | 98 | | | | | | | | | | | |
| DELT | 97 | 98 | | | | | | | | | | | |
| DELT | 97 | 98 | | | | | | | | | | | |
| DPI | 16 | 21 | 61 | 101 | 105 | | | | | | | | |
| DR | 98 | 99 | 100 | 101 | 105 | | | | | | | | |
| OSORT | 98 | | | | | | | | | | | | |
| EXIT | 244 | | | | | | | | | | | | |
| EXP | 217 | | | | | | | | | | | | |
| F1 | 107 | 108 | 114 | | | | | | | | | | |
| F2 | 108 | 117 | | | | | | | | | | | |
| FC | 116 | 122 | 123 | 135 | 139 | 146 | | | | | | | |
| FLOAT | 105 | | | | | | | | | | | | |

| | | | | | | | | | | | | |
|--------|-----|-----|-----|-----|-----|-----|-----|-----|-----|-----|-----|-----|
| G | 113 | 117 | | | | | | | | | | |
| GROUND | 15 | | | | | | | | | | | |
| M1 | 17 | 123 | 133 | 139 | | | | | | | | |
| MR | 17 | 122 | 131 | 139 | | | | | | | | |
| I | 57 | 241 | | | | | | | | | | |
| IEL | 15 | 88 | 92 | 93 | 94 | 142 | 143 | 144 | 148 | 149 | 150 | |
| IF | 34 | | | | | | | | | | | |
| IFILE | 42 | 54 | | | | | | | | | | |
| IL | 101 | 105 | | | | | | | | | | |
| ILABL | 1 | 34 | 36 | 43 | 43 | 55 | 56 | | | | | |
| ILBL | 52 | 54 | | | | | | | | | | |
| INPUT | 68 | | | | | | | | | | | |
| IPDAT | 2 | 8 | 28 | 242 | | | | | | | | |
| K | 15 | 45 | | | | | | | | | | |
| LAMBDA | 14 | 14 | 57 | 59 | 60 | 61 | 146 | | | | | |
| NEL | 57 | 88 | | | | | | | | | | |
| NRP | 3 | 8 | 39 | 161 | 162 | | | | | | | |
| NRIZE | 13 | | | | | | | | | | | |
| OFILE | 24 | | | | | | | | | | | |
| PLXT | 3 | | | | | | | | | | | |
| R | 99 | 133 | 145 | | | | | | | | | |
| R1 | 111 | 113 | | | | | | | | | | |
| R2 | 84 | 104 | 108 | 111 | 112 | | | | | | | |
| REAL | 157 | 158 | | | | | | | | | | |
| REC | 13 | | | | | | | | | | | |
| RELEAL | 46 | 58 | 240 | 243 | | | | | | | | |
| RT | 13 | 171 | 181 | 190 | 191 | 202 | 211 | 212 | 217 | 222 | 224 | |
| RIFT | 3 | 181 | | | | | | | | | | |
| RTLT | 3 | 202 | | | | | | | | | | |
| RTMN | 3 | 190 | 212 | | | | | | | | | |
| RTMX | 3 | 191 | 211 | | | | | | | | | |
| RX | 13 | 84 | 95 | 108 | 113 | 178 | 184 | 185 | 199 | 205 | 206 | 234 |
| RXFT | 3 | 178 | | | | | | | | | | |
| RXLT | 3 | 199 | | | | | | | | | | |
| RXMN | 3 | 184 | 205 | | | | | | | | | |
| RXMX | 3 | 185 | 206 | | | | | | | | | |
| RY | 13 | 96 | 179 | 186 | 187 | 200 | 207 | 208 | 234 | | | |
| RYFT | 3 | 179 | | | | | | | | | | |
| RYLT | 3 | 200 | | | | | | | | | | |
| RYMN | 3 | 186 | 207 | | | | | | | | | |
| RYMX | 3 | 187 | 208 | | | | | | | | | |
| PZ | 13 | 84 | 97 | 145 | 180 | 188 | 189 | 201 | 209 | 210 | 234 | |
| RZFT | 3 | 180 | | | | | | | | | | |
| RZLT | 3 | 201 | | | | | | | | | | |
| RZMN | 3 | 188 | 210 | | | | | | | | | |
| RZMX | 3 | 189 | 209 | | | | | | | | | |
| S | 112 | 113 | | | | | | | | | | |
| SAK | 62 | 114 | 145 | | | | | | | | | |
| SCAT | 127 | | | | | | | | | | | |
| SY | 115 | 122 | 123 | 134 | 139 | 146 | | | | | | |
| SIN | 115 | 134 | 146 | | | | | | | | | |
| SNGL | 62 | 99 | | | | | | | | | | |
| SORT | 59 | 84 | 107 | 109 | 112 | | | | | | | |

| | | | | | | | | |
|--------|-----|-----|-----|-----|-----|-----|-----|-----|
| 30RT2L | 88 | 131 | 122 | | | | | |
| TO | 271 | 217 | 222 | | | | | |
| TAU | 34 | 217 | | | | | | |
| TC | 100 | 110 | 111 | 112 | | | | |
| TD | 110 | 113 | 122 | 123 | | | | |
| TEMP | 106 | 107 | 108 | 109 | 114 | | | |
| TEMP2 | 60 | 105 | 114 | 115 | 116 | 117 | 122 | 133 |
| VAL | 17 | | 114 | 115 | 116 | 117 | 122 | 133 |
| X | 10 | 57 | 92 | | | | | |
| X1 | 13 | 45 | | | | | | |
| X2 | 13 | 45 | | | | | | |
| Y | 10 | 37 | 93 | | | | | |
| Z | 10 | 37 | 94 | | | | | |
| Z1 | 13 | 45 | | | | | | |
| Z2 | 15 | 45 | | | | | | |

| | | | | |
|-----|-----|----|----|----|
| 191 | 43 | 40 | 55 | 50 |
| 192 | 80 | | | |
| 193 | 102 | | | |
| 194 | 40 | | | |
| 195 | 40 | | | |
| 196 | 35 | | | |
| 197 | 52 | | | |
| 198 | 50 | | | |
| 199 | 234 | | | |
| 200 | 234 | | | |
| 201 | 30 | | | |
| 202 | 40 | | | |
| 203 | 200 | | | |
| 204 | 200 | | | |
| 205 | 200 | | | |
| 206 | 200 | | | |
| 207 | 200 | | | |
| 208 | 200 | | | |
| 209 | 200 | | | |
| 210 | 200 | | | |
| 211 | 200 | | | |
| 212 | 200 | | | |
| 213 | 200 | | | |
| 214 | 200 | | | |
| 215 | 200 | | | |
| 216 | 200 | | | |
| 217 | 200 | | | |
| 218 | 200 | | | |
| 219 | 200 | | | |
| 220 | 200 | | | |
| 221 | 200 | | | |
| 222 | 200 | | | |
| 223 | 200 | | | |
| 224 | 200 | | | |
| 225 | 200 | | | |
| 226 | 200 | | | |
| 227 | 200 | | | |
| 228 | 200 | | | |
| 229 | 200 | | | |
| 230 | 200 | | | |
| 231 | 200 | | | |
| 232 | 200 | | | |
| 233 | 200 | | | |
| 234 | 200 | | | |
| 235 | 200 | | | |
| 236 | 200 | | | |
| 237 | 200 | | | |
| 238 | 200 | | | |
| 239 | 200 | | | |
| 240 | 200 | | | |
| 241 | 200 | | | |
| 242 | 200 | | | |
| 243 | 200 | | | |
| 244 | 200 | | | |
| 245 | 200 | | | |
| 246 | 200 | | | |
| 247 | 200 | | | |
| 248 | 200 | | | |
| 249 | 200 | | | |
| 250 | 200 | | | |
| 251 | 200 | | | |
| 252 | 200 | | | |
| 253 | 200 | | | |
| 254 | 200 | | | |
| 255 | 200 | | | |
| 256 | 200 | | | |
| 257 | 200 | | | |
| 258 | 200 | | | |
| 259 | 200 | | | |
| 260 | 200 | | | |
| 261 | 200 | | | |
| 262 | 200 | | | |
| 263 | 200 | | | |
| 264 | 200 | | | |
| 265 | 200 | | | |
| 266 | 200 | | | |
| 267 | 200 | | | |
| 268 | 200 | | | |
| 269 | 200 | | | |
| 270 | 200 | | | |
| 271 | 200 | | | |
| 272 | 200 | | | |
| 273 | 200 | | | |
| 274 | 200 | | | |
| 275 | 200 | | | |
| 276 | 200 | | | |
| 277 | 200 | | | |
| 278 | 200 | | | |
| 279 | 200 | | | |
| 280 | 200 | | | |
| 281 | 200 | | | |
| 282 | 200 | | | |
| 283 | 200 | | | |
| 284 | 200 | | | |
| 285 | 200 | | | |
| 286 | 200 | | | |
| 287 | 200 | | | |
| 288 | 200 | | | |
| 289 | 200 | | | |
| 290 | 200 | | | |
| 291 | 200 | | | |
| 292 | 200 | | | |
| 293 | 200 | | | |
| 294 | 200 | | | |
| 295 | 200 | | | |
| 296 | 200 | | | |
| 297 | 200 | | | |
| 298 | 200 | | | |
| 299 | 200 | | | |
| 300 | 200 | | | |

ILSCIO.F4 P40 V20(14) 21-JUL-74 17151 PAGE 7

```

1
2
3
4
5
6
7
8
9
10
11
12
13
14
15
16
17
18
19
C
C THIS SUBROUTINE OPENS THE FLIGHT PATH FILE AND INPUTS THE
C FLIGHT PATH PLOT LABEL AND THE INERTIAL TIME CONSTANT
C
C THIS SUBROUTINE INPUTS THE RECEIVER LOCATION
C COORDINATES OF THE NEXT POINT ON THE FLIGHT PATH, IF THERE
C ARE NO MORE POINTS THE SUBROUTINE ENDS TO THE
C END RETURN POINT
C SUBROUTINE IF(ILABL,TAU)
C DIMENSION ILABL(8)
C COMMON/REC/ DUM(4),MSIZE
C CALL JOVSET(1,'PATH,DAT',MS)
C WRITE(5,1000) MS
1000 FORMAT(12,' RECORDS IN PATH,DAT',/)
C MSIZE=(MS-8)/4
C CALL JOVSET(1,ILABL,8,0)
C CALL JOVSET(1,TAU,1,8)
C RETURN
C END

```

CONSTANTS

0 000000000001 1 302032000134 2 423033020:06 3 000000000000 4 000000000000

GLOBAL DUMMIES

ILABL 66 TAU 67

COMMON

DUM /REC /+0 MSIZE /REC /+4

SUBPROGRAMS

JOVSET INTO. INT1. JOVW1

SCALARS

IF 70 MS 71 MSIZE 4 TAU 67

ARRAYS

ILABL 66 DUM 0

| | | | |
|--------|----|----|----|
| DUM | 1: | | |
| IF | 9 | | |
| ILABL | 9 | 10 | 16 |
| JOVSET | 12 | | |
| JOV#1 | 16 | 17 | |
| VS | 12 | 13 | 15 |
| VS122 | 11 | 15 | |
| REC | 11 | | |
| TAU | 9 | 17 | |

| | | |
|-------|----|----|
| 1030P | 13 | 14 |
|-------|----|----|

ILSGLD.F4 F10 V20(16) 21-JUL-74 17151 PAGE 8

```

1      SUBROUTINE INPUT(4)
2      COMMON /REC/ RI(4),NSIZE
3      IF(NSIZE .LE. 0) RETURN 1
4      CALL JOVNI(1,RX,4,0)
5      NSIZE=NSIZE-1
6      RETURN
7      END

```

CONSTANTS

```

0      000000000001      1      000000000004      2      000000000000

```

COMMON

```

RX      /REC      /+0      NSIZE      /REC      /+4

```

SUBPROGRAMS

JOVNI

SCALARS

```

INPUT  16      NSIZE  4

```

ARRAYS

```

RX      0

```

| | | | |
|-------|---|---|---|
| INPUT | 1 | | |
| JOYMI | 4 | | |
| NOISE | 2 | 3 | 3 |
| REC | 2 | | |
| RZ | 2 | 4 | |

```

1      C
2      C      THIS SUBROUTINE SUMS THE EFFECTS OF THE STRIPS THAT MAKE
3      C UP THE GROUND SURFACE. THERE ARE 'K' STRIPS DESCRIBED IN COMMON
4      C GROUND AS FOLLOWS:
5      C      X1(I)  THE X-COORDINATE OF THE LEADING EDGE OF THE I'TH STRIP
6      C      X2(I)  THE X-COORDINATE OF THE LEADING EDGE OF THE I'TH STRIP
7      C      X3(I)  THE X-COORDINATE OF THE ENDING EDGE OF THE I'TH STRIP
8      C      X4(I)  THE X-COORDINATE OF THE ENDING EDGE OF THE I'TH STRIP
9      C      SUBROUTINE SCAT
10     C      COMMON /SEC/ RX,RY,RZ
11     C      COMMON /ANT/AX,AZ
12     C      COMMON /GROUND/ E,X1(20),X2(20),X3(20),X4(20),IEL
13     C      COMMON /SEC/ X1,X2,X3,X4,N
14     C
15     C      THESE ARE INITIAL VALUES FOR THE PARAMETERS USED IN SHADOWING
16     C      S; P=0.
17     C      PH=0.
18     C
19     C      THIS IS THE LOOP OVER THE STRIPS
20     C      DO 1 I=1,K
21     C
22     C      THESE ARE THE VALUES TO BE USED IN THE STRIP
23     C      INTEGRATION SUBROUTINE
24     C      X1  LEADING X-COORDINATE
25     C      X2  LEADING X-COORDINATE
26     C      X3  TRAILING X-COORDINATE
27     C      X4  TRAILING X-COORDINATE
28     C      X1=X1(I)
29     C      X2=X2(I)
30     C      X3=X3(I)
31     C      X4=X4(I)
32     C
33     C      THIS IS A TEST TO SEE IF THE SUMMATION OVER THE GROUND
34     C STRIPS HAS REACHED THE RECEIVER LOCATION. IF IT HAS THE SUMMATION
35     C IS STOPPED. THIS IS TO GIVE THE EFFECT OF FORWARD LOOKING RECEIVER
36     C ANTENNA PATTERN.
37     C      IF( X1,RC, RX) GO TO 6
38     C
39     C      IF THE RECEIVER IS LOCATED OVER THE MIDDLE PORTION OF A STRIP
40     C THE STRIP WILL BE INTEGRATE ONLY UP TO THE VALUE OF THE
41     C RECEIVER X-COORDINATE
42     C      IF(X2,LE, RX) GO TO 5
43     C      X3=X3+(RX-X1)*(X4-X3)/(X2-X1)
44     C      X4=RX
45     C      CONTINUE
46     C
47     C      THIS SECTION DOES THE SHADOWING. IF PART OR ALL OF THE STRIP
48     C IS IN THE SHADOW OF A PREVIOUS STRIP, THIS STRIP WILL BE ELIMINATED
49     C OR MASKED TO GIVE THE EFFECT OF SHADOWING.
50     C      DELX=X2-AX
51     C      IF(DELX,LE, 0.) GO TO 1
52     C      PHIE=(AZ-X3)/DELX
53     C      IF(SLOPE,LT, 0.) GO TO 1

```

```

94 IF(PHIZ-GE, SLOPE) GO TO 1
95 PHIB=(AS-221)/(X1-AX)
96 IF( PHIB .LE. ALOPE) GO TO 3
97 IF( X1 .GE. X2) GO TO 4
98 AS=(222-221)/(X2-X1)
99 AS21=AS*(X1-AX)
00 X1=(AS-B)/(A-SLOPE)*AX
01 X2=(SLOPE*(X1-AX)+AS
02 C
03 C THIS SUBROUTINE WILL INTEGRATE OVER THE STRIP THE
04 C COMPLEX 'GAIN' EFFECT OF THIS STRIP WILL BE ADDED TO MR AND MI
05 C IN COMMON 'VALL'
06 CALL SUB
07 SLOPE=PHIB
08 CONTINUE
09 RETURN
10 ENO

```

CONSTANTS

0 201400000000

COMMON

| | | | | | | | | | | | | | | |
|-----|-------------|-----|-----|--------------|-----|-----|------------|-----|----|-------------|-----|-----|------------|-----|
| RX | /REC | /0 | RY | /SEC | /01 | RZ | /SEC | /02 | AX | /AMT | /00 | AY | /AMT | /01 |
| AZ | /AMT | /02 | K | /GROUND/00 | | H | /GROUND/01 | | Z1 | /GROUND/030 | | X2 | /GROUND/01 | |
| Z2 | /GROUND/030 | | TEL | /GROUND/0123 | | X21 | /SEC | /00 | Z1 | /SEC | /01 | X23 | /SEC | /02 |
| Z23 | /SEC | /01 | M | /SEC | /04 | | | | Z1 | | | | | |

SUBPROGRAMS

SUM

SCALARS

| | | | | | | | |
|------|-----|-------|-----|------|-----|-----|-----|
| SCAT | 143 | GLOPE | 144 | PHIZ | 145 | K | 0 |
| X1 | 0 | Z21 | 1 | X23 | 2 | RX | 0 |
| DELX | 147 | AX | 0 | AZ | 3 | X2 | 131 |
| B | 152 | RY | 1 | PHIB | 150 | A | 131 |
| M | 4 | | | AY | 1 | TEL | 133 |

ARRAYS

| | | | | | | | |
|----|---|----|----|----|----|----|----|
| X1 | 1 | Z1 | 20 | X2 | 01 | Z2 | 70 |
|----|---|----|----|----|----|----|----|

| | | | | | | | | | |
|--------|----|----|----|----|----|----|----|----|----|
| A | 50 | 59 | 60 | | | | | | |
| AST | 11 | | | | | | | | |
| AX | 11 | 50 | 55 | 59 | 60 | 61 | | | |
| AY | 11 | | | | | | | | |
| AS | 11 | 52 | 55 | 60 | 61 | | | | |
| B | 59 | 60 | | | | | | | |
| DELX | 50 | 51 | 52 | | | | | | |
| QADUHO | 12 | | | | | | | | |
| I | 20 | 20 | 20 | 30 | 31 | | | | |
| IEL | 12 | | | | | | | | |
| K | 12 | 20 | | | | | | | |
| H | 12 | | | | | | | | |
| PHIO | 55 | 56 | | | | | | | |
| PHIC | 17 | 52 | 54 | 67 | | | | | |
| HOC | 10 | | | | | | | | |
| OX | 10 | 37 | 42 | 43 | 44 | | | | |
| OT | 10 | | | | | | | | |
| RZ | 10 | | | | | | | | |
| SCAT | 9 | | | | | | | | |
| SGS | 13 | | | | | | | | |
| SL/PPC | 16 | 53 | 54 | 56 | 60 | 61 | 67 | | |
| SPH | 66 | | | | | | | | |
| X1 | 12 | 20 | | | | | | | |
| X2 | 12 | 30 | | | | | | | |
| X21 | 13 | 20 | 37 | 43 | 55 | 57 | 58 | 59 | 60 |
| X22 | 13 | 30 | 42 | 45 | 44 | 30 | 57 | 58 | 61 |
| X1 | 12 | 29 | | | | | | | |
| X2 | 12 | 31 | | | | | | | |
| X21 | 13 | 29 | 43 | 55 | 50 | 59 | 61 | | |
| X22 | 13 | 31 | 43 | 52 | 50 | | | | |

| | | | | |
|----|----|----|----|----|
| 19 | 20 | 54 | 60 | |
| 39 | 51 | 53 | 56 | 58 |
| 49 | 57 | 61 | | |
| 59 | 42 | 45 | | |
| 69 | 37 | 69 | | |

```

1      C
2      C      THIS SUBROUTINE INTEGRATES OVER THE SURFACE STRIP DEFINED
3      C BY X1,Z1,X2,Z2 IN COMMON 'SEC', TO GIVE THE FIELD EFFECT
4      C OF THE ANTENNA ELEMENT IN COMMON 'ANT' AT RECEIVER DEFINED
5      C IN COMMON 'REC'. THE VARIABLES ARE AS FOLLOWS:
6      C      AX      ANTENNA X-COORDINATE
7      C      AY      ANTENNA Y-COORDINATE
8      C      AZ      ANTENNA Z-COORDINATE
9      C      LAMBDA   WAVELENGTH OF CARRIER
10     C      AZ      TWO*PI/LAMBDA
11     C      DPI      TWO*PI (DOUBLE PRECISION)
12     C      RX      RECEIVER X-COORDINATE
13     C      RY      RECEIVER Y-COORDINATE
14     C      RZ      RECEIVER Z-COORDINATE
15     C      NR      REAL PART OF 'GAIN' FACTOR
16     C      NI      IMAGINARY PART OF 'GAIN' FACTOR
17     C      X1      LEADING EDGE OF STRIP'S X-COORDINATE
18     C      Z1      LEADING Z-COORDINATE
19     C      X2      TRAILING EDGE X-COORDINATE
20     C      Z2      TRAILING Z-COORDINATE
21     C THE INTEGRATION IS PERFORMED BY A MODIFIED TRAPIZOID RULE.
22     C THE SPACING BETWEEN POINTS ALONG THE VARIABLE OF INTEGRATION
23     C IS VARIED BY THE RATE OF CHANGE OF THE INTEGRAND.
24     C      SUBROUTINE SUP
25     C      COMMON /SEC/ X1,Z1,X2,Z2,N
26     C      DOUBLE PRECISION A1,A2,B1,B2,X1,AY2
27     C      REAL JR,J1,J0R,J0I,JNR,JNI
28     C      REAL LAMBDA
29     C      DOUBLE PRECISION AX,DPI,DP
30     C      COMMON /ANT/AX,AY,AZ,LAMBDA,AX,DPI
31     C      COMMON /REC/RX,RY,RZ
32     C      COMMON /VAL/NR,NI
33     C      REAL L3,L10
34     C
35     C      THIS IS THE INITIALIZATION SECTION
36     C      AY2=0.0LE(AY)*0.0LE(AY)
37     C      AX2=0.0LE(AX)*0.0LE(AX)
38     C      SE=Z2-Z1
39     C      CE=X2-X1
40     C
41     C      XMAX IS THE LENGTH ALONG THE SURFACE OF THE STRIP
42     C      XMAX=SQRT(SE*SE+CE*CE)
43     C
44     C      THESE ARE THE SIN AND COS OF THE ANGLE THE STRIP MAKES WITH
45     C A HORIZONTAL PLANE
46     C      SE=SE/XMAX
47     C      CE=CE/XMAX
48     C      JR=0.
49     C      JI=0.
50     C
51     C      XL IS THE VARIABLE OF INTEGRATION. IT IS THE DISTANCE
52     C LONG THE SURFACE OF THE STRIP STARTING FROM THE LEADING EDGE
53     C      XL=0.

```


IL04LD.F4

F40

V26(10) 21-JUL-75

17:52 PAGE 12

```

54      XI=1
55      IT=0
56      C
57      C      THESE ARE THE LOWER AND UPPER BOUNDS FOR THE SPACING BETWEEN
58      C POINTS ALONG THE VARIABLE OF INTEGRATION
59      L1= LAMBDA/24.
60      L10=20.*LAMBDA
61      A1=XI-X1
62      A2=XI-X1
63      B1=X1
64      B2=X1-A2
65      A=0.1
66      TEMP=A2
67      A= SQRT(A+A*TEMP*TEMP)
68      B=0.1
69      TEMP=B2
70      B= SQRT(B+B*TEMP*TEMP)
71      TEMP=A+B
72      DO=SSCAT(SBLE(TEMP)*DBLE(TEMP)*DBLE(AT*AT))
73      C=0.0
74      DO=DO+A
75      I=0.0/DO
76      F=0.0-DBLE(FLGAT(I))*99.1
77      C=C/TEMP
78      D=C*0.0
79      E=C*A
80      S=SQRT((1./A+1./B)/C/C/C)
81      G=1/7/3/2/R/R/2
82      TEMP=C/(A+G*B)
83      CF=CCG(F)
84      SF=SSIN(F)
85      JCM=C*CF*TEMP*SF
86      JCI=C*CF*TEMP*CF
87      AP=(A1*CX-A2*CX)/A
88      BP=(B1*CX-B2*CX)/1
89      C
90      C      FP IS THE DERIVATIVE OF THE PHASE FUNCTION
91      C OF THE INTEGRAND
92      FP=ABS((AP-BP)/C)
93      C
94      C      DL IS DELTA XL
95      DL=L1/FP
96      IF(DL .GT. L10) DL=L10
97      IF(DL .LT. L1) DL=L1
98      XL=XL+DL
99      C
100     C      THIS IS THE LOOP OVER THE SURFACE OF THE STRIP. XL IS
101     C INCREMENTED BY DL (OF VARIABLE SIZE) UNTIL THE END OF THE STRIP
102     C IS REACHED (XMAX)
103     C      CONTINUE
104     I
105     C      THIS SECTION CALCULATE VARIOUS TERMS USED IN EVALUATING THE
106     C INTEGRAND, THE AMPLITUDE AND PHASE FUNCTION

```

```

107 C ARE EVALUTATED SEPARATELY. THE DERIVATIVE OF THE PHASE FUNCTION
108 C IS EVALUATED TO DETERMINE THE SIZE FOR DELTA X
109 DLSE=DL*SE
110 DLCE=DL*CE
111 A1=A1-DLCE
112 A2=A2-DLSE
113 B1=B1-DLCE
114 B2=B2-DLSE
115 A=A1
116 TEMP=A2
117 A= SQRT(A*A+TEMP*TEMP)
118 B=B1
119 TEMP=B2
120 B= SQRT(B*B+TEMP*TEMP)
121 TEMP=A*B
122 DR=DSORT(DBLE(TEMP)+DBLE(TEMP)+DBLE(AY*AY))
123 C=ENGL(DR)/TEMP
124 DR=DR*AK
125 I=DR/DPI
126 C
127 C THIS IS THE PHASE ANGLE "MODULO TWO PI"
128 F=DR-DBLE(FLOAT(I))*DPI
129 D=C*B
130 R=C*A
131 S=SQRT((1./A+1./B)/C)/C
132 G=A1/(D*D*R*R*R)
133 C
134 C THIS IS THE AMPLITUDE FUNCTION
135 TEMP=G/(AKK*D)
136 CF=COS(F)
137 SF=SIN(F)
138 C
139 C THIS IS THE REAL PART OF THE INTEGRAND FOR THE
140 C INTEGRATION VARIABLE VALUE OF XL
141 JNR=G*CF-TEMP*EF
142 C
143 C THIS IS THE IMAGINARY PART
144 JNI=G*SF+TEMP*CF
145 TEMP=DL
146 C
147 C THESE ARE THE REAL AN IMAGINARY PARTS OF THE THE SUMMATION
148 C OF THE TRAPIZOID MAKING U. THE APPROXIMATION TO THE INTEGRAL
149 JR=JR+(JOR*JNR)*TEMP
150 JI=JI+(JOI*JNI)*TEMP
151 IF(IT,NE,0) GO TO 2
152 JOR=JNR
153 JOI=JNI
154 AP=(-A1*CE-A2*SE)/A
155 BP=(B1*CE+B2*SE)/B
156 C
157 C FP IS THE DERIVATIVE OF THE PHASE FUNCTION
158 FP=ABS((AP*BP)/C)
159 C

```

```

160 C DL IS DELTA X AND IS LIMITED BY THE BOUNDS L3,L10
161 DL=L3/PP
162 IF(DL.GT. L10) DL=L10
163 IF(DL.LT. L3) DL=L3
164 HX=DX+1
165
166 C THE VARIABLE OF INTEGRATION IS INCREMENTED AND IF THE END OF THE
167 C STRIP IS REACHED THE LAST TRAPIZOID IS ADDED
168 XLEXL=DL
169 IF( XL.LT. XMAX) GO TO 1
170 DL=DL+DX
171 XLEXL=XL
172 IF( XL.LT. XMAX) GO TO 1
173
174 C THIS SECTION ADDS THE FIELD EFFECT FROM THE STRIP TO THE
175 C TOTAL FIELD SUM AND TEN SUBROUTINE TERMINATES
176 C
177 CONTINUE
178 H=H+X
179 H=H+J*TEMP
180 H=H+J*TEMP
181 H=H+J*TEMP
182 RETURN
183 END

```

CONSTANTS

0 208600000000

COMMON

| | | | | | | | | | | | | | | |
|-----|------|-----|----|------|-----|----|------|-----|--------|------|-----|----|------|-----|
| X1 | /SEC | /+0 | Z1 | /SEC | /+1 | X2 | /SEC | /+2 | Z2 | /SEC | /+3 | N | /SEC | /+4 |
| AX | /ANT | /+0 | AY | /ANT | /+1 | AZ | /ANT | /+2 | LAMBDA | /ANT | /+3 | AK | /ANT | /+4 |
| DP1 | /VAL | /+0 | RX | /REC | /+0 | RY | /REC | /+1 | RZ | /REC | /+2 | NR | /VAL | /+0 |
| W1 | | | | | | | | | | | | | | |

SUBPROGRAMS

| | | | | | | | | | | | | | | | |
|-------|-------|-------|-------|-------|-------|-------|-------|-------|-------|-------|-------|-------|-------|-------|-------|
| DBLK | DPN.6 | SHGL | DSRT | DPN.2 | DPN.0 | DPN.2 | DPN.2 | DPN.2 | DPN.2 | DPN.2 | DPN.2 | DPN.2 | DPN.2 | DPN.2 | DPN.2 |
| DPN.6 | DPN.6 | DPN.6 | DPN.6 | DPN.6 | DPN.6 | DPN.6 | DPN.6 | DPN.6 | DPN.6 | DPN.6 | DPN.6 | DPN.6 | DPN.6 | DPN.6 | DPN.6 |

SCALARS

| | | | | | | | | | |
|-----|------|------|------|------|------|--------|------|-----|------|
| SUN | 1064 | A/2 | 1065 | AY | 1 | AKK | 1067 | AK | 2 |
| SE | 1070 | Z1 | 1071 | Z1 | 1072 | CE | 1074 | X2 | 1075 |
| X1 | 0 | XMAX | 1073 | JR | 1074 | J1 | 1076 | XL | 1077 |
| WX | 1077 | TX | 1078 | L3 | 1079 | LAMBDA | 1080 | L10 | 1081 |
| A1 | 1103 | RX | 1104 | A2 | 1105 | RZ | 1106 | B1 | 1107 |
| B2 | 1111 | AZ | 1112 | A | 1113 | TEMP | 1114 | B | 1115 |
| DR | 1116 | C | 1117 | I | 1118 | DP1 | 1119 | F | 1120 |
| D | 1123 | R | 1124 | S | 1125 | G | 1126 | CP | 1127 |
| 87 | 1130 | JOR | 1131 | JOI | 1132 | AP | 1133 | BP | 1134 |
| PP | 1135 | DL | 1136 | DLSE | 1137 | DPCE | 1138 | JNR | 1139 |

17 103 169 173

APPENDIX B

FMAKE LISTING

PNAKE,F4

F40

V26(14) 21-JUL-74

17:52

PAGE 1

```

1      DIMENSION IDUM(2)
2      DATA IDUM(2)/'.DAT'/
3      COMMON XI,YY,ZZ,TT
4      DIMENSION ILABL(8)
5      DIMENSION X(20),Y(20),Z(20)
6      IMPLICIT COMPLEX (C)
7      DIMENSION C1(20),C2(20),C3(20)
8      COMMON /GROUND/ R,X1(20),Z1(20),X2(0/20),Z2(0/20),.C'.
9
10     C      THIS SECTION ACCEPTS THE INPUT OF THE SWITCH (ONE ' ' -C VLA) TO
11     C DETERMINE WHAT KIND OF FILE TO GENERATE.
12     C      <BLANK> TO END THE PROGRAM
13     C      Y      TO SET ANTENNA OFFSET AND EMISSION WAVELENGTH
14     C      G      FOR GROUND DESCRIPTION
15     C      P      FOR FLIGHT PATH
16     C      A      FOR ANTENNA DESCRIPTION
17     2      WRITE(5,1013)
18     READ(5,1009) NAME
19     IF(NAME.EQ.' ') GO TO 3
20     IF(NAME.EQ.'Y') GO TO 20
21     IF(NAME.EQ.'G') GO TO 21
22     IF(NAME.EQ.'P') GO TO 22
23     IF(NAME.EQ.'A') GO TO 23
24     WRITE(5,1012)
25     GO TO 2
26
27     C      THIS IS THE INPUT FOR THE ANTENNA OFFSET AND FOR THE
28     C TRANSMISSION WAVELENGTH, BOTH ARE IN FEET AND ARE FLOATING POINT.
29     20      WRITE(5,1011)
30     READ(5,1011) TO,RL
31     GO TO 2
32
33     C      THIS SECTION IS FOR GROUND DESCRIPTION
34     21      WRITE(5,1014)
35
36     C      THIS IS TO INPUT THE FILE NAME FOR GROUND DESCRIPTION
37     READ(5,103) IDUM(1)
38     WRITE(5,104)
39
40     C      THIS IS TO INPUT THE PLOT LABEL FOR GROUND DESCRIPTION
41     READ(5,105) ILABL
42     WRITE(5,106)
43
44     C      THIS IS THE INPUT FOR THE GROUND STRIP EDGE COORDINATES
45     C      R      DELTA X-COORDINATE FOR CARTESIAN AND
46     C      RANGE FOR POLAR COORDINATES
47     C      ZZ      DELTA Y-COORDINATE FOR CARTESIAN AND
48     C      USUALLY ZERO FOR POLAR COORDINATES
49     C      THETA    ZERO FOR CARTESIAN COORDINATES AND
50     C      THE ELEVATION ANGLE FOR POLAR
51     C      THIS IS THE INPUT FOR THE STARTING EDGE OF THE FIRST STRIP
52     READ(5,101,END=2) R,ZZ,THETA
53     X2(0)=R+COSD(THETA)-ZZ*SIND(THETA)

```



```

34      ZZ(0)=R*SIND(TNETHA)+Z2*COSD(TNETHA)
35      K=0
36      WRITE(5,102)
37  C
38  C      THIS IS THE INPUT LOOP FOR THE REST OF THE STRIP EDGES. THE
39  C EDGES ARE THE TRAILING EDGE OF THE PREVIOUS STRIP AND THE
40  C LEADING EDGE OF THE NEXT. THE LOOP WILL CONTINUE TO A MAXIMUM OF
41  C TWENTY STRIPS OR UNTIL BOTH 'R' AND 'Z2' ARE ZERO,
42  11  READ(5,101,END=2) R,Z2,TNETHA
43      IF(R.NE.0.) GO TO 5
44      IF(Z2.NE.0.) GO TO 5
45      IF(K.EQ.0) GO TO 2
46      GO TO 4
47  5      K=K+1
48      X1(K)=X2(K-1)
49      Z1(K)=Z2(K-1)
50      X2(K)=X2(K-1)+R*COSD(TNETHA)-Z2*SIND(TNETHA)
51      Z2(K)=Z2(K-1)+R*SIND(TNETHA)+Z2*COSD(TNETHA)
52      IF(K.LT.20) GO TO 4
53      WRITE(5,103)
54      GO TO 4
55  6      WRITE(5,102)
56      GO TO 11
57  C
58  C      THIS OPENS A FILE FOR THE GROUND DESCRIPTION, OUTPUTS IT
59  C IN BINARY AND CLOSSES THE FILE. FLOW THEN RETURNS TO THE SWITCH POINT.
60  4      CALL CFILE(20,IDUM(1))
61      WRITE(20,105) ILABL
62      WRITE(20) K,X1,Z1,X2,Z2
63      CALL DELEAS(20)
64      GO TO 2
65  C
66  C      THIS IS THE SECTION TO GENERATE A FLIGHT PATH FILE.
67  22  WRITE(5,1015)
68  C
69  C      THIS INPUTS THE FLIGHT PATH FILE NAME
70  READ(5,105) IDUM(1)
71  C
72  C      THIS IS TO CREATE THE FILE IF ONE DOES NOT ALREADY EXIST.
73  C THIS IS NECESSARY AS JOVRAX DOES NOT CREATE FILES.
74  CALL CFILE (20,IDUM(1))
75  CALL DELEAS(20)
76  C
77  C      THIS IS TO GEN THE FILE FOR JOVRAX
78  CALL JOVSET(1,IDUM(1),N5IZE)
79  WRITE(5,1003)
80  C
81  C      THIS IS TO INPUT THE FLIGHT PATH PLOT LABEL AND OUTPUT IT TO
82  C THE FILE
83  READ(5,105) ILABL
84  CALL JOVNO(1,ILABL,0,0)
85  WRITE(5,1008)

```

```

107 C
108 C THIS SWITCH IS TO SELECT EITHER STRIGHT LINE FLIGHT OR
109 C HYPERBOLIC. "C" INPUT WILL SELECT HYPERBOLIC ANYTHING ELSE WILL
110 C GIVE STRIGHT LINE.
111 READ(5,1009) I
112 IF(I .NE. 'C') GO TO 12
113 C
114 C THIS IS THE HYPERBOLIC FLIGHT SECTION
115 WRITE(5,1010)
116 C
117 C THIS IS THE INPUT TO DESCRIBE THE FLIGHT
118 C X0 STARTING X-COORDINATE
119 C X1 ENDING X-COORDINATE
120 C N HEIGHT OF MAIN ELEMENT USED TO DETERMINE GLIDE ANGLE
121 C AND HEIGHT ABOVE GROUND OF ZERO CDI SURFACE AT CLOSEST
122 C APPROACH
123 READ(5,1011) X0,X1,N
124 WRITE(5,1006)
125 C
126 C THIS INPUT IS FOR THE FLIGHT PATH QUANTIZATION PARAMETERS
127 C NK IS THE NUMBER OF POINTS ALONG THE FLIGHT PATH
128 C V IS THE VELOCITY (FT./SEC.) OF THE AIRCRAFT
129 C TAU IS THE TIME CONSTANT (SEC.) FOR THE DYNAMIC CDI
130 READ(5,1007) NK,V,TAU
131 IF(NK .LE. 0) GO TO 22
132 CALL JOVNO(1,TAU,1,0)
133 C
134 C THIS LOOP GENERATES THE COORDINATES OF THE POINTS ALONG THE
135 C HYPERBOLA AND OUTPUTS THEM TO THE FLIGHT PATH FILE
136 A1=RL*RL+.25*N*N*Y0*Y0
137 A2=1./((1.-4.*N*N/RL/RL)
138 DX=(X1-X0)/FLOAT(NK-1)
139 XX=X0
140 YY=0.
141 TT=0.
142 XCL=XX
143 ZCL=SQRT((A1-XX*XX)*A2)
144 DO 13 I=1,NK
145 ZZ=SQRT((A1-XX*XX)*A2)
146 TEMP=XX-XCL
147 TEMP2=ZZ-ZCL
148 TT=TT+SQRT(TEMP*TEMP+TEMP2*TEMP2)/V
149 CALL JOVNO(1,XX,4,0)
150 XCL=XX
151 ZCL=ZZ
152 XX=XX+DX
153 CONTINUE
154 GO TO 14
155 C
156 C THIS SECTION IS FOR STRIGHT LINE FLIGHT
157 CONTINUE
158 WRITE(5,1004)
159 C

```

FMARE,P4

F40

V26(14) 21-JUL-74

17:52 PAGE 4

```

160 C      THESE INPUTS ARE TO DESCRIBE THE FLIGHT PATH
161 C      XX      STARTING X-COORDINATE (FEET)
162 C      YY      STARTING Y-COORDINATE (FEET)
163 C      ZZ      STARTING Z-COORDINATE (FEET)
164 C      XF      ENDING X-COORDINATE (FEET)
165 C      YF      ENDING Y-COORDINATE (FEET)
166 C      ZF      ENDING Z-COORDINATE
167 C      NK      NUMBER OF POINTS ALONG THE FLIGHT PATH
168 C      V      VELOCITY OF AIRCRAFT (FEET/SEC.)
169 C      TAU     TIME CONSTANT FOR DYNAMIC CDI (SE)
170      READ(5,101) XX,YY,ZZ
171      WRITE(5,1005)
172      READ(5,101) XF,YF,ZF
173      WRITE(5,1006)
174      READ(5,1007) NR,V,TAU
175      IF( NR .LE. 0) GO TO 22
176      CALL JOVNO(1,TAU,1.0)
177      F=NR-1
178      DX=(XF-XX)/F
179      DY=(YF-YY)/F
180      DZ=(ZF-ZZ)/F
181      DT=SQRT(DX*DX+DY*DY+DZ*DZ)/V
182      TT=0.
183 C
184 C      LOOP TO GENERATE X-,Y-, AND Z-COORDINATES AND OUTPUT THEM
185 C TO THE FLIGHT PATH FILE
186      DO 1 1=1,NR
187      CALL JOVNO(1,XX,4.0)
188      XX=XX+DX
189      YY=YY+DY
190      ZZ=ZZ+DZ
191      TT=TT+DT
192 C
193 C      THIS CLOSSES THE FLIGHT PATH FILE AND RETURNS TO SWITCH POINT
194 14  CALL JOVREL(1)
195      GO TO 2
196 C
197 C      THIS SECTION IS TO GENERATE ANTENNA DESCRIPTION FILE
198 2)  *NO
199      WRITE(5,107)
200 C
201 C      INPUT FOR ANTENNA FILE NAME
202      READ(5,2000) ILBL
203      WRITE(5,108)
204 C
205 C      INPUT FOR ANTENNA PLOT LABEL
206      READ(5,103) ILARL
207      N=1
208 C
209 C      THIS IS THE INPUT FOR ELEMENT DESCRIPTION
210 C      X(1)  X-COORDINATE OF 1ST ELEMENT (FEET)
211 C      Z(1)  Z-COORDINATE OF 1ST ELEMENT (FEET)
212 C      C(1)  COMPLEX AMPLITUDE OF CARRIER COMPONENT OF 1ST ELEMENT

```

```

213 C      C2(I)  COMPLEX AMPLITUDE OF 150 HZ SIDEBAND OF ITH ELEMENT
214 C      C3(I)  COMPLEX AMPLITUDE OF 90 HZ SIDEBAND OF ITH ELEMENT
215 C THE PROGRAM WILL LOOP THRU IS FOR ADDITIONAL ELEMENTS UNTIL A
216 C      ZERO IS ENCOUNTERED FOR Z(N)
217 WRITE(5,1017)
218 10 READ(5,2001) X(N),Z(N),C1(N),C2(N),C3(N)
219 IF( Z(N) .EQ. 0) GO TO 9
220 C
221 C      THIS SECTION DETERMINES THE Y OFFSET OF EACH ELEMENT. THIS
222 C IS NOMINALLY Y0 BUT THERE IS A SMALL CHANGE (LESS THAN ONE WAVELENGTH)
223 C FOR NEAR FIELD CORRECTION PURPOSES
224 S=SIGN(1.,Z(N)-Z(1))
225 IF(N .NE. 1) GO TO 15
226 Y(1)=Y0
227 F=SQRT(Y0-Y0+Z(1)-Z(1))
228 GO TO 16
229 15 X=Y0-SQRT(F+F-Z(N)+Z(N))
230 IF(X=0 .LT. 0.) GO TO 17
231 19 Y=Y0-SQRT((F+RL)-(F+RL)-Z(N)+Z(N))
232 IF(XP=0 .LT. 0.) GO TO 18
233 F=F+PL+S
234 X=X+P
235 GO TO 19
236 17 F=F+PL+S
237 GO TO 15
238 18 Y(N)=Y0-X
239 16 CONTINUE
240 N=N+1
241 GO TO 10
242 C
243 C      THIS SECTION OUTPUTS THE ANTENNA DESCRIPTION TO THE FILE
244 C AND ON THE LINE PRINTED, CLOSES THE FILE AND RETURNS TO THE SWITCH
245 C POINT
246 9 NELL=1
247 CALL CFILE(20,ILBL)
248 WRITE(20,105) ILBL
249 WRITE(20) PL,NEL,(X(1),Y(1),Z(1),C1(1),C2(1),C3(1),I=1,NEL)
250 WRITE(3,1016) ILBL
251 WRITE(3,2001) (X(1),Y(1),Z(1),C1(1),C2(1),C3(1),I=1,NEL)
252 CALL DELRAN(20)
253 GO TO 2
254 C
255 C      THIS IS THE PROGRAM TERMINATION POINT
256 3 CALL EXIT
257 STOP
258 1012 FORMAT('* UNKNOWN SWITCH,')
259 1013 FORMAT(' INPUT SWITCH,')
260 1014 FORMAT(' INPUT GROUND FILE NAME,')
261 1015 FORMAT(' INPUT FLIGHT PATH FILE NAME,')
262 1017 FORMAT(' INPUT ELEMENT VALUES,')
263 1016 FORMAT(2X,8A5)
264 1014 FORMAT(' INPUT GROUND LABEL ,')
265 105 FORMAT(8A5)

```


FMJHC,PA

P40

V26(14) 21-JUL-74

17152 PAGE 7

20
-
20

IDUM
C1
X2

1447
1554
91

ILABL 1451
C2 1028
23 76

X C)
1461
1475

Y X1
1803
1

Z 21
1531
23

| | | | | | | | | | | | | |
|----|-----|-----|-----|-----|-----|-----|-----|-----|-----|-----|-----|-----|
| Y0 | 30 | 138 | 226 | 227 | 229 | 231 | 238 | | | | | |
| Y1 | 172 | 179 | 170 | 179 | 189 | | | | | | | |
| Y2 | 3 | 140 | 170 | 224 | 227 | 229 | 231 | 249 | 251 | | | |
| Y3 | 5 | 218 | 219 | 82 | | | | | | | | |
| Y4 | 8 | 69 | 82 | 71 | 82 | | | | | | | |
| Y5 | 8 | 94 | 69 | | | | | | | | | |
| Y6 | 172 | 180 | 181 | 94 | 62 | 64 | 70 | 71 | 148 | 147 | 151 | 170 |
| Y7 | 143 | 147 | 93 | | | | | | | | | 180 |
| Y8 | 3 | 52 | | | | | | | | | | 190 |

| | | | | | | | | | |
|-------|-----|-----|-----|-----|-----|-----|-----|-----|-----|
| 1P | 186 | 191 | | | | | | | |
| 2P | 17 | 25 | 31 | 52 | 62 | 63 | 84 | 195 | 253 |
| 3P | 19 | 256 | | | | | | | |
| 4P | 66 | 74 | 80 | | | | | | |
| 5P | 63 | 64 | 67 | | | | | | |
| 6P | 72 | 75 | | | | | | | |
| 9P | 219 | 246 | | | | | | | |
| 10P | 218 | 241 | | | | | | | |
| 11P | 62 | 76 | | | | | | | |
| 12P | 112 | 157 | | | | | | | |
| 13P | 144 | 153 | | | | | | | |
| 14P | 154 | 194 | | | | | | | |
| 15P | 225 | 229 | 217 | | | | | | |
| 16P | 228 | 230 | | | | | | | |
| 17P | 230 | 236 | | | | | | | |
| 18P | 232 | 238 | | | | | | | |
| 19P | 231 | 235 | | | | | | | |
| 20P | 20 | 29 | | | | | | | |
| 21P | 21 | 34 | | | | | | | |
| 22P | 22 | 87 | 131 | 179 | | | | | |
| 23P | 23 | 190 | | | | | | | |
| 100P | 42 | 266 | | | | | | | |
| 101P | 30 | 52 | 62 | 123 | 170 | 172 | 271 | | |
| 102P | 56 | 75 | 276 | | | | | | |
| 103P | 73 | 272 | | | | | | | |
| 104P | 38 | 264 | | | | | | | |
| 105P | 37 | 41 | 81 | 90 | 104 | 206 | 238 | 265 | |
| 107P | 199 | 284 | | | | | | | |
| 108P | 203 | 285 | | | | | | | |
| 1003P | 99 | 275 | | | | | | | |
| 1004P | 156 | 230 | | | | | | | |
| 1005P | 171 | 381 | | | | | | | |
| 1006P | 524 | 173 | 282 | | | | | | |
| 1007P | 130 | 174 | 283 | | | | | | |
| 1008P | 106 | 276 | | | | | | | |
| 1009P | 12 | 111 | 277 | | | | | | |
| 1010P | 115 | 278 | | | | | | | |
| 1011P | 29 | 279 | | | | | | | |
| 1012P | 24 | 258 | | | | | | | |
| 1013P | 17 | 259 | | | | | | | |
| 1014P | 34 | 260 | | | | | | | |
| 1015P | 47 | 261 | | | | | | | |
| 1016P | 250 | 263 | | | | | | | |
| 1017P | 217 | 262 | | | | | | | |
| 2000P | 202 | 265 | | | | | | | |
| 2001P | 218 | 251 | 284 | | | | | | |

APPENDIX C
GLDPLT LISTING

GLDPLT,F4

F40

V26(14) 17-JUL-74

15158 PAGE 2

```

54      CALL PLOT(7,,0,,3)
55      1      READ(20,1000,END=2) X,Y,Z,T,C,P,CD,ND
56      1000  FORMAT(8F)
57      I=1
58      GO TO (300,301) ISY
59      300  CONTINUE
60      DY(I)=C
61      DX(I)=P
62      GO TO 302
63      301  DY(I)=C
64      DX(I)=P
65      302  CONTINUE
66      GO TO (200,201,202) ISX
67      200  CALL=ATAN2(2,50*(X-X1)+Y))=57,205)
68      GO TO 100
69      201  DX(I)=X
70      GO TO 100
71      202  DX(I)=Y
72      GO TO 100
73      199  IF(I,1,1) GO TO 100
74      CONTINUE
75      CALL=ATAN2(2,50*(X-X1)+Y))=57,205)
76      198  CALL=ATAN2(2,50*(X-X1)+Y))=57,205)
77      CALL=ATAN2(2,50*(X-X1)+Y))=57,205)
78      1001  PLOT(5,3F)
79      IF(I,1,1) GO TO 1
80      2  IF(I,1,1) GO TO 3
81      CALL=ATAN2(2,50*(X-X1)+Y))=57,205)
82      CALL=ATAN2(2,50*(X-X1)+Y))=57,205)
83      CALL=ATAN2(2,50*(X-X1)+Y))=57,205)
84      CALL=ATAN2(2,50*(X-X1)+Y))=57,205)
85      CALL=ATAN2(2,50*(X-X1)+Y))=57,205)
86      CALL=ATAN2(2,50*(X-X1)+Y))=57,205)
87      CALL=ATAN2(2,50*(X-X1)+Y))=57,205)
88      CALL=ATAN2(2,50*(X-X1)+Y))=57,205)
89      CALL=ATAN2(2,50*(X-X1)+Y))=57,205)
90      CALL=ATAN2(2,50*(X-X1)+Y))=57,205)
91      IF(I,1,1) GO TO 101
92      CONTINUE
93      121  CALL=ATAN2(2,50*(X-X1)+Y))=57,205)
94      CALL=ATAN2(2,50*(X-X1)+Y))=57,205)
95      CALL=ATAN2(2,50*(X-X1)+Y))=57,205)
96      IF(I,1,1) GO TO 102
97      CALL=ATAN2(2,50*(X-X1)+Y))=57,205)
98      CALL=ATAN2(2,50*(X-X1)+Y))=57,205)
99      CALL=ATAN2(2,50*(X-X1)+Y))=57,205)
100     CALL=ATAN2(2,50*(X-X1)+Y))=57,205)
101     CALL=ATAN2(2,50*(X-X1)+Y))=57,205)
102     CALL=ATAN2(2,50*(X-X1)+Y))=57,205)
103     CALL=ATAN2(2,50*(X-X1)+Y))=57,205)
104     CALL=ATAN2(2,50*(X-X1)+Y))=57,205)
105     CALL=ATAN2(2,50*(X-X1)+Y))=57,205)
106     CALL=ATAN2(2,50*(X-X1)+Y))=57,205)

```


UC191 1274

Y24(14) 17-JUL-74

543

SECRET

IPYDAT 0 11571
DY

147
151
155

SIACF 1197
ILIF 5101

11011
11011
11011

(- 6)

| | | | | | | | | | |
|-------|-----|-----|-----|-----|-----|----|----|----|----|
| 1P | 55 | 70 | | | | | | | |
| 2P | 55 | 80 | | | | | | | |
| 3P | 75 | 80 | 112 | | | | | | |
| 4P | 105 | 105 | | | | | | | |
| 4P | 104 | 110 | | | | | | | |
| 7P | 16 | 52 | | | | | | | |
| 109P | 47 | 51 | | | | | | | |
| 121P | 44 | 60 | | | | | | | |
| 122P | 84 | 82 | | | | | | | |
| 121P | 91 | 93 | | | | | | | |
| 134P | 73 | 70 | | | | | | | |
| 149P | 66 | 70 | 72 | 73 | | | | | |
| 200P | 66 | 67 | | | | | | | |
| 271P | 66 | 66 | | | | | | | |
| 232P | 66 | 71 | | | | | | | |
| 273P | 74 | 75 | 26 | 27 | 113 | | | | |
| 309P | 90 | 90 | | | | | | | |
| 311P | 68 | 63 | | | | | | | |
| 312P | 62 | 65 | | | | | | | |
| 1001P | 55 | 56 | | | | | | | |
| 1001P | 78 | 100 | 102 | 104 | | | | | |
| 1002P | 13 | 14 | | | | | | | |
| 1003P | 15 | 16 | | | | | | | |
| 1004P | 17 | 18 | 30 | 40 | 41 | 42 | 43 | 44 | 45 |
| 1005P | 22 | 23 | | | | | | | |
| 1006P | 20 | 21 | | | | | | | |

```

1      SUBROUTINE AXIS3(X0,Y0,AX,AY,DELTA,AINCH,BCD,ACH,BDFC,PJW,CELN)
2      DIMENSION PC(11)
3      AT = .10
4      DELTA=SIGN(DELTA,(AX-AXI))
5      *100.
6      *200.
7      *3 * U.
8      *EXP = 0
9      *CH=IARS('C')
10     IF(P=0,0,0) *EXP = 0
11     C1=CH*ABS(AINCH)
12     IF(IARS(A-AY-AVIN)+A*4(OFF),LT,1,F-3) GO TO 50
13     IF((A-AX-AVIN)/(PI*E-5),GT,3,0,C1/CH) DELTA = (AX-AXI)/CINCH
14     IF(-CP,LT,0) *3 = 1.
15     *CH=IARS(A-AX-AVIN)/CELTA*1.0)
16     *CH=IARS(A-AX-AVIN)/CELTA*1.0)
17     *CH=IARS(A-AX-AVIN)/CELTA*1.0)
18     *CH=IARS(A-AX-AVIN)/CELTA*1.0)
19     *CH=IARS(A-AX-AVIN)/CELTA*1.0)
20     *CH=IARS(A-AX-AVIN)/CELTA*1.0)
21     *CH=IARS(A-AX-AVIN)/CELTA*1.0)
22     *CH=IARS(A-AX-AVIN)/CELTA*1.0)
23     *CH=IARS(A-AX-AVIN)/CELTA*1.0)
24     *CH=IARS(A-AX-AVIN)/CELTA*1.0)
25     *CH=IARS(A-AX-AVIN)/CELTA*1.0)
26     *CH=IARS(A-AX-AVIN)/CELTA*1.0)
27     *CH=IARS(A-AX-AVIN)/CELTA*1.0)
28     *CH=IARS(A-AX-AVIN)/CELTA*1.0)
29     *CH=IARS(A-AX-AVIN)/CELTA*1.0)
30     *CH=IARS(A-AX-AVIN)/CELTA*1.0)
31     *CH=IARS(A-AX-AVIN)/CELTA*1.0)
32     *CH=IARS(A-AX-AVIN)/CELTA*1.0)
33     *CH=IARS(A-AX-AVIN)/CELTA*1.0)
34     *CH=IARS(A-AX-AVIN)/CELTA*1.0)
35     *CH=IARS(A-AX-AVIN)/CELTA*1.0)
36     *CH=IARS(A-AX-AVIN)/CELTA*1.0)
37     *CH=IARS(A-AX-AVIN)/CELTA*1.0)
38     *CH=IARS(A-AX-AVIN)/CELTA*1.0)
39     *CH=IARS(A-AX-AVIN)/CELTA*1.0)
40     *CH=IARS(A-AX-AVIN)/CELTA*1.0)
41     *CH=IARS(A-AX-AVIN)/CELTA*1.0)
42     *CH=IARS(A-AX-AVIN)/CELTA*1.0)
43     *CH=IARS(A-AX-AVIN)/CELTA*1.0)
44     *CH=IARS(A-AX-AVIN)/CELTA*1.0)
45     *CH=IARS(A-AX-AVIN)/CELTA*1.0)
46     *CH=IARS(A-AX-AVIN)/CELTA*1.0)
47     *CH=IARS(A-AX-AVIN)/CELTA*1.0)
48     *CH=IARS(A-AX-AVIN)/CELTA*1.0)
49     *CH=IARS(A-AX-AVIN)/CELTA*1.0)
50     *CH=IARS(A-AX-AVIN)/CELTA*1.0)
51     *CH=IARS(A-AX-AVIN)/CELTA*1.0)
52     *CH=IARS(A-AX-AVIN)/CELTA*1.0)
53     *CH=IARS(A-AX-AVIN)/CELTA*1.0)

```

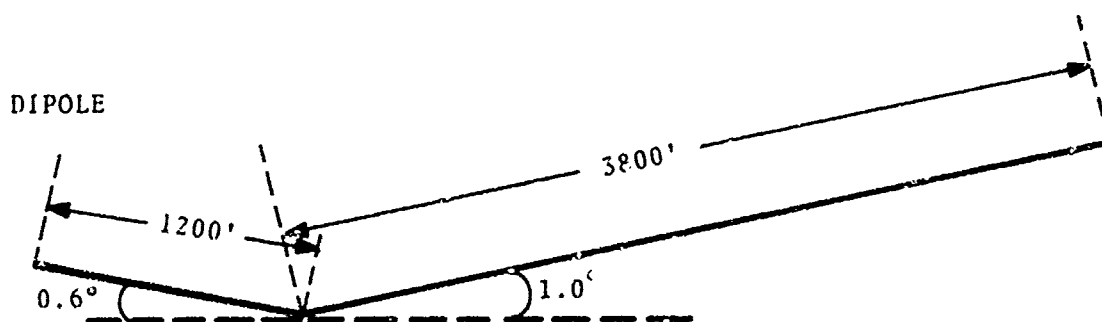

C-11

| | | |
|------|----|----|
| 50 | 17 | 27 |
| 100 | 19 | 21 |
| 200 | 30 | 13 |
| 250 | 30 | 12 |
| 400 | 27 | 50 |
| 500 | 12 | 43 |
| 1000 | 64 | 65 |

APPENDIX D
EXAMPLE

In this Appendix a test case is presented which the programmer may duplicate to gain experience in running the model.

The test case uses a Null Reference antenna over a terrain as sketched below.



The results are shown in Figure 9.

1 2 3 4 5 6 7 8 9 10 11 12 13 14 15 16 17 18 19 20 21 22 23 24 25 26 27 28 29 30 31 32 33 34 35 36 37 38 39 40 41 42 43 44 45 46 47 48 49 50 51 52 53 54 55 56 57 58 59 60 61 62 63 64 65 66 67 68 69 70 71 72 73 74 75 76 77 78 79 80 81 82 83 84 85 86 87 88 89 90 91 92 93 94 95 96 97 98 99 100

Figure 9.. Test Case Results

```

14150130 SVEPS SATCON (14150130) INP: SUBJOB 01 OF 01
14150130 DATE 17-AUG-74
14150130 BASUM TEST(14150130) FOR ANTIMON(14150130) LOG FILE IN 14150130
          REQUEST CHECKED AT 14150130 17-AUG-74
          UNIQUE 2 DESIGNS 9
14150130 MONTR ,LOGIN 14150130
14150130 MONTR JCE 16 TET DECRYPTION=14150130 14150130
14150130 USER OTHER JOB DATA DPM
14150130 USER 14150130 17-AUG-74 TWO
14150130 MONTR ,GET TIME SACS
14150130 MONTR ,SET SPOOL ALL
14150130 MONTR ,RUN FRANK
14150130 USER
14150130 USER INPUT SWITCHING
14150130 USER INPUT TO LAMBDA(14150130,,),
14150130 JCE INPUT SWITCHING
14150130 USER INPUT GROUND FILE NAME:GND
14150130 USER INPUT GROUND LAMP
14150130 USER THIS IS A DEMONSTRATION CASE
14150130 JCE INPUT GROUND ELEMENTS, STARTING FROM ANTENNA,
14150130 USER GIVE CONSECUTIVELY SPIN 1 AND 2 INCREMENTS, OR THE
14150130 USER LENGTH AND ANGLE FROM HORIZONTAL IN DEGREES, SEPARATED
14150130 USER BY A SPACE, HIT CARriage RETURN FOR END OF DATA,
14150130 USER OR IF THERE ARE NO MORE STD. 16,
14150130 JCE *END*
14150130 USER *1200,0.0,0,0
14150130 USER *1300,0.0,1,0
14150130 USER *
14150130 USER INPUT SWITCHING
14150130 USER INPUT FLIGHT PATH FILE NAME:FLIGHT
14150130 USER INPUT FLIGHT PATH TITLE
14150130 USER HYPERBOLIC FLIGHT FROM 14150130
14150130 USER INPUT FLIGHT DATA TYPE:G
14150130 USER INPUT 10,17,14150130,14150130,14150130
14150130 USER INPUT 3 60 POINTS, VELOCITY, TIME CONSTANT:14150130,14150130...4
14150130 USER INPUT SWITCHING
14150130 USER INPUT ANTENNA FILE NAME:ANTENNA
14150130 USER INPUT ANTENNA DESCRIPTION

```

41-3

